

# Supported Heteropoly Acids for Acid Catalysed Reactions

PhD 2011

Peter Llewelyn

UMI Number: U516563

All rights reserved

INFORMATION TO ALL USERS

The quality of this reproduction is dependent upon the quality of the copy submitted.

In the unlikely event that the author did not send a complete manuscript and there are missing pages, these will be noted. Also, if material had to be removed, a note will indicate the deletion.



UMI U516563

Published by ProQuest LLC 2013. Copyright in the Dissertation held by the Author.  
Microform Edition © ProQuest LLC.

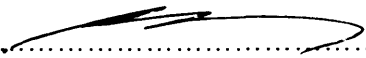
All rights reserved. This work is protected against  
unauthorized copying under Title 17, United States Code.



ProQuest LLC  
789 East Eisenhower Parkway  
P.O. Box 1346  
Ann Arbor, MI 48106-1346


**DECLARATION**

This work has not previously been accepted in substance for any degree and is not concurrently submitted in candidature for any degree.

Signed  .....  
Date ..... 10.08.11 .....

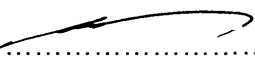
**STATEMENT 1**

This thesis is being submitted in partial fulfilment of the requirements for the degree of PhD

Signed  .....  
Date ..... 10.08.11 .....


**STATEMENT 2**

This thesis is the result of my own independent work/investigation, except where otherwise stated.  
Other sources are acknowledged by explicit references.

Signed  .....  
Date ..... 10.08.11 .....

**STATEMENT 3**

I hereby give consent for my thesis, if accepted, to be available for photocopying and for inter-library loan, and for the title and summary to be made available to outside organisations.

Signed  .....  
Date ..... 10.08.11 .....

## **Acknowledgements**

Since starting this work there are a few people I'd like to thank.

Thanks to Prof Graham Hutchings and Dr Stuart Taylor for their supervision and guidance over this project.

I'd like to thank Johnson Matthey Crystal Faraday and EPSRC for funding this research.

I'd like to thank my fiancé, Vic, who gave me endless words of encouragement and probably got as stressed as me during this Ph.D.

Thanks to my parents and my family who probably didn't understand what this PhD's about but sounded interested when I talked about it.

Thanks to all the people in lab 1.88 who finished, about to finish or were just starting out who made the day-to-day labour that little bit more bearable.

# Abstract

Keggin type heteropoly acids (HPA) either pure, supported or their salts have been synthesised, characterised and their catalytic activity tested against the cyclodehydration of 1,4-butanediol gas phase and liquid phase reactions, the dehydration of geraniol in liquid phase reactions and bio-diesel synthesis using rapeseed oil and methanol.

Raman spectroscopy, B.E.T isotherms, powder XRD, ammonia TPD and TGA indicate that the supported HPAs are present on the surface of the supports investigated. B.E.T experiments show that substituting all but one the acidic protons with caesium increases the surface area of the HPA. Once the remaining proton is substituted, the surface area decreases but remains higher than the unsubstituted free HPA.

The dehydration of 1,4-butanediol was performed and it was found that under the conditions investigated that the reaction was irreproducible. The dehydration and isomerisation of geraniol showed that the reaction proceeds at relatively low temperatures and that the super acidic nature of the heteropoly acids was a key factor in the reaction. The geraniol experiments were found to be first order.

Keggin type HPAs were able to catalyse the transesterification of rapeseed oil (RSO) to fatty acid methyl esters (FAME) however, the highly solubility of HPAs in methanol prevented reusing the catalyst. The transesterification of RSO with methanol were found to be first order. The conversions obtained in the transesterification of RSO were lower than mineral acids in comparison under the same reaction conditions.

**Chapter One**

1.1 Introduction .....	1
1.2 Heteropoly Acids History and Structure.....	2
1.3 Synthesis of Heteropoly Acids.....	3
1.4 Acidity of HPAs.....	4
1.5 Acid Catalysed Reactions .....	6
1.5.1 Homogeneous Catalysis .....	6
1.5.2 Heterogeneous Catalysis.....	11
1.6 Conclusions.....	33

**Chapter Two**

2.1 Synthesis of Catalysts.....	39
2.1.1 Synthesis of Keggin heteropoly acids .....	39
2.1.2 Synthesis of $H_3PW_{12}O_{40}$ (PTA) .....	39
2.1.3 Synthesis of $H_3PMo_{12}O_{40}$ (PMA) .....	39
2.1.4 Preparation of Supported STA .....	40
2.1.5 Synthesis of Keggin salts .....	40
2.1.6 Silica supported caesium salts of STA .....	41
2.2 Experimental Catalyst Testing Apparatus .....	41
2.2.1 Catalyst synthesis and liquid phase apparatus.....	41
2.2.2 Vapour Phase Apparatus.....	41
2.2.3 Gas chromatography analysis set up.....	43
2.2.4 Autoclave reactor set up.....	44
2.3 Catalyst Characterisation Techniques.....	44
2.3.1 B.E.T isotherms.....	44
2.3.2 Raman Spectroscopy.....	45
2.3.3 Powder X-ray Diffraction.....	46
2.3.4 Thermal Gravimetric Analysis (TGA).....	46
2.3.5 Ammonia Temperature Programmed Desorption (TPD).....	47
2.4 Methods.....	47
2.4.1 Liquid Phase Alcohol Dehydration Procedure.....	47
2.4.1.1 1,4-Butanediol Cyclodehydration.....	47
2.4.1.2 Geraniol Dehydration.....	47
2.4.2 Vapour Phase Alcohol Dehydration Procedure.....	47

2.4.3 Alcohol calibration and blank tests.....	48
2.4.4 1,4-butanediol blank tests and calibration.....	49
2.4.5 Isobutanol blank tests and calibration.....	54
2.4.6 Vegetable Oil Transesterification Experimental Procedure.....	57
2.4.7 Materials Used.....	57

### **Chapter Three**

3.1 Catalyst Characterisations.....	59
3.1.1 BET isotherms.....	59
3.1.2 Raman Spectroscopy.....	60
3.1.3 Powder X-ray Diffraction.....	61
3.1.4 Thermal Gravimetric Analysis (TGA).....	63
3.1.5 Ammonia Temperature Programmed Desorption (TPD).....	66

### **Chapter Four**

4.1 introduction.....	72
4.2 Cyclodehydration of 1,4-butanediol.....	73
4.2.1 Introduction.....	73
4.2.2 Reaction of 1,4-butanediol.....	74
4.2.3.1 Initial Reactions.....	75
4.3 Dehydration of Isobutanol.....	83
4.3.1 Activity over time.....	83
4.4 Conclusions.....	88

### **Chapter Five**

5.1 Introduction.....	91
5.2 Geraniol Dehydration.....	94
5.2.1 Initial Reactions.....	95
5.2.2 Caesium Salts of Silicotungstic Acid.....	101
5.2.3 Silica supported reactions.....	104
5.2.4 Effect of Water on activity.....	108
5.2.5 Effect of competitive absorption.....	110
5.2.6 Comparison with mineral acids.....	117
5.2.7 Filtering of the supported catalysts.....	118

5.2.8 Leaching of catalysts.....	119
5.3 Cyclodehydration of 1,4-butanediol.....	120
5.3.1 Initial reactions.....	120
5.4 Conclusions.....	131

**Chapter Six**

6.1 Introduction.....	135
6.2 Reactions.....	138
6.2.1 Initial Reactions.....	138
6.2.2 Transesterification of rapeseed oil to bio-diesel using an autoclave.....	139
6.2.3 Comparisons with other acid catalysts.....	144
6.3 Conclusions.....	145

**Chapter Seven**

7.1 Conclusions.....	147
7.2 Further Work.....	149



# Chapter One: Introduction

## 1.1 Introduction

New classes of acid catalysts that can operate efficiently while using lower quality feed stocks will be important in the future, as oil reserves decrease in quantity and quality. Since the growth of the global economy is driving unsustainable consumption, there is a need for sustainable products and manufacturing processes to be invented and utilised by industry. Traditional acid catalysts are used in the petroleum industry to convert lower value commodities into higher value or higher functionality products<sup>(1)</sup>. The mechanisms for acid catalysed cracking reactions are well understood<sup>(2-8)</sup>, and usually involve the formation of carbonium ions that can undergo isomerisation. In industry, many homogeneous stoichiometric amounts of Lewis acids (e.g.  $\text{AlCl}_3$ ) and mineral acids (e.g.  $\text{H}_2\text{SO}_4$ ) are used in acid catalysis and result in significant volumes of waste, as the acids need to be quenched before discharging or disposal<sup>(9)</sup>. Increasingly, environmental legislation is making disposing of waste acid more expensive forcing companies to adopt 'greener' solutions to waste management<sup>(7)</sup>.

Heterogeneous catalysis is a more favoured approach. Solid heteropoly acids offer safer working conditions and more eco-friendly approach to acid catalysis than traditional soluble acid catalysts.

The aim of the project is to investigate the catalytic properties of the Keggin-type heteropoly acid in various reactions in order to synthesise fine chemicals from lower value chemicals. Supported and unsupported heteropoly acids will be used in order to compare and contrast the differences in both homogeneous and

heterogeneous reaction conditions. Caesium salts of the heteropoly acid silicotungstic acid have been synthesised. The heteropoly acids will be characterised by Raman spectroscopy, powder XRD, TGA, ammonia TPD and BET to assess the identification and purity of the compounds.

A gas phase heterogeneous reactor with on-line GC analysis has been constructed to test the activity of the catalysts under investigation. The dehydration of alcohols has been used as a way of assessing the acid strength of the heteropoly acids. The transesterification of vegetable oil with methanol has been assessed with supported, unsupported heteropoly acids and their caesium salts.

## 1.2 Heteropoly acids history and structure

Heteropoly acids (HPA) were discovered by Berzelius in 1826<sup>(10)</sup> but the formula and crystal structure was not determined until 1933 by Keggin by powder X-ray diffraction. The Keggin structure of HPAs has the general formula  $H_{8-x}X^xM_{12}O_{40}$  where X is typically, but not limited to,  $P^V$ ,  $Si^{IV}$ ,  $Ge^{IV}$  or  $As^V$  and where the M atom is typically  $Mo^{VI}$  or  $W^{VI}$ .



**Figure 1.2.1: The Keggin structure**

Since the discovery of the Keggin structure, two other structures have been identified, the Wells-Dawson  $[(X^{n+})_2M_{18}O_{62}]^{(16-2n)}$  (where X represents  $P^V$ ,  $Ge^{IV}$  or  $As^V$  and M represents  $Mo^{VI}$  or  $W^{VI}$ ) and the Anderson structure  $(XM_6O_{24}^{n-})^{(9,10)}$ . The Keggin structure is built on a distorted edge and corner-sharing  $WO_6$  octahedra, with the length of the W-O bonds between 2.44Å in bridging oxygens ( $O_b$ ) to 1.7Å in terminal oxygens ( $O_t$ ). Tungsten and Molybdenum are the favoured metals as the radii of the

metal cations are 0.74Å and 0.73Å respectively, which allow them to fit into the framework of the HPA anion. This is complemented by the accessibility of empty d orbitals for metal-oxygen  $\pi$  bonding.<sup>(12,13)</sup>

Other atoms have similar radii to 0.74Å but lack the ability to change their coordination to oxygen from 4→6 upon polymerisation in solution or they lack the empty d orbital for  $\pi$  bonding. For example,  $\text{Cr}^{6+}$  is a good  $\pi$  electron acceptor, but its small size means it can only coordinate to 4 oxygen atoms,  $\text{Te}^{6+}$  has the right coordination number but it is a poor  $\pi$  electron acceptor and is unable to form double bonds with unshared oxygen by  $p\pi$ - $d\pi$  interaction.<sup>(13)</sup>

Solid heteropoly acids have a discrete ionic structure of reasonably mobile structural units (the heteropoly anions and their counterions e.g.,  $\text{H}^+$ ,  $\text{H}_3\text{O}^+$ , etc) unlike zeolites and polymer based solid acids, for example Amberlyst-15, the protons are extremely mobile and heteropoly acids exhibit a 'pseudoliquid' phase<sup>(15,16)</sup>. This is where small polar molecules are absorbed into the bulk of the heteropoly anion. Heteropoly acids are extremely soluble in polar solvents such as water, lower alcohols, ethers, esters, ketones, etc. Heteropoly acids are not readily soluble in non-polar solvents like hydrocarbons<sup>(11)</sup>.

### 1.3 Synthesis of heteropoly acids

The synthesis of heteropoly acids is based on the polymerisation of octahedrally coordinated metal oxides around a heteroatom in an acidified solution. The external oxygens prevent the heteropoly acid from forming larger structures by being polarised towards the W or Mo atoms<sup>(12)</sup>. The  $\text{MO}_6$  octahedra formed are slightly distorted which allows the heteroatom to be accommodated. The external oxygens are weakly basic and so as a consequence can only weakly bond to protons. Keggin HPAs can be easily synthesised at room temperature. The simplest method to synthesise a Keggin

HPA is by the acidification of phosphoric acid ( $\text{H}_3\text{PO}_4$ ) and sodium tungstate ( $\text{Na}_2\text{WO}_4$ ), which undergoes the following reaction:



The solution must be of a pH of less than 1, as the HPA isomer is only stable at this pH. It is also easily isolated by solvent extraction to yield a white powder<sup>(16)</sup>.

#### 1.4 Acidity of HPAs

HPAs are strong Bronsted acids due to the surface charge density of the anion being delocalised over the large sized polyanion<sup>(14)</sup>, leading to a weak interaction with the counter-ions. There are six acid sites present in HPAs:<sup>(17)</sup>

1. Proton sites in HPAs (e.g.  $\text{H}_3[\text{PW}_{12}\text{O}_{40}]$ ).
2. Proton sites in acidic salts (e.g.  $\text{Cs}_{2.5}\text{H}_{0.5}\text{PW}_{12}\text{O}_{40}$ ).
3. Lewis acid sites in salts (metal counter-ions e.g.  $\text{La}^{\text{III}}[\text{PW}_{12}\text{O}_{40}]$ )
4. Proton sites generated by dissociation of co-ordination water:  

$$\text{Ln}(\text{H}_2\text{O})_n^{3+} \rightarrow \text{Ln}(\text{H}_2\text{O})_n(\text{OH})^{2+} + \text{H}^+$$
5. Proton sites generated by reduction of salts:  $\text{Pd}_2[\text{SiW}_{12}\text{O}_{40}] + 4\{\text{H}\} \rightarrow 2\text{Pd}^0 + \text{H}_4[\text{SiW}_{12}\text{O}_{40}]$
6. Protons generated by partial hydrolysis of polyanions:  $[\text{PW}_{12}\text{O}_{40}]^{3-} + 2\text{H}_2\text{O} \rightarrow [\text{PW}_{11}\text{O}_{39}]^{-7} + \{\text{WO}_3\} + 4\text{H}^+$

The dissociation constants of HPAs in acetic acid have been studied and have been shown to be stronger than normal mineral acids such as sulphuric acid, HBr and HCl. The dissociation constants were given in the form  $\text{p}K_i = -\log K_i$ , where  $K_i$  is the acid dissociation constant.<sup>(18)</sup>

Acid	$pK_1$
$H_4[SiW_{12}O_{40}]$	4.87
$H_3[PW_{12}O_{40}]$	4.70
$H_3[PMo_{12}O_{40}]$	4.68
HBr	5.60
$H_2SO_4$	7.00
HCl	8.40

**Table 1.4.1: Dissociation constants of HPA and mineral acids at 25°C in acetic acid<sup>(18)</sup>**

Acid strength can also be determined by the Hammett acidity function  $H_o$ <sup>(16)</sup>

( $H_o = pK_{BH^+} - \log ([BH^+]/[B])$ ) where [B] is the concentration of the indicator B,  $[BH^+]$  is the concentration of the conjugated acid and  $K_{BH^+}$  is the equilibrium constant for the reaction:  $BH^+ \rightarrow B + H^+$

The Hammett acid strength value of 100%  $H_2SO_4$  is -11.94, while acids with a Hammett value less than -12 are classed as superacids.

Solid Acid	$-H_o$
Nafion	12
$H_3[PW_{12}O_{40}]$	13.2
$AlCl_3-CuCl_2$	13.7
$SbF_5/SiO_2-Al_2O_3$	13.7

**Table 1.4.2: Hammett function for some solid acid catalysts<sup>(16)</sup>**

The acid strength decreases when tungsten is replaced by molybdenum or vanadium and when the central atom phosphorus is replaced by silicon. The general

acidity increases with a decrease in the negative charge of the heteropoly anion, or an increase in the charge of the central atom.<sup>(11)</sup>

## 1.5 Acid Catalysed Reactions

### 1.5.1 Homogeneous Catalysis

Tungsten containing HPAs exhibit high catalytic activity and are more active than sulphuric acid and phosphoric acid in terms of molar concentration of the catalyst or the proton concentration when the HPA are assumed to be a tri or tetra basic acid.<sup>(5)</sup> Variations in the water content in the systems examined found no cause of the difference in catalytic activity. Determination of the acidity of HPAs by use of Hammett indicators found that the HPAs acidity ranged from between -8.2 to -3.7 on the  $H_o$  scale at concentrations at  $\leq 0.01$  mol/l, while conventional acids such as  $H_2SO_4$  and  $H_3PO_4$  required to be at concentrations of 5.0 and 4.5 mol/l, respectively, to be in the same range.

In the etherification of diethylene glycol with ethanol<sup>(19)</sup>,  $H_3[PW_{12}O_{40}]$  and  $H_4[SiW_{12}O_{40}]$  catalyse the reaction with 60% conversion and 75% selectivity and with 56% conversion and 78% selectivity to diethylene glycol ethyl ether respectively.  $H_2SO_4$  was used in molar amounts 1000 times more concentrated and converted 18% of the diethylene glycol with a selectivity of 41%.

The electrical conductivity of the reaction medium containing  $H_2SO_4$  decreased during reaction time and decreased the acidity. This was not observed in any of the HPAs studied. The acidity losses were thought to of been from the formation of sulphuric esters of alcohol, while the HPAs do not form its esters with alcohol.

Catalyst	Catalyst concentration $10^{-3}$ mol/l	Conversion (%)	Selectivity to diethylene glycol ethyl ether (%)
H <sub>3</sub> [PW <sub>12</sub> O <sub>40</sub> ]	1.6	60	75
H <sub>4</sub> [SiW <sub>12</sub> O <sub>40</sub> ]	1.6	56	78
H <sub>4</sub> [SiMo <sub>12</sub> O <sub>40</sub> ]	1.6	48	76
H <sub>3</sub> [PW <sub>12</sub> O <sub>40</sub> ]	1.6	30	77
H <sub>2</sub> SO <sub>4</sub>	1620	18	41

**Table 1.5.1.1: Etherification of diethylene glycol with ethanol at 200°C<sup>(19)</sup>**

In the homogeneous cyclodehydration reaction of diols<sup>(20)</sup> (1,4-butanediol, 2,5-hexanediol, 2,5-dimethyl-2,5-hexanediol and 1,5-pentanediol) with four unsupported HPAs (H<sub>3</sub>[PW<sub>12</sub>O<sub>40</sub>], H<sub>3</sub>[PMo<sub>12</sub>O<sub>40</sub>], H<sub>4</sub>[SiW<sub>12</sub>O<sub>40</sub>], H<sub>4</sub>[SiMo<sub>12</sub>O<sub>40</sub>]), all the diols were dehydrated to yield the corresponding cyclic ethers with high selectivity. One diol, 1,6-hexanediol was found to produce oxa-cycloheptane, five- and six-membered cyclic ethers. It was found that the weaker acid H<sub>4</sub>[SiMo<sub>12</sub>O<sub>40</sub>] gave higher selectivity in this reaction, due to the limited ability to generate ring contraction by carbocationic processes. 2,5-dimethyl-2,5-hexanediol undergoes cyclodehydration with high selectivity with HPAs and is stereospecific, producing *cis*-2,5-dimethyltetrahydrofuran from racemic 2,5-hexanediol and *trans*-2,5-dimethyltetrahydrofuran from *meso*-2,5-hexanediol. The cyclodehydration occurs by an intramolecular S<sub>N</sub>2 mechanism. 1,2-diols (1,2-propanediol, isomeric 2,3-butanediols and 2,3-dimethyl-2,3-butanediol) undergo highly selective transformations into the analogous carbonyl compound (propanal, 2-butanone and

3,3-dimethyl-2-butanone). The four HPAs studied were all highly active and selective for this reaction, with highest selectivity from  $H_3[PW_{12}O_{40}]$ .

In the homogeneous dehydration of pentaerythritol (PE) to dipentaerythritol (DPE) at  $150^\circ\text{C}$  in a sealed Teflon tube with HPAs<sup>(21)</sup>, water was found to increase the formation of DPE over  $H_3[PW_{12}O_{40}]$  due to the water suppressing the consecutive reaction of DPE.

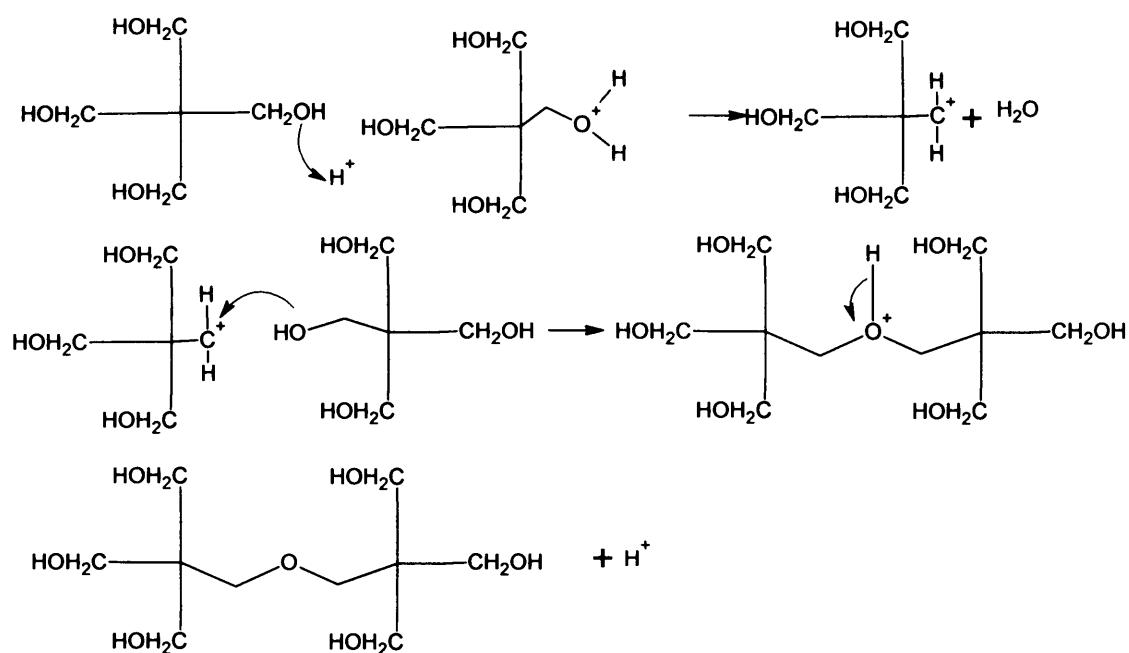


**Figure 1.5.1 Mechanism of DPE formation** <sup>(21)</sup>

The yield of the DPE decreased with the increase of water added because of a decrease in conversion. Supported  $H_4[\text{SiW}_{12}\text{O}_{40}]$  exhibited some activity without water present. The addition of water produced a negative effect on yield.

HPAs have been studied in the homogeneous tetrahydropyranlation of alcohols<sup>(22)</sup>. The reaction is used to protect alcoholic and phenolic hydroxyl groups by forming stable 2-tetrahydropyranyl ethers. Four HPAs, ( $H_3[PW_{12}O_{40}]$ ,  $H_3[PMo_{12}O_{40}]$ ,  $H_4[\text{SiW}_{12}O_{40}]$ , and  $H_4[\text{SiMo}_{12}O_{40}]$ ), were used in the tetrahydropyranlation of benzyl alcohol and were found to catalyse the reaction. HPAs  $H_3[PW_{12}O_{40}]$  and



$H_4[SiMo_{12}O_{40}]$  were tested with other alcohols to assess their catalytic activity. Compounds with electron withdrawing or electron donating substituents were found to react slowly and give low yields. The deprotection step was performed with  $H_3[PW_{12}O_{40}]$  at room temperature for four hours with methanol as the deprotecting agent.

Product	$H_4[SiMo_{12}O_{40}]$	$H_3[PMo_{12}O_{40}]$	$H_4[SiW_{12}O_{40}]$	$H_3[PW_{12}O_{40}]$
2,3-dimethyl-1-butene	17	10	-	-
2,3-dimethyl-1,3-butadiene	15	20	29	22
Acetone	15	27	-	-
3,3-dimethyl-2-butanone	44	43	71	78
Unidentified	9	-	-	-

Table 1.5.1.2: selectivity of the dehydration of 2,3-dimethyl-2,3-butanediol at 150°C <sup>(21)</sup>

HPAs have been studied in the acetylation of cyclic ethers<sup>(23)</sup>. Tetrahydrofuran (THF) was completely converted in two hours at 60°C in a reaction mixture of acetic acid/acetic anhydride (9:1 volume ratio). In this reaction,  $H_3[PW_{12}O_{40}]$  was used and only one product was obtained, 1,4-diacetoxybutane. The high selectivity and efficiency of the reaction was reasoned to be due to acetyl cations formed by the acetic anhydride with the HPA and an excess of acetate anions to react with the acetylated THF oxocations. Sulphuric and *p*-toluenesulphonic acid were found to be nearly inactive in this reaction, as was HPA  $H_3[PMo_{12}O_{40}]$ . Molybdenum containing HPAs are well known to be more susceptible to being reduced in organic media,

which explains its low activity. Both  $H_3[PW_{12}O_{40}]$  and  $H_4[SiW_{12}O_{40}]$  were found to be highly active and is thought to be due to their higher acidity, higher ability to form ether complexes and the heteropoly anion stabilising the organic cationic intermediates.

Catalyst	Rate constant ( $l\text{ Mol}^{-1}\text{ min}^{-1}$ )
$H_4[SiW_{12}O_{40}]$	20.4
$H_3[PW_{12}O_{40}]$	20.2
$H_3[PMo_{12}O_{40}]$	0.06
<i>p</i> -Toluenesulphonic acid	0.03
Sulphuric acid	0.16

Table 1.5.1.3: Catalytic activity of THF acetolysis at 60°C <sup>(23)</sup>

Caesium ion-exchanged HPAs have been tested as water tolerant catalysts<sup>(25)</sup>.  $H_3PW_{12}O_{40}$ ,  $Cs_3PW_{12}O_{40}$ ,  $Cs_{2.5}H_{0.5}PW_{12}O_{40}$  (Cs2.5), H-ZSM, (Si/Al = 628), H=ZSM-5 (Si/Al = 40),  $SiO_2$ ,  $Al_2O_3$  and  $SiO_2-Al_2O_3$  were all tested in the hydrolysis of ethyl acetate in excess water and their activities compared. It was found that the activity of the Cs2.5 (per unit weight) was 3 and 35 times greater than H-ZSM, (Si/Al = 628), H=ZSM-5 (Si/Al = 40) respectively. It was noted that  $SiO_2-Al_2O_3$  and  $Al_2O_3$  were inactive under the same reaction conditions. The activity per acid amount was 7 times greater for Cs2.5 than the H-ZSM catalysts. In the hydrolysis of 2-methylphenyl acetate, Cs2.5 was found to be less active (per unit weight) than  $H_2SO_4$  and *para*-toluenesulphonic acid for the hydrolysis of 2-methylpheny acetate, the activity per acid weight was 15 times greater than the liquid acids.

In conclusion, HPAs can be used to catalyse reactions in homogeneous conditions where traditional acids such as sulphuric acid and hydrochloric acid

cannot. HPAs are able to be active at concentrations several orders of magnitude lower than the equivalent mineral acid, this enables less workup and less waste in purifying the end products after the required reaction is over. In general, the stronger HPAs (PTA and STA) are able to catalyse reactions that the weaker (PMA and SMA) are not, the weaker HPAs generally produce different selectivities to the stronger HPAs due to interactions with the HPA with intermediate reaction products. The major disadvantage of HPAs in homogeneous reactions is that they are more expensive per gram than conventional mineral acids.

### 1.5.2 Heterogeneous Catalysis

HPAs have been supported on silica<sup>(12,14,16,24-30,60)</sup>, zeolites<sup>(31-36)</sup>, alumina<sup>(27,28,36)</sup>, carbon<sup>(28,37,25)</sup>, titania<sup>(27,28,38,60)</sup>, zirconia<sup>(39,40,43,60)</sup>, niobia<sup>(54,60)</sup> and clays<sup>(28,33,35,41,50)</sup>. This can increase the surface area of the HPA from  $\sim 10\text{m}^2/\text{g}$  to  $100\text{-}300\text{m}^2/\text{g}$ <sup>(30)</sup>. The most common support is silica with the HPA either supported on the surface by incipient wetness (silica supported) or incorporated into the silica by hydrolysis of ethyl orthosilicate (silica included)<sup>(23, 27, 30)</sup>

In gas and liquid phase heterogeneous catalysis, reactions take place on the surface of the catalyst. This can be on the pore walls or on the outer surface. Reactions with HPAs can take place within the heteropoly anion leading to two possible mechanisms, surface and bulk mechanisms. Small, polar molecules are taken up into the bulk of the heteropoly anion and cause swelling. The rate at which this happens is determined by basicity and by molecular size.

In the hydrolysis of ethyl acetate by silica included  $\text{Cs}_{2.5}\text{H}_{0.5}[\text{PW}_{12}\text{O}_{40}]$  it was found that the salt remained an insoluble solid during the reaction<sup>(23)</sup>. The activity of the unsupported and non-included Cs salt was found to be related to the bulk acidity of the salt, with the activity decreasing with increasing Cs content. In the hydrolysis

of ethyl acetate, the Cs salt could be separated by filtration under low water concentrations, under a large excess of water, the salt particles formed a colloidal solution and become unrecoverable in water.

Other acidic salts  $(\text{NH}_4)_2\text{H}[\text{PW}_{12}\text{O}_{40}]$ ,  $\text{Cs}_2\text{H}[\text{SiW}_{12}\text{O}_{40}]$  and  $\text{Cs}_{2.5}\text{H}_{0.5}[\text{PMo}_{12}\text{O}_{40}]$  partly dissolved in the reaction mixture. The  $\text{SiO}_2/\text{Cs}_{2.5}\text{H}_{0.5}[\text{PMo}_{12}\text{O}_{40}]$ , water/ $(\text{EtO})_4\text{Si}$  and ethanol/ $(\text{EtO})_4\text{Si}$  ratios were investigated to determine the optimum conditions for  $\text{Cs}_{2.5}\text{H}_{0.5}[\text{PMo}_{12}\text{O}_{40}]$  inclusion. It was found that a high  $\text{SiO}_2$  content reduced leaching of the salt and high water content accelerated the hydrolysis of the  $(\text{EtO})_4\text{Si}$ , which resulted in more leaching of the salt due to the lack of inclusion within the support. The included Cs salt was compared with two other catalysts, Amberlyst-15 and H-ZSM and were found to be less active than Amberlyst-15 and more active than H-ZSM. On the basis of rate per unit catalyst weight, the TOF of the Cs salt were found to be higher than both Amberlyst-15 and H-ZSM. A silica included Cs salt with a silica/ $\text{Cs}_{2.5}\text{H}_{0.5}[\text{PW}_{12}\text{O}_{40}]$  ratio of 8 was found to be easily filtered and reusable for the hydrolysis up four times without deactivation.

$\text{H}_3[\text{PW}_{12}\text{O}_{40}]$  included silica requires higher loadings due to the solubility of the HPA in water and are more catalytically active than the silica included Cs salt based on unit weight in the hydrolysis of ethyl acetate. When compared to reaction systems containing a physical mixture of silica and  $\text{H}_3[\text{PW}_{12}\text{O}_{40}]$  and homogeneous  $\text{H}_3[\text{PW}_{12}\text{O}_{40}]$ , the mixed and silica supported  $\text{H}_3[\text{PW}_{12}\text{O}_{40}]$  systems behaved similarly to the  $\text{H}_3[\text{PW}_{12}\text{O}_{40}]$  dissolved into the reaction medium. The silica included  $\text{H}_3[\text{PW}_{12}\text{O}_{40}]$  was catalytically more active than the other systems. It is thought that the  $\text{H}_3[\text{PW}_{12}\text{O}_{40}]$  is trapped in the silica matrix and acting as a highly concentrated solution.

The liquid phase alkylation of benzene with ethylene have been performed with silica supported phosphotungstic acid (PTA) it was found that catalytic activity increases with loading of the PTA on silica until it reaches a maximum of 50wt. %<sup>(24)</sup> and decreases. It was found that the bulk PTA had the lowest activity. While 75wt. % PTA had the greatest number of acid sites and acid strength determined by ammonia TPD, it was not as active as the 50wt. %. This is explained by the fact that ammonia can be absorbed into the bulk of the PTA, due to the pseudo-liquid phase exhibited by HPAs. Pyridine adsorption FT-IR studies support that the Bronsted and Lewis acid sites in the 75wt % PTA are actually less than the 50wt. % PTA. It was determined that the pores of the silica of the 75wt. % have been filled with the PTA, therefore, reactants have less chance of reacting on the surface acid sites.

Catalyst	Catalytic activity (kg E kg <sub>cat</sub> <sup>-1</sup> h <sup>-1</sup> )	Selectivity to ethyl benzene (%)	Selectivity to ethylene(%)
10 wt.% PTA	1.11	73.2	99.3
20 wt.% PTA	2.28	71.9	99.4
30 wt.% PTA	2.48	71.2	99.4
50 wt.% PTA	3.16	70.7	99.5
75 wt.% PTA	1.68	69.9	99.4
PTA	1.05	72.2	99.2

**Table 1.5.2.1: Transalkylation activity and selectivity of supported PTA and bulk PTA<sup>(24)</sup>**

Friedel-Crafts type alkylations have been studied with silica supported and included HPAs<sup>(30)</sup>. HPAs demonstrate varying activities and regioselectivities in the adamantylation of substituted benzene derivatives depending on the strength of the acid used. Molybdenum containing HPAs give para-substituted isomers with high selectivities as the para isomers were formed under kinetic control. No isomerisation

was observed with the molybdenum containing HPAs after prolonged reaction time. Tungsten containing HPAs give high meta/para ratios due to the para isomer isomerising to give the meta compound in the presence of strong acids. For the silica included HPAs  $\text{H}_3[\text{PW}_{12}\text{O}_{40}]$  and  $\text{H}_4[\text{SiW}_{12}\text{O}_{40}]$  gave 100% conversion in 35 minutes while the HPAs supported on silica also produced 100% conversion and are more selective to the meta isomer in 35 minutes. The reduced conversion is due to diffusional hindrance of 1-bromoadamantane to the active sites in the molybdenum containing HPAs.

In the Friedel-Crafts alkylation of toluene with 5-*tert*-butyl-1,2,3-trimethylbenzene the silica included tungsten containing HPAs are more catalytically active than the silica supported tungsten containing HPAs. After 10 hours reaction time the conversion is 90% with the silica included HPAs compared to the silica supported HPAs (50% with  $\text{H}_3[\text{PW}_{12}\text{O}_{40}]$  and 60% with  $\text{H}_4[\text{SiW}_{12}\text{O}_{40}]$ ) Conversion of the silica included HPAs after recovery was reported to be 40% after 5 hours compared to 60% when fresh catalyst was used. The silica supported HPAs were inactive after recovery and reuse. The silica included and silica supported molybdenum-containing HPAs were inactive, this would be due to molybdenum containing HPAs being less acidic than tungsten containing HPAs. The formation of the *tert*-butyl cation in the transalkylation requires stronger acidity than the generation of the adamantyl cation in the adamantylation.

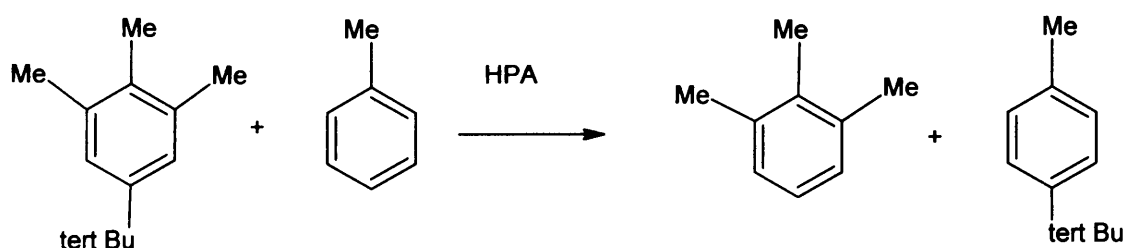
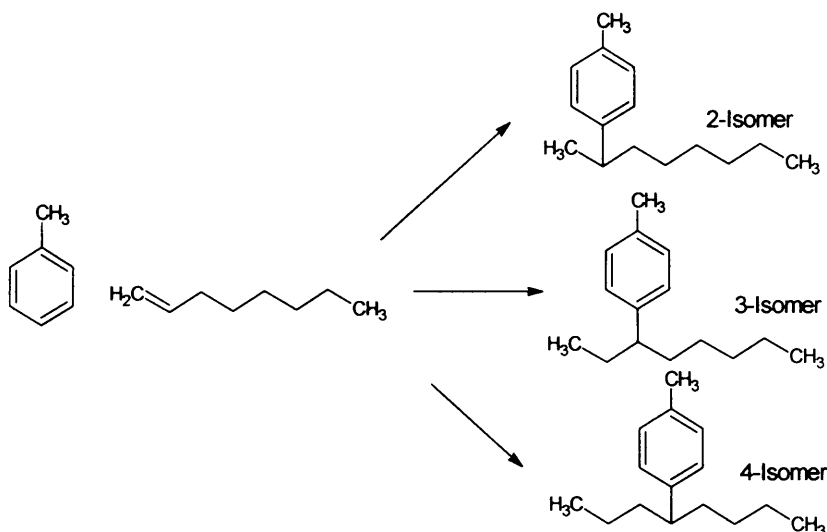


Figure 1.5.2 Transalkylation of 5-*tert*-butyl-1,2,3-trimethylbenzene <sup>(30)</sup>

Alkylation of toluene with 1-octene using HPAs supported by MCM-41 showed 100% conversion of 1-octene and a selectivity of 99% for monoalkylation products<sup>(52)</sup>. All the catalysts tested (supported and unsupported HPA) showed varying degrees of activity high selectivity except for the support MCM-41. The catalyst with the highest conversion and selectivity to the 2-isomer was STA 50%wt supported on MCM-41. The selectivity to the 2-isomer is dependent on temperature. While the conversion increases with temperature, the distribution of products after four hours at 120°C was 43.7% 2-isomer, 24.7% 3-isomer and 31.6% 4-isomer.



**Figure 1.5.3 Toluene alkylation scheme**<sup>(52)</sup>

It was found that PTA on MCM-41 was slightly less active than STA on MCM-41 under the same conditions. PTA on MCM-41 reached 100% conversion in two hours, while under the same conditions STA on MCM-41 reached 100% conversion in 1.5 hours. Since PTA is generally stronger in acid strength it is likely that the difference is due to the interaction between the HPA and the support.

In the dehydration of 1,2-diphenylethanol to stilbene with silica supported HPAs it was found that the reaction was 100% selective to *trans*-stilbene<sup>(29)</sup>. The dehydration of 1,2-diphenylethanol was carried out at reflux in chloroform and it was

observed that the reaction proceeded at a high rate with >99% conversion at 30 minutes for silica supported  $H_3[PW_{12}O_{40}]$  and  $H_3[PMo_{12}O_{40}]$ . At 15 minutes the  $H_3[PW_{12}O_{40}]$  HPA converted 90% of the 1,2-diphenylethanol and the  $H_3[PMo_{12}O_{40}]$  converted 54% in the same time, the reason for this was the highly dispersed  $H_3[PW_{12}O_{40}]$  on the silica. The same reaction was carried out with 50% sulphuric acid with similar results but the HPA catalysed reaction was faster and more environmentally friendly.

The gas phase isomerisation of *n*-hexane with silica supported  $H_3[PW_{12}O_{40}]$  the catalysts show isomerisation activity without a promoter<sup>(26)</sup>. The selectivity of the isomerisation is greater than that of the cracking with the main products of isomerisation being 2-methylpentane, 3-methylpentane, 2,3-dimethylbutane and 2,2-dimethylbutane and the main cracking products were isopentane and isobutane. The catalyst activity decreases with time on stream, which may be due to coking on the surface of the catalyst. The HPA has strong acid sites able to isomerise *n*-hexane but it requires a promoter with hydrogenating/dehydrogenating function to stabilise the activity. An increase in the loading of the silica with HPA leads to an increase in the conversion of *n*-hexane and a decrease in selectivity for the isomerisation, but the selectivity to isobutane and isopentane increase. These are the main cracking products and are thought to result from uncompleted secondary isomerisation.

	<b>10% HPA loading</b>	<b>20% HPA loading</b>	<b>30% HPA loading</b>	<b>40% HPA loading</b>	<b>50% HPA loading</b>	<b>60% HPA loading</b>
Conversion %	0.8	1.3	3.6	4.4	5.7	5.6

**Table 1.5.2.2: Conversion of *n*-hexane over silica supported HPA at 22 minutes. Selectivity of samples to 2-methylpentane is 75.6-79.3%<sup>(26)</sup>**



The isomerisation of styrene oxide to phenylacetaldehyde using PTA on silica (20% wt) has been investigated under mild conditions<sup>(58)</sup>. Due to styrene oxide polymerising under solvent-free conditions, cyclohexane was used as a solvent. The reaction was highly efficient as only 0.08 wt% of the silica supported was needed for 98% conversion in 30 minutes at 25°C with selectivity to phenylacetaldehyde of 50%, remaining 50% was attributed to oligomers, which were not detectable, by GC. Upon increasing the temperature to 70°C the selectivity increased to 87% in two hours reaction time. It was noted that the conversion stopped and was only increased with the addition of fresh catalyst, which was possibly due to styrene oxide polymer poisoning the catalyst surface.

HPA promoted by Pt/Al<sub>2</sub>O<sub>3</sub> (1:1 ratio in weight) increased the selectivity for the isomerisation to 98.9% and the conversion of *n*-hexane is increased compared to the non-promoted HPA on silica. 1 wt.% Pt/Al<sub>2</sub>O<sub>3</sub> alone did not produce any products under the same reaction conditions as the silica supported HPA.

<b>Catalyst</b>	<b>10% HPA loading</b>	<b>20% HPA loading</b>	<b>30% HPA loading</b>	<b>40% HPA loading</b>	<b>50% HPA loading</b>	<b>60% HPA loading</b>
Conversion %	9.8	25.2	37.7	46.6	50.1	46.1

**Table 1.5.2.3: Conversion of *n*-hexane over silica supported HPA promoted by Pt/Al<sub>2</sub>O<sub>3</sub> at 60 minute on stream<sup>(26)</sup>**

Isomerisation of *n*-butane over zirconia supported Pt<sup>(40)</sup> promoted HPAs has been studied and it was shown that Pt free systems showed little activity for the reaction with only 7% yield of isomers at optimal temperatures. The HPA free system also showed little activity for the reaction with yields of isohexane of 18% at 350°C with selectivity below 50%. The effect of HPA loading at a fixed temperature of 210°C showed that loading of 20% HPA on zirconia gave a yield of 77% and a selectivity of 95% to isohexane. The selectivity of isohexane is a maximum of ~99%

at 180°C, at this temperature the yield would drop to 65%. An increase in the temperature above 210°C leads to a decrease in the yield of isohexanes. The selectivity drops to below 90% at 250°C. Introducing Zr atoms into the HPA structure decreases activity as the yield of isohexanes at 160°C with Pt/H<sub>3</sub>[PW<sub>11</sub>ZrO<sub>40</sub>] was less than 5%.

The conversion of glycerol to acrolin has been reported with Cs salts of PTA under gas phase conditions<sup>(53)</sup>. Unsupported Cs<sub>2.5</sub>H<sub>0.5</sub>PW<sub>12</sub>O<sub>40</sub> showed high activity with 100% glycerol conversion with 98% selectivity to acrolin after one hour on stream. After six hours the conversion decreased to around 40% with around 9% (w%) coking found on the catalyst surface, however, the selectivity to acrolin was still high (92% after twelve hours on stream) despite the decrease in conversion. When doped with Pd there is a decrease in the amount of coke deposited on the surface of around 4.5%, half that of the undoped catalyst.

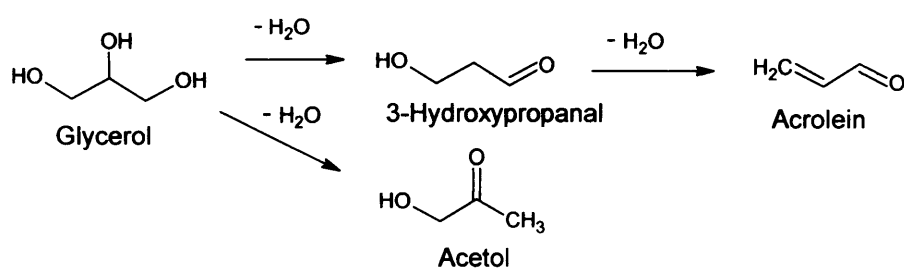


**Figure 1.5.4 Dehydration of Glycerol** <sup>(53)</sup>

The gas phase isomerisation of *n*-butane using H<sub>3</sub>[PW<sub>12</sub>O<sub>40</sub>] on natural montmorillonite clay and acid activated montmorillonite clay have been studied<sup>(33)</sup>. The reactions were carried out at 473K and the activity decreased with time on stream. The products formed were isobutane, propane, isopentane and *n*-pentane. The isomerisation of *n*-butane was considered to be a surface type reaction as the TON increases with increasing HPA content up to a plateau corresponding to pure HPA, which is an indicator to a surface type reaction.

The isomerisation of longifolene and  $\alpha$ -pinene has been investigated using 20 wt% PTA supported on silica in solvent free conditions<sup>(51)</sup>. To determine catalysis leaching, the catalyst was removed at reaction temperature to avoid re-adsorption of HPA onto the silica. The supernatant was added to fresh substrate and the reaction restarted. No further isomerisation products were observed in the leaching experiments, demonstrating that the level of leaching was insufficient to catalyse the reaction further. This was attributed to the fact HPAs are insoluble in non-polar solvents. The isomerisation of longifolene was performed at 80°C for 300 minutes with 60% conversion to isolongifolene with 95% selectivity. The conversion increased to 96% at 100°C with 98% selectivity in only 70 minutes reaction time. Upon increasing the temperature to 120°C the conversion was 100% in 10 minutes reaction time, however the conversion had decreased to 76%, which was attributed to the formation of high boiling products, which were not determinable. The isomerisation of  $\alpha$ -pinene to camphene was able to proceed at relatively low temperatures (60-100°C) with a selectivity of 40-50% to camphene with other products being formed (tricyclene, limonene,  $\alpha$ -terpinene,  $\gamma$ -terpinene, terpinino-lene as well as other products which were not determined). The temperature had a significant effect on the rate as the reaction at 60°C took five hours to reach completion, whereas the reaction at 100°C reached 90% conversion after one hour.

After optimisation, camphene and limonene accounted for around 80% of the products with the remainder made up of  $\alpha$ -terpinene,  $\gamma$ -terpinene and terpinino-lene. The catalyst was reused three times without loss of activity, showing that leaching under non-polar conditions is negligible. Camphene and other bi-cyclic products form in the presence of Lewis sites, while mono-cyclic products form in the presence of Bronsted sites. The effectiveness of the HPA catalyst in the isomerisation of  $\alpha$ -pinene

is related to the weak interaction of the heteropoly anion with the reaction intermediates, which unlike the anions of other Bronsted acids, do not strongly affect the products and therefore do not promote side reactions.

$\alpha$ -pinene isomerisation has been carried out in gas phase conditions<sup>(60)</sup> with PTA supported on silica, titania, zirconia and niobia at 15 wt% loadings. Reactions were carried out at 200°C with  $\alpha$ -pinene at a concentration of 2.0% by volume in nitrogen (flow rate 20ml/min) with 0.1g catalyst used. Camphene was the main reaction product with limonene, terpinolenes, terpinenes,  $\beta$ -pinene, *p*-cymene and a number of unidentified monoterpene by-products. Coke deposits were observed on the catalyst surfaces, it was found that during the first hour of reaction only 50-60% of the carbon fed ended in the products detected. After three hours on stream 90-100% of the carbon fed ended up in the products. This shows that the majority of coking occurs in the first three hours, after three hours little coking occurs on the catalyst surface.

Catalyst	Conversion (%)	Selectivity (mol%)		
		Camphene	Limonene	Others
15% $H_3PW_{12}O_{40}/SiO_2^a$	100	27	0	73
15% $H_3PW_{12}O_{40}/TiO_2^a$	94	39	3	73
15% $H_3PW_{12}O_{40}/TiO_2^b$	88	56	7	37
15% $H_3PW_{12}O_{40}/Nb_2O_5^a$	88	32	7	61
15% $H_3PW_{12}O_{40}/Nb_2O_5^b$	85	36	8	56
15% $H_3PW_{12}O_{40}/ZrO_2^a$	74	55	19	26

15% $\text{H}_3\text{PW}_{12}\text{O}_{40}/\text{ZrO}_2^{\text{b}}$	75	51	18	31
$\text{CS}_{2.5}\text{H}_{0.5}\text{PW}_{12}\text{O}_{40}^{\text{a}}$	48	67	10	23

**Table 1.5.2.4: Gas phase isomerisation of pinene after ten hours reaction time.**

**a: Catalyst calcined at 300°C**

**b: Catalyst calcined at 500°C**

The selectivity to camphene and limonene increased with reaction time, in line with catalyst deactivation. The coke is most likely blocking the stronger acid sites of the catalyst, which indicates that the formation of camphene and limonene is favoured with the strongest sites deactivated.

PTA supported on niobia, titania and zirconia calcined at 500°C were weaker acids and showed higher camphene selectivity as well as stronger resistance to deactivation. This also suggests that the less active acid sites are favour the formation of camphene and that the stronger acid sites increase the isomerisation and catalyst coking, which reduces the camphene selectivity.

The alkylation of aniline with methyl-*tert*-butyl ether (MTBE) and *tert*-butanol using  $\text{H}_3[\text{PW}_{12}\text{O}_{40}]$  supported on K-10 clay<sup>(41)</sup> gave a conversion of 70% with MTBE and a selectivity of 84% to the mono-alkylated products, 53% being 2-*tert*-butylaniline. The same catalyst gave a 34% conversion with *tert*-butanol with 50% selectivity to both 2-*tert*-butylaniline and 4-*tert*-butylaniline. The HPA loaded clay was found to be more catalytically active than the clay or HPA alone on a unit weight basis. The  $\text{H}_3[\text{PW}_{12}\text{O}_{40}]$  supported on K-10 clay could be reused twice without appreciable loss of activity as the conversions were 70% in both cases. During the third run the conversion was 63% and on the fourth reuse the conversion dropped to 58%. The alkylation of phenol with benzyl alcohol on zirconia supported<sup>(43)</sup> phosphotungstic acid (PTA) was found to be an efficient catalyst at a 15wt.% loading. Zirconia alone does not show any activity for the reaction. At

15wt.% loading the conversion is 65%, upon an increase in catalyst loading the conversion decreases. The selectivity of the reaction also depends on the loading of the catalyst. The selectivity to benzyl phenol increases from 65% to 75% as the loading of PTA on zirconia increased from 5% to 15%.

HPA trapped in the channels of MCM-41 are active for the synthesis of bisphenol-A<sup>(32)</sup>. The HPA used is the Cs salt and is introduced by impregnating the silica surface with caesium carbonate followed with impregnation with HPA. This results in the insoluble  $\text{Cs}_{2.5}\text{H}_{0.5}[\text{PW}_{12}\text{O}_{40}]$  supported on the silica at the entrances of the channels. This blocks the channels and reduces the surface area from about  $900\text{m}^2/\text{g}$  to  $220\text{m}^2/\text{g}$ . It was thought that when the caesium salt is introduced it covers the channel with very little distance between neighbouring molecules. Once the HPA is introduced the resulting salt blocks the channel.

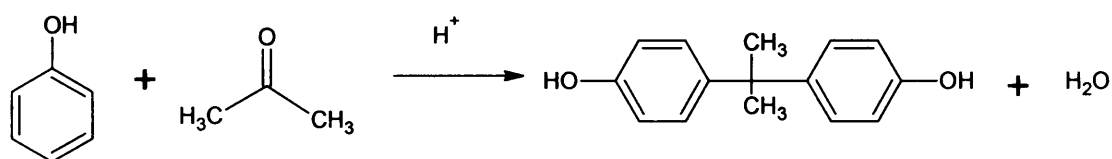


**Figure 1.5.5 Synthesis of Bisphenol A** <sup>(32)</sup>

An alternate route for supporting HPA on MCM-41 was to first impregnate the surface with HPA solution then introduce the caesium carbonate to form the caesium salt. This is thought to result in a high dispersion of the HPA but with enough distance between HPA molecules to prevent blockage of the channel once caesium is introduced. The supported HPA on MCM-41 obtained in this method had a surface area of  $500\text{m}^2/\text{g}$ . Washing the sample with methanol had little effect on surface area and pore volume indicating that the HPA anions were bonded to the support. The resulting catalysts were used in the synthesis of bisphenol-A and showed high activity for phenol conversion at  $160^\circ\text{C}$  and a high selectivity of 60% to *p-p*-bisphenol-A

The Friedel-Crafts isopropylation of benzene with isopropyl mesylate<sup>(43)</sup> and transalkylation of toluene with 5-*tert*-butyl-1,2,3-trimethylbenzene catalysed with MCM-41 supported HPAs with low caesium content are more active than MCM-41 supported HPAs with high caesium content.

Catalyst	Isopropylation conversion (%)	Transalkylations	
		Conversion (%)	TOF (min <sup>-1</sup> )
Cs <sub>2.8</sub> /MCM-41	44	0	-
Cs <sub>1.8</sub> /MCM-41	100	69 <sup>a</sup> (81) <sup>b</sup>	1.3

**Table 1.5.2.5: Activity of catalysts in Friedel-Crafts alkylations. Catalyst amount: 0.1g, under reflux conditions (43)**

a: reaction time 3 hours

b: reaction time 7 hours

The transalkylation of toluene with 5-*tert*-butyl-1,2,3-trimethylbenzene requires a high concentration of acid sites to generate the *tert*-butyl carbocation by dealkylation of the aromatic compound. The high content HPA salts have a low concentration of acid sites and are unable to facilitate the reaction by generating the carbocations. The isopropyl mesylate is able to yield the 2-propyl carbocation intermediate with supported HPAs with low concentrations of acid sites. Reuse studies of the silica supported Cs<sub>1.7</sub> H<sub>1.3</sub>[PW<sub>12</sub>O<sub>40</sub>] catalyst show a repeated drop in activity for the transalkylation of toluene, from 90% in the first run, 70% in the second run and 58% in the third run of 7 hours reaction time.

Ion-exchanged HPAs are not restricted to mono-valent cations, cations of alkaline earth cations (Be, Mg, Ca, Sr and Ba) have been reported<sup>(44)</sup> to have been exchanged with the protons from phosphotungstic acid and still retained strong Bronsted acid sites when determined by ammonia absorption. While the substitution exchanged two acidic protons for one alkaline earth cation, the heat of ammonia absorption was reported to have been higher than 150kJ/mol.

The catalytic performance of  $\text{Cs}(\text{NH}_4)_2\text{PMo}_{12}\text{O}_{40}$  and  $\text{Cs}_2(\text{NH}_4)\text{PMo}_{12}\text{O}_{40}$  in the conversion of methacrolein (MA) to methacrylic acid (MAA)<sup>(45)</sup> was investigated and it was found that the conversion, selectivity to MAA and catalyst lifetime were greater than that of the parent HPA, phosphomolybdic acid. (PMA). The addition of the  $\text{Cs}^+$  cations enhanced the thermal stability of the HPA. The introduction of one  $\text{Cs}^+$  cation significantly improves the conversion and selectivity to MAA, while the addition of two  $\text{Cs}^+$  cations improves the lifetime of the catalyst, but adversely effects the conversion and selectivity while still outperforming the parent acid PMA.

Catalyst	Conversion (%)	Selectivity MAA (%)	Lifetime (h)
$\text{H}_3\text{PMo}_{12}\text{O}_{40}$	36.4	50.2	Ca.15
$\text{Cs}(\text{NH}_4)_2\text{PMo}_{12}\text{O}_{40}$	63.7	56	Ca.200
$\text{Cs}_2(\text{NH}_4)\text{PMo}_{12}\text{O}_{40}$	50.7	54	>380

**Table 1.5.1.6:**The lifetime is defined as the point at which the conversion and selectivity begin to decrease<sup>(45)</sup>

Vanadium substituted ( $\text{H}_{3+x}[\text{PMo}_{12-x}\text{V}_x\text{O}_{40}]$   $x = 0-3$ ) polymer supported HPAs have been used in the heterogeneous lactonisation of 1,4-butanediol<sup>(46)</sup>. The polymer support was polyaniline and the HPAs were supported by two methods. In the first method a solution of free  $\text{H}_3[\text{PMo}_{12}\text{O}_{40}]$  and aniline was polymerised at room temperature for 24 hours, washed and dried. The two-step method involved deprotonating the emeraldine salt of aniline with 3% ammonium hydroxide solution to obtain the emeraldine base. This was then reacted with a solution of  $\text{H}_3[\text{PMo}_{12}\text{O}_{40}]$  dissolved in acetonitrile. The resulting catalyst was then washed and dried. The lactonisation of 1,4-butanediol was done at 80°C for 20 hours in the liquid phase. The vanadium substituted HPA supported on the polymer made by the second method were the most active with the order of activity following the trend  $\text{PMo}_9\text{V}_3 >$



$\text{PMo}_{10}\text{V}_2 > \text{PMo}_{11}\text{V}_1 > \text{PMo}_{12}$ . The same trend in activity was seen in the catalysts prepared with the first method and with unsupported vanadium substituted HPA. The higher activity of the two-step prepared catalysts was thought to be the HPA immobilised on the surface of the polyaniline and have higher surface areas than the one-step catalysts. The enhanced activities are thought to down to two factors. The first is the molecular level dispersion of  $\text{PMo}_{12-x}\text{V}_x$  ( $x = 0-3$ ) catalyst on and in the polymer support, the other effect could be due to electronic modification of the  $\text{PMo}_{12-x}\text{V}_x$  ( $x = 0-3$ ) contributed by the support by ionic immobilisation.

Catalyst	BET surface area ( $\text{m}^2/\text{g}$ )
$\text{PMo}_{12}$ (one-step)	49
$\text{Pmo}_{12}$ (two-step)	140
$\text{PMo}_{11}\text{V}_1$ (one-step)	70
$\text{PMo}_{11}\text{V}_1$ (two-step)	184
$\text{PMo}_{10}\text{V}_2$ (one-step)	52
$\text{PMo}_{10}\text{V}_2$ (two-step)	100
$\text{Pmo}_9\text{V}_3$ (one-step)	66
$\text{Pmo}_9\text{V}_3$ (two-step)	142

**Table 1.5.2.7: Surface areas of vanadium substituted HPA supported on polyaniline(46)**

Copper exchanged PTA has been used in the cyclopropanation of alkenes <sup>(59)</sup>. The copper PTA was synthesised by precipitating an aqueous solution containing 2.0g of PTA with 0.18g barium hydroxide to neutralise the three acidic protons. To the neutralised PTA, 0.16g of  $\text{CuSO}_4 \cdot 5\text{H}_2\text{O}$  was added to exchange the barium with copper. The resulting PTA had the formula  $\text{Cu}_{1.5}\text{PW}_{12}\text{O}_{40}$  and was recovered from the solution by recrystallisation. Reactions were conducted at  $27^\circ\text{C}$  with 5 mol% of the copper exchanged PTA (Cu-PTA) in a solution of dichloromethane catalysing the reaction between ethyl diazoacetate (1mmol) and an alkene under test. Styrene was

reacted with ethyl diazoacetate in the presence of 10mmol% Cu-PTA in dichloromethane.

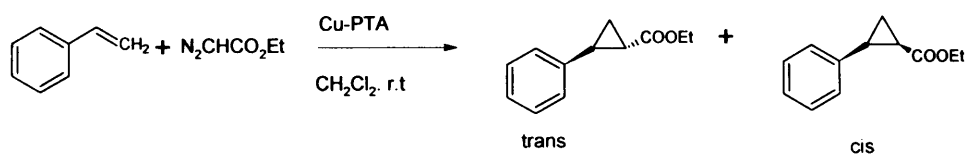


Figure 1.5.6: Styrene cyclopropanation <sup>(59)</sup>

The reaction was complete in 2.5 hours at room temperature and the product, ethyl-2-phenyl-1-cyclopropanecarboxylate was isolated as two isomers (*trans* and *cis*) with a 90% yield. The reaction of cyclohexene with ethyl diazoacetate gave two isomers (endo and exo) of ethyl bicycloheptane-7-carboxylate, with the endo isomer the favoured product. The catalyst was separated by filtration and was reused up to four times with minimal decrease in activity.

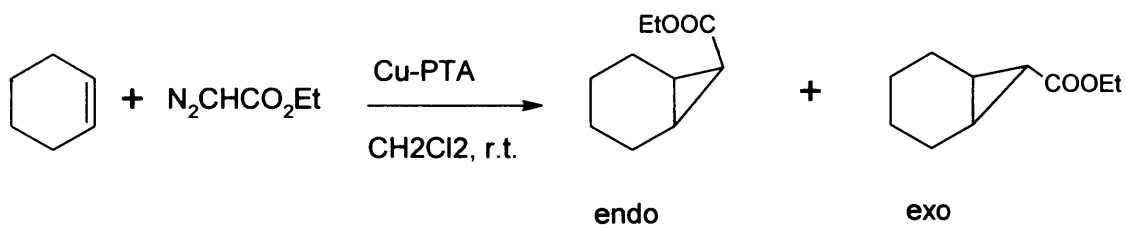


Figure 1.5.7: Cyclopropanation of cyclohexene <sup>(59)</sup>

The esterification of propanoic acid with butanol using carbon supported  $H_3[PW_{12}O_{40}]$  and  $H_4[SiW_{12}O_{40}]$  have been studied<sup>(37)</sup>. The catalysts were prepared by impregnating the supports with an acidified solution of the HPAs. The reaction was carried out with 0.3 mol of propanoic acid and 0.3 mol of butanol with elimination of water by formation of an azeotrope with toluene.

Support	HPA loading	Apparent formula of	Surface areas
---------	-------------	---------------------	---------------

	(wt%)	HPA	(m <sup>2</sup> /g)
Aldrich charcoal	50	H <sub>1.1</sub> [PW <sub>12</sub> O <sub>40</sub> ]	1500
Strem charcoal	31	H <sub>0.6</sub> [PW <sub>12</sub> O <sub>40</sub> ]	1000
Lonza graphite	27	H <sub>1</sub> [PW <sub>12</sub> O <sub>40</sub> ]	310
Vucan-6	27	H <sub>1.4</sub> [PW <sub>12</sub> O <sub>40</sub> ]	115
Vucan-3	14	H <sub>2</sub> [PW <sub>12</sub> O <sub>40</sub> ]	75

Table 1.5.2.8: Apparent formula of HPA on carbon supports <sup>(37)</sup>

The amount of acid was  $5.0 \times 10^{-4}$  mol. The unsupported H<sub>4</sub>[SiW<sub>12</sub>O<sub>40</sub>] had slightly higher activity than the unsupported H<sub>3</sub>[PW<sub>12</sub>O<sub>40</sub>] catalyst, converting >90% of the propanoic acid in 175 minutes compared to 85% conversion for the H<sub>3</sub>[PW<sub>12</sub>O<sub>40</sub>]. This can be explained by the H<sub>4</sub>[SiW<sub>12</sub>O<sub>40</sub>] HPA having more proton sites than H<sub>3</sub>[PW<sub>12</sub>O<sub>40</sub>] and showing that the acid strength of the weaker acid is sufficient enough to catalyse the esterification. The initial reaction rates were calculated to be  $4.8 \times 10^{-3}$  mol min<sup>-1</sup> for H<sub>3</sub>[PW<sub>12</sub>O<sub>40</sub>] and  $6.5 \times 10^{-3}$  mol min<sup>-1</sup> for H<sub>4</sub>[SiW<sub>12</sub>O<sub>40</sub>] which is proportional to the number of protons in the HPA.

For the carbon supported HPAs the highest loading were used on various carbons. Two active charcoals, one from Aldrich and one from Strem Chemicals, Lonza graphite, two carbon blacks, Vulcan-3 Cabot and Vulcan-6 Cabot. The Aldrich charcoal was the most active with 66% conversion but its loading was 50% compared to the other supports. The activity for the supported HPAs is related to how many catalytically active protons there are in the solid. This was calculated as the mean number of active protons per Keggin unit. The carbon supported HPAs were all less active than the unsupported HPAs. The charcoal supported HPA is more active than the other carbon supports as the surface of the charcoal is not uniform, but covered

with different functional groups from the process of making charcoal from the pyrolysis of wood. These functional groups are able to help anchor the HPA to the carbon support.

The carbon supported HPAs are active catalysts for the esterification of propanoic acid with butanol or 2-ethyl hexanol but the activity per Keggin unit is lower than that of the unsupported HPA. The best results with carbon supported HPAs were with supports, which had a low surface area with the HPA loading as high as possible. The high surface area supports encapsulated the HPAs, which led to a neutralisation of charge. On the low surface area supports there is a slight repulsion of charge that inhibits such encapsulation.

The esterification of acetic acid with butanol (*n*-butanol, *sec*-butanol and *ter*-butanol) catalysed by different HPAs supported on activated clay has been investigated<sup>(50)</sup>. The major product was butyl acetate with selectivity of around 100%, the conversion depended on the HPA and the alcohol used in the reaction. The different HPAs used were phosphotungstic acid, phosphomolybdic acid and silicotungstic acid with loadings of 10, 20 and 30% by incipient wetness impregnation. The highest conversions were made by the PTA catalysts, followed by STA, followed by PMA. The conversions with the supported PTA increased with loading from 10 to 20% but decreased after the loading is increased to 30%. It was noted that the activity of the free HPA was significantly lower when compared to the clay supported HPA under the same reaction conditions. The higher activity was attributed to a high dispersion of the HPA on the clay support, enabling a higher surface area and more active sites when compared to free HPA.

The esterification of mandelic acid with methanol was investigated with silica supported PTA with different weight percent of PTA to silica at room temperature<sup>(57)</sup>.

Weight percentages of PTA to silica were 20%, 40% and 60% and it was found that the reaction was more efficient at a loading of 40 wt% since no increase in yield or time were observed when using loadings higher than 40 wt%. Upon using different alcohols in the esterification of mandelic acid (ethanol, 1-butanol, 1-heptanol and 1-octanol) it was found that no side products were found during these reactions.

The vapour phase dehydration of isopropanol has been studied with  $H_3[PW_{12}O_{40}]$  supported on alumina and titania at  $180^\circ C^{(27)}$ . It was found that the isopropanol does not react with the supports and decomposes to propene with the HPA present on the supports. The solid  $H_3[PW_{12}O_{40}]$  had a surface area of  $2m^2/g$ , but on the supports the acid becomes highly dispersed and increases the catalytically active surface. The acidity order for the different catalysts studied in this reaction were  $TiO_2=SiO_2 > \text{carbon} > \text{acidic alumina} > \text{basic alumina}$ . The acidity of  $H_3[PW_{12}O_{40}]$  on both types of alumina is similar to that of the solid  $H_3[PW_{12}O_{40}]$ . The interaction between the support and HPA determines if the ion will be degraded or not. The acidic alumina contains the  $[PW_{12}O_{40}]^{3-}$  anion and dimeric heteropoly anions and the basic alumina causes the HPA anion to form tungstodiphosphate ( $[P_2W_{21}O_{71}]^{6-}$ ) and the lacunar species  $[PW_{11}O_{39}]^{7-}$  on the support.

The  $H_3[PW_{12}O_{40}]$  acid remains intact on the surface of titania and is more active in the dehydration reaction than the bulk  $H_3[PW_{12}O_{40}]$  while the acidic alumina had similar acidity to the bulk  $H_3[PW_{12}O_{40}]$  and the basic alumina had lower acidity than the bulk  $H_3[PW_{12}O_{40}]$ .

<b>Catalyst</b>	<b>Isopropanol Conversion (%)</b>	<b>Concentration (g W/100g)</b>	<b>Specific conversion(1/mgW)</b>
Bulk $H_3[PW_{12}O_{40}]$	40	70.43	0.113
HPA/ $TiO_2$	30.4	16.13	0.377

HPA/Al <sub>2</sub> O <sub>3</sub> (acidic)	14.2	25.31	0.112
HPA/Al <sub>2</sub> O <sub>3</sub> (basic)	4.3	22.31	0.038

**Table 1.5.2.9: Isopropanol specific conversion <sup>(28)</sup> Conditions: Atmospheric pressure, 180°C, time: 4 hours, catalyst mass: 0.5g Isopropanol/helium volumetric ratio:  $9.8 \times 10^{-3}$**

The synthesis of fructose using Cs salts of PTA supported on alumina has been reported<sup>(55)</sup>. In the liquid phase reactions of ethyl acetoacetate with ethylene glycol to synthesise fructose, alumina supported Cs<sub>2.5</sub>H<sub>0.5</sub>PW<sub>12</sub>O<sub>40</sub> (30% wt) was highly stable and water tolerant catalyst. Conversion of ethyl acetoacetate was 98.7% and selectivity to fructose was over 97%. The catalyst could be reused without regeneration for up to five reactions.

The dehydration of isopropanol with PTA, CsPTA and 15% PTA on various supports (SiO<sub>2</sub>, TiO<sub>2</sub>, Nb<sub>2</sub>O<sub>5</sub> and ZrO<sub>2</sub>.) In these experiments, propene was the major product with all the catalysts used<sup>(48)</sup>. The activity of the supported catalysts decreases with increasing calcination temperature from 300°C to 500°C in correlation with catalysts acid strength. This is due to the loss of proton sites due to dehydration of the catalysts and a decrease in surface area.

PTA supported on niobia has been used to catalyse the esterification of palmitic acid or sunflower fatty acid with methanol<sup>(54)</sup>. The loadings on the niobia of the PTA were at 25% wt% to be the most active in the esterification of the fatty acids with methanol. The esterification of the fatty acids depends on the acid strength of the catalysts. The calcination temperature influenced the activity of the catalyst, as calcination temperatures over 400°C. Upon calcination over 400°C, the Keggin anion begins to decompose. XRD patterns indicate that the Keggin anions were decomposing to WO<sub>3</sub> at these higher temperatures. The activity of the catalysts increased with temperature, at a temperature of 35°C the conversion for palmitic acid

reached a near constant conversion of 28% after three hours with little increase after four hours. The conversion of sunflower fatty acid reached 18.9% conversion at 35°C after two hours, after four hours the conversion reached 22.5%. Upon increasing the temperature to 65°C the conversion for palmitic acid reached 99.1% after four hours and the conversion of sunflower fatty acid reached 97.3% after four hours.

Supported Cs salts of HPAs have been used in biphasic reactions. In the conversion of D-xylose to furfural, Cs salts of PTA impregnated in silica have been used in a water-toluene mix<sup>(47)</sup>. The xylose conversion takes place primarily in the aqueous phase, the product furfural has a higher affinity for toluene and is separated as it is formed. This leads to higher conversions than as if water alone was used as a reaction medium. Higher catalytic activity is observed for supported CsHPA with a loading of 15% (w/w) and is attributed to the higher number of effective acid sites when compared to supported CsHPA with a loading of 34% and may be due to the greater dispersion on the silica. Apparent pore blocking is less severe with the lower loading CsHPA that would also extend the catalysis lifetime.

The doping of HPAs with platinum group metals enhances the regeneration when used in propene oligomerisation<sup>(49)</sup>. 20% PTA on silica was coked by propene in a fixed bed reactor at 200°C. When no Pd is present, the coke burns at approximately 500°C, with the Pd doped PTA at levels of 1.6, 2.0 and 2.5% the coke burns at approximately 375, 350 and 340°C respectively. The higher the Pd loading, the lower the combustion temperature of the coke, this enables the regeneration of the Pd doped PTA to be conducted at temperatures well below the decomposition temperature of PTA. The Pd doping affects the type of coking on the catalyst, undoped PTA has both aliphatic and polyaromatic coke deposits. Upon doping with

Pd, only aliphatic coke is deposited with combusts more readily than polyaromatic coke.

The catalytic lifetime of HPAs can be extended in supercritical fluids<sup>(56)</sup>. HPAs could be regenerated by extracting the carbonaceous deposits from the catalyst surface by supercritical fluids. The isomerisation of *n*-butane under supercritical conditions using PTA and STA supported on titania (20% wt) at 260°C and 110 bar, supported on sulphated zirconia at 215°C and 61 bar and H-mordenite at 300°C and 138 bar as catalysts. During gas phase isomerisation (non-supercritical isomerisation) the catalysts deactivated due to coking. Under supercritical conditions, the catalyst activity was stable for over five hours when using titania supported HPAs. The catalysts coked in the gas phase reactions could be regenerated in supercritical *n*-butane to achieve activity close to their original unused state.

In conclusion, HPAs in heterogeneous catalysis can be used in a wide range of reactions, isomerisation, dehydration, hydrolysis, alkylations, esterifications and etherifications. They are easily supported on many different supports without losing their primary Keggin structure at high loadings (up to 50%), but do suffer from deactivation and loss of active HPA to polar liquids. The leaching of active sites by polar solvents can be decreased by increasing the loading of the HPA to include the HPA in the bulk of the supports, rather than on the surface. In experiments where the solvents are non-polar, little leaching is observed with supported HPAs and the catalysts can be reused many times.

The deactivation by coking can be partially solved by calcining the catalysts and can be further enhanced by doping the catalysts with platinum group metals, in particular, platinum at doping level of 2.5% as this promotes aliphatic carbon deposits, which are burned off at a lower temperature than polyaromatic carbon



deposits, crucially below the temperature that HPAs decompose (450°C for PTA). Caesium salts of HPAs are water insoluble and can also be supported on many different solid supports. The substitution of one or more of the acidic protons with caesium results in a water insoluble HPA can increase the thermal stability of the Keggin anion, but at the expense of acidity as the most acidic protons are substituted preferentially.

### 1.6 Conclusions

HPAs can be used as supported acids for a number of acid catalysed reactions. The activity of the catalysts depends on the nature of the support, the acidity of the HPA, and the loading of the HPA on the support. HPAs can be supported on a wide range of inert or acidic supports, but basic supports will deactivate the active Keggin structure. Too high loading and interactions with the support and the acidic properties of the HPA are lost through transformation of the HPA structure to less catalytically active ones. The most acidic HPAs contain tungsten as the heteroatom and are commonly used to demonstrate the superacidic nature of HPAs, as molybdenum containing HPAs are less active when compared to the tungsten containing HPAs. Molybdenum containing HPAs while less active do provide different selectivities to products as the tungsten HPAs can often catalyse intermediate products to give the kinetic products of a reaction. Molybdenum HPAs are often reduced during reactions. Supported HPAs are easily recovered from the reactions and are reusable with lowered activity unlike traditional acid catalysts (e.g.  $\text{AlCl}_3$ ). Caesium salts, while water tolerant, can form unrecoverable colloidal suspensions under a large excess of water. Caesium salts supported in the channels of MCM-41 show high reusability and minimal leaching when washed with methanol. HPAs are tuneable catalysts with the acidity being controlled by the introduction of metal ions to form salts thereby

changing the number of protons the HPA has, by changing the heteroatom from P to Si and by changing the metal in the polyanion cage (W or Mo). Further substitution of other metal atoms in the framework can alter the acidic properties.

## References

1. K. Tanabea, W. F. Hoelderich, *Applied Catalysis A: General* 181 (1999) 399-434
2. E. Inglesia, S. L. Soled, G. M. Kramer, *Journal of Catalysis* 144 (1993) 238-253
3. T. K. Cheung, F.C. Lange, B. C. Gates, *Journal of Catalysis* 159 (1996) 99-106
4. V. B. Kazansky, *Catalysis Today*, 51 (1999) 419-434
5. A. Sassi, J. Sommer, *Applied Catalysis A: General* 199 (1999) 155-162
6. J. Bandiera, M. Dufaux, Y. B. Taârit, *Applied Catalysis A: General* 148 (1997) 283-300
7. S. van Donk, J. H. Bitter, K. P. de Jong, *Applied Catalysis A: General* 212 (2001) 97-116
8. L.H. Nguyen, T. Vazhnova, S. T. Kolaczkowski, D. B. Lukyanov, *Chemical Engineering Science* 61 (2006) 5881-5894
9. J. H. Clark, *Pure Applied Chemistry* 70 (2001) 103-111
10. U. B. Mioc, M. R. Davidovic, Ph. Colomban, I. Holclajtner-Antunovic, *Solid State Ionics*, 176 (2005) 3005-3017
11. I. V. Kozhevnikov, *Chemical Reviews* 98 (1998) 171-198
12. N. Ohler, *Chem. Eng. 245: Catalysis*, (2002)
13. W. Zuoping, G. Shuang, X. Lin, S. Enhong, W. Enbo, *Polyhedron* 15 (1996) 1383-1388
14. A. Bielanski, A. Lubanska, J. Pozniczek, A. Micek-Ilnicka *Applied Catalysis A: General* 256 (2003) 153-171

15. G. Li, Y. Ding, J. Wang, X. Wang, J. Suo, *Journal of Molecular Catalysis A: Chemical* 262 (2007) 67–76
16. F. Cavani, *Catalysis Today* 41 (1998) 73-86
17. I.V. Kozhevnikov *Applied Catalysis A: General* 256 (2003) 3–18
18. M.N. Timofeeva, *Applied Catalysis A: General* 256 (2003) 19-35
19. J.F. Liu, P.G Yi, Y.S.Qi, *Journal of Molecular Catalysis A: Chemical* 170 (2001) 109-115
20. B. Török, I. Bucsi, T. Beregszászi, I. Kapocsi Á. Molnár *Journal of Molecular Catalysis A: Chemical* 107 (1996) 305-311
21. L. Li, Y. Kamiya, T. Okuhara *Applied Catalysis A: General* 253 (2003) 29-32
22. A. Molnar, T. Beregszaszi, *Tetrahedron Letters*, Vol. 37, No. 47. (1997) 8597-8600
23. Y. Izumi, K. Iida, K. Usami, T. Nagata, *Applied Catalysis A: General* 256 (2003) 199-202
24. Y. Zhang, Z. Du, E. Min, *Catalysis Today* 93-95 (2004) 327-332
25. T. Okuhara, *Catalysis Today* 73 (2002) 167-176
26. W. Kuang, A. Rives, M. Fournier, R. Hubaut, *Applied Catalysis A: General* 250 (2003) 221-229
27. Á. Kukovecz, Zs. Balogi, Z. Kónya, M. Toba, P. Lentz, S. -I. Niwa, F. Mizukami, Á. Molnár, J. B. Nagy, I. Kiricsi, *Applied Catalysis A: General* 228 (2002) 83-94
28. L. R. Pizzio, C. V. Cáceres, M. N. Blanco, *Applied Catalysis A: General* 167 (1998) 283-294
29. P. Vázquez, L. Pizzio, C. Cáceres, M. Blanco, H. Thomas, E. Alesso, L. Finkielstein, B. Lantaño, G. Moltrasio, J. Aguirre, *Journal of Molecular Catalysis A: Chemical* 161 (2000) 223-232

30. Á. Molnár, C. Keresszegi, B. Török, *Applied Catalysis A: General* 189 (1999) 217-224
31. M. J. Verhoef, P. J. Kooyman, J. A. Peters, H. van Bekkum, *Microporous and Mesoporous Materials* 27 (1999) 365-371
32. K. Nowinska, W. Kaleta, *Applied Catalysis A: General* 203 (2000) 91-100
33. F. Marme, G. Coudurier, J. C. Védrine, *Microporous and Mesoporous* 22 (1998) 151-163
34. T. Blasco, A. Corma, A. Martínez, P. Martínez-Escolano, *Journal of Catalysis* 177 (1998) 306-313
35. I. V. Kozhevnikov, K. R. Kloetstra, A. Sinnema, H. W. Zandbergen, H. van Bekkum, *Journal of Molecular Catalysis A: Chemical* 114, (1996) 287-298
36. A. Bielanski, A. Lubańska, J. Poźniczek, A. Micek-Ilnicka, *Applied Catalysis A: General* 238 (2003) 239-250
37. P. Dupont, F. Lefebvre, *Journal of Molecular Catalysis A: Chemical* 114, (1996) 299-307
38. A. Lapkin, B. Bozkaya, T. Mays, L. Borello, K. Edler, B. Crittenden, *Catalysis Today* 81 (2003) 611-621
39. E. Lopez-Salinas, J. G. Hernández-Cortéz, I. Schifter, E. Torres-García, J. Navarrete, A. Gutiérrez-Carrillo, T. López, P. P. Lottici, D. Bersani, *Applied Catalysis A: General* 193 (2000) 215-225
40. A. V. Ivanov, T. V. Vasina, V. D. Nissenbaum, L. M. Kustov, M. N. Timofeeva, J. I. Houzvicka, *Applied Catalysis A: General* 259 (2004) 65-72
41. G. D. Yadav, N. S. Doshi, *Journal of Molecular Catalysis A: Chemical* 194, (2003) 195-209

42. B.M. Devassy, G.V. Shanbhag, F. Lefebvre, W. Böhringer, J. Fletcher, S.B. Halligudi, *Journal of Molecular Catalysis A: Chemical* 230 (2005) 113-119
43. A. Molnar, T. Beregszászi, Á. Fudala, P. Lentz, J. B. Nagy, Z. Kónya, I. Kiricsi, *Journal of Catalysis* 202 (2001) 379-386
44. Lj. Damjanovic, V. Rakić, U.B. Mioč, A. Auroux, *Thermochimica Acta* 434 (2005) 81-87
45. L. Marosi, C. O. Arean, *Journal of Catalysis* 213 (2003) 235-240
46. S. S. Lim, G. I. Park, J. S. Choi, I. K. Song, W. Y. Lee, *Catalysis Today* 74 (2002) 299-307
47. A. S. Dias, S. Lima, M. Pillinger, A. A. Valente, *Carbohydrate Research* 341 (2006) 2946-2953
48. A. M. Alsalme, P. V. Wiper, Y. Z. Khimyak, E. F. Kozhevnikova, I. V. Kozhevnikov, *Journal of Catalysis* 276 (2010) 181-189
49. I. V Kozhevnikov *Journal of Molecular Catalysis A: Chemical* 305 (2009) 104-111
50. S.K. Bhorodwaj, D. K. Dutta, *Applied Clay Science* 378 (2011) 221-226
51. K. A. S. Rocha, P. A. Robles-Dutenhefner, I. V. Kozhevnikov, E. V. Gusevskay, *Journal of Catalysis A: General* 352 (2009) 188-192
52. Y. Liu, B. Xu, Z. Li, L. Jia, W. Guo, *Journal of Molecular Catalysis A: Chemical* 297 (2009) 86-92
53. A. Alhanash, E. F. Kozhevnikova, I. V. Kozhevnikov, *Applied Catalysis A: General* 378 (2010) 11-18
54. K. Srilatha, N. Lingaiah, B. L. A. Prabhavathi, R. B. N. Prasad, S. Venkateswar, P. S. Sai Prasad, *Applied Catalysis A: General* 365 (2009) 28-33

55. F. Zhang, C. Yuan, J. Wang, Y. Kong, H. Zhu, C. Wang, *Journal of Molecular Catalysis A: Chemical* 247 (2006) 130-137
56. I. V. Kozhevnikov *Journal of Molecular Catalysis A: Chemical* 262 (2007) 86-92
57. E. Rafiee, M. Joshaghani, F. Tork, A. Fakhri, S. Eavani *Journal of Molecular Catalysis A: Chemical* 283 (2008) 1-4
58. V. V. Costa, K. A. S. Rocha, I. V. Kozhevnikov, E. V. Gusevskaya *Applied Catalysis A: General* 383 (2010) 217-220
59. J. S. Yadav, B. V. Subba Reddy, K. V. Purnima, K. Nagaiah, N. Lingaiah *Journal of Molecular Catalysis A: Chemical* 285 (2008) 36-40
60. A. Alsalme, E. F. Kozhevnikova, I. V. Kozhevnikov *Applied Catalysis A: General* (2010) 219-224
61. J. F. Liu, Y. Liu, P. G. Yi *Applied Catalysis A: General* 277 (2004) 167-171

# Chapter Two: Experimental

## 2.1 Synthesis of catalysts

### 2.1.1 Synthesis of Keggin heteropoly acids

Phosphotungstic and phosphomolybdic Keggin type heteropoly acids were synthesised using the etherate method as described in the literature. <sup>(1,2)</sup> HPAs are highly soluble in diethyl ether and can be used to extract them from strongly acidified aqueous solutions.

### 2.1.2 Synthesis of H<sub>3</sub>PW<sub>12</sub>O<sub>40</sub> (PTA)

Sodium tungstate dihydrate (Na<sub>2</sub>WO<sub>4</sub>·2H<sub>2</sub>O, ≥99%, Aldrich, 25g, 0.076 moles) was dissolved in water. Phosphoric acid (H<sub>3</sub>PO<sub>4</sub>, 85%, 8.5g, 0.074 moles) was dissolved in water (distilled, 10ml) to make an 85% H<sub>3</sub>PO<sub>4</sub> solution. 2.5ml of the H<sub>3</sub>PO<sub>4</sub> solution was added to the sodium tungstate solution. Concentrated HCl (20ml) was added to the mixture. The solution was stirred overnight at room temperature. A white precipitate was found in the flask and was collected. The HPA in the acidified solution was extracted by adding diethyl ether and extracting the lowest of three layers after vigorous shaking. The acid was dried on a rotary evaporator until a white powder was collected.

### 2.1.3 Synthesis of H<sub>3</sub>PMo<sub>12</sub>O<sub>40</sub> (PMA)

Sodium molybdate dihydrate (Na<sub>2</sub>MoO<sub>4</sub>·2H<sub>2</sub>O ≥99%, Aldrich, 18.3g, 0.076 moles) was dissolved in water (distilled, 45ml). H<sub>3</sub>PO<sub>4</sub> (H<sub>3</sub>PO<sub>4</sub>, 85%, 8.5g, 0.074 moles) was dissolved in water (distilled, 10ml). 2.5ml of the H<sub>3</sub>PO<sub>4</sub> solution was added to the sodium molybdate solution. Concentrated HCl (20ml) was added to the

conical flask. The solution was stirred overnight at room temperature. A dark green precipitate was found in the flask and was collected. The HPA in the acidified solution was extracted by adding diethyl ether and extracting the lowest of three layers after vigorous shaking. The acid was dried on a rotary evaporator until a green powder was collected.

#### 2.1.4 Preparation of Supported STA

$\text{H}_3\text{SiW}_{12}\text{O}_{40}$  supplied by Johnson Matthey (STA) on silica powder was made by saturating the support with a solution of silicotungstic acid (26% w/w) for two hours followed by filtering of the support. The support was divided into two batches, one batch was dried in a conventional oven and the other batch was dried in a fluidised bed drier. Base treated alumina (200g) and alumina beads (200g) were saturated with STA (26% w/w) solution for two hours and dried in a conventional oven. Carbon-coated silica (100g) and carbon-coated alumina (100g) were saturated with STA solution (26% w/w) and dried in a conventional oven. All supports were supplied by Johnson Matthey.

#### 2.1.5 Synthesis of Keggin salts

Caesium salts of silicotungstic acid were prepared by ion exchange <sup>(3)</sup>. To synthesise CsSTA, Silicotungstic acid ( $\text{H}_4\text{SiW}_{12}\text{O}_{40}$ , Aldrich, 6.22g, 0.019 moles, 99%) was dissolved in a minimum of water (distilled) while under stirring. To this solution, caesium nitrate ( $\text{CsNO}_3$ , Aldrich,  $\geq 99\%$ , 0.42g, 0.002 moles) dissolved in water (distilled, 10ml) was added drop wise. Upon addition of the  $\text{CsNO}_3$ , a white precipitate is formed. The water was evaporated off until the precipitate was a fine white paste. The precipitate was dried in an oven and then calcined ( $200^\circ\text{C}$ , two



hours, under helium). To synthesise caesium salts with a greater number of caesium cations, the weight of the caesium nitrate was calculated to achieve the required molar ratio.

### **2.1.6 Silica supported caesium salts of STA**

Silica supported CsSTA were prepared by precipitating the Cs salt in a silica slurry. Silica supplied by Johnson Matthey (surface area: 317m<sup>2</sup>/g) was used as the support. To this slurry, the free HPA was added to dissolve before adding the caesium salt solution. Upon addition of the caesium nitrate solution a white precipitate was observed. After the caesium nitrate was added, the solutions were left to evaporate to a paste and then calcined at 200°C under helium for two hours. The loading amount was kept at 16.6wt%. As an example:  $(\text{g HPA} / (\text{g silica} + \text{g HPA})) \times 100 = 16.6$

## **2.2 Experimental Catalyst Testing Apparatus**

### **2.2.1 Catalyst synthesis and liquid phase apparatus**

A hot plate stirrer, equipped with a fuzzy logic temperature controller, was used with an oil bath for heating and stirring the solutions. Chemicals and inert supports were mixed in a two-necked round-bottomed flask with a magnetic stirrer. A condenser was used when reflux was required. A rubber septum was used to facilitate samples for analysis.

### **2.2.2 Vapour Phase Apparatus**

The vapour phase reactions of the dehydration of 1,4-butanediol (BTD), isopropanol and isobutanol were performed in a conventional fixed bed micro reactor.

The apparatus for the reaction is shown in the scheme below:

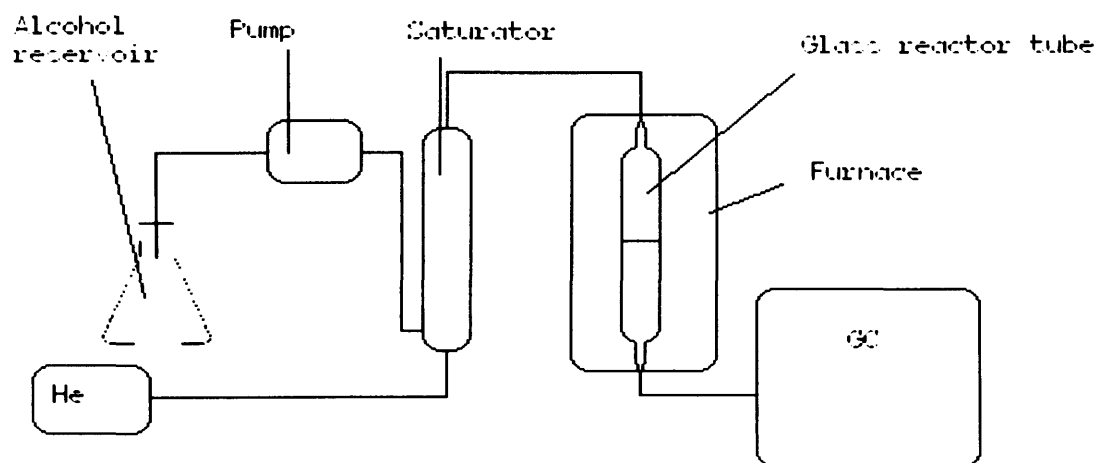


**Figure 2.2.2.1 Schematic diagram of gas phase apparatus**

The reactor was constructed from a 15cm long, fused silica tube with an internal diameter of 12mm, fitted half-length with a porous frit to hold the catalyst in place. The fused silica tube is held in place with Cajun Ultra-Torr joints to facilitate removal. The catalyst was placed vertically in a Carbolite furnace. Reaction temperature was measured using a thermocouple placed in the silica reactor, just above the catalyst bed. The reactor was operated at atmospheric pressure. The reactant was pumped into the heating oven by a peristaltic pump at a flow rate of 0.019ml/hour and mixed with the He carrier gas. The carrier gas and the alcohol enter the heated saturator, where the alcohol is swept up by the carrier gas.

The reactor inlet and outlet lines were heated with heating tape to prevent condensation of reactants and products. A Brooks Instruments SMART mass flow controller, calibrated for a flow rate of 0-100ml/min, controlled by a Brooks Instrument control box regulated the helium flow rate which varied depending on the reaction. The reaction products were measured on a Varian 3400 Gas Chromatograph (GC) fitted with a six-foot tubular column coated with 10% sp-2100 on 100/120 supelcoport. The detector used on the GC was an FID

### 2.2.3 Gas chromatography analysis set up

The GC analysis system was provided by a Varian 3400 CG and Varian Star software. The column was chosen to separate out polar compounds (BTD, tetrahydrofuran, isopropanol and isobutanol). Helium was used as a carrier gas for the GC. The reactants and products were introduced to the GC by a 6-port valve driven pneumatically and controlled by the GC timed event program. Figure 2 shows the sampling valve in the filling position, where the sample flows through the sample loop and is vented, while the carrier gas flows directly to the column. When the valve is switched to the injection position, the helium carrier gas sweeps the sample onto the column. The detector output was recorded on a PC and the data processed by Varian Star software to allow the peak area to be quantified.

#### Flame ionisation detector

The flame ionisation detector (FID) was an ion detector, which burns compounds in a hydrogen/air flame to produce ions. The hydrogen introduced into the carrier gas from the column is burned in air to produce a noise free flame. When an organic compound is burnt in the detector, the ions migrate to the collector electrode under the influence of a polarising field applied to the jet of the detector. The charge generated by the ions is proportional to the concentration of analyte present. The current generated is amplified and plotted on screen as a chromatogram.

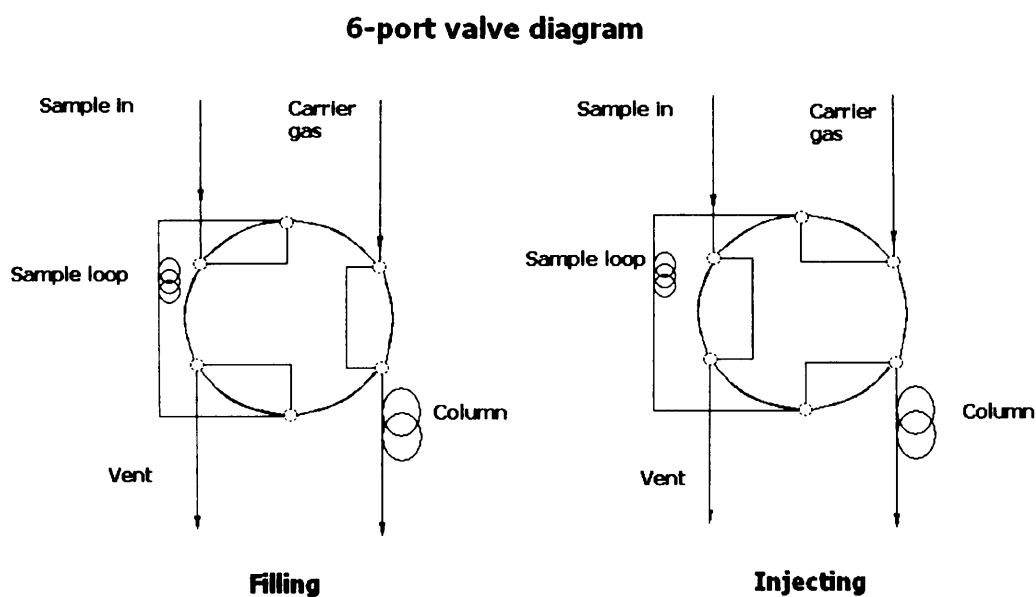


Figure 2.2.3.1 Diagram of 6-port valve showing filling and injecting positions

## 2.2.4 Autoclave reactor set up

The autoclave used was a Baskerville single vessel autoclave fitted with a glass insert with an internal volume of 100ml. Mixing of the reactants was done by an overhead impeller. Heating was provided by a Baskerville control unit connected to a heating jacket.

## 2.3 Catalyst Characterisation Techniques

### 2.3.1 B.E.T isotherms

Surface area measurements were carried out on a Micromeritics Gemini surface area analyser. A Micromeritics Flow Prep 060 was used to degas the samples (200°C, nitrogen, two hours) before measurement of the adsorption isotherms. During operation, the sample tube and the reference tube are cooled in liquid nitrogen and the adsorptive gas (nitrogen) is dosed into the sample and reference tubes. As the sample

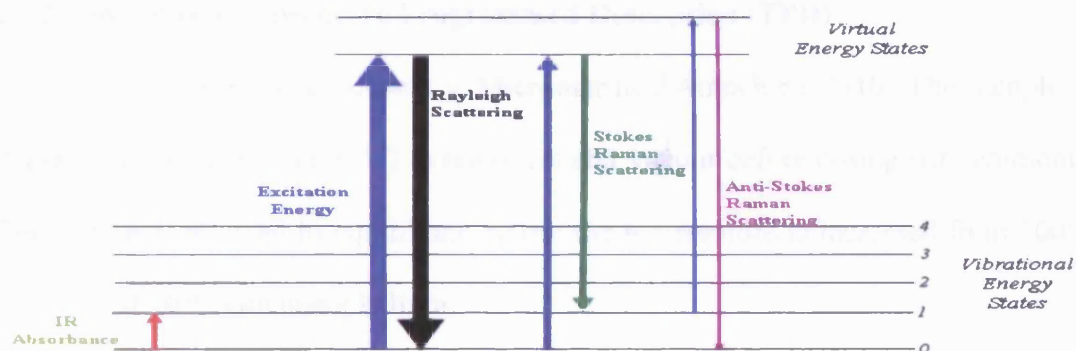
adsorbs the gas, a transducer located between the sample and balance tubes detects any pressure difference between the two tubes and causes a valve to balance the pressures in both tubes. This method of dosing and accounting for the volume of gas uptake enables the surface area to be calculated using the Brunauer, Emmett and Teller (BET) method<sup>(4)</sup>.

### 2.3.2 Raman Spectroscopy

Raman spectra were obtained using a Renishaw Ramascope Spectrograph fitted with a green Ar<sup>+</sup> laser ( $\lambda = 514\text{nm}$ ) operated at 20mW. Samples were analysed in powdered form.

The Raman effect occurs when a symmetric molecule absorbs a quantum of light and this excites the molecule into a higher vibrational energy state. Upon relaxation of the molecule into the first vibration energy state, the molecule will emit a photon that is called Stokes Raman scattering. If the molecule was already at an elevated energy state, the Raman scattering is called Anti-Stokes Raman scattering<sup>(4)</sup>. In practice, monochromatic light is used.

Figure 2.3.2.1: Energy levels in Raman Spectroscopy



### 2.3.3 Powder X-ray Diffraction

Powder X-ray diffraction (XRD) was performed using an Enraf Nonius FR590 X-ray generator with a Cu-K $\alpha$  source fitted with an Inel CPS 120 hemispherical detector. X-rays are generated and are reflected by the powdered sample. The crystallites of the sample are randomly ordered due to the fact they are not a single crystal and under ideal conditions expose every possible orientation while being rotated on the sample holder. When the sample is a powder, a proportion of the crystallites will satisfy the Bragg equation,  $\lambda = 2d \sin \theta$  (where  $\theta$  is the glancing angle,  $\lambda$  is the wavelength of incident radiation and  $d$  is the spacing between the planes in the atomic lattice). Some of the crystallites will be orientated so that their (111) planes give rise to diffracted intensity at their glancing angle  $\theta$ . The X-rays are diffracted by the crystal lattice and lie on a cone around the incident beam of half-angle  $2\theta^{(4)}$ .

### 2.3.4 Thermal Gravimetric Analysis (TGA)

Thermal gravimetric analysis (TGA) was performed using a Perkin Elmer TGA 7 thermogravimetric analyser. The samples were heated from 25°C to 500°C at a rate of 15°C/min.

### **2.3.5 Ammonia Temperature Programmed Desorption (TPD)**

The instrument used was a Micromeritics Autochem 2910. The sample is degassed under helium (100°C) to remove water vapour before dosing with ammonia. The sample is allowed to equilibrate before the temperature is increased from 100°C to 600°C at 10°C/min under helium.

## **2.4 Methods**

### **2.4.1 Liquid Phase Alcohol Dehydration Procedure**

#### **2.4.1.1 1,4-Butanediol Cyclodehydration**

1,4-butanediol (10ml, Aldrich), internal standard (cyclohexene, 1ml, Aldrich) 1,4-dioxane (40ml, Aldrich) and catalyst (0.05g-0.1g) were refluxed for up to five hours. Samples (40µl) were taken at regular intervals (0, 5, 10, 30, 60, 120, 180 and 300 minutes) and analysed by GC.

#### **2.4.1.2 Geraniol Dehydration**

Geraniol (40ml, Aldrich) was heated to the desired reaction temperature 50-90°C) and catalyst (0.05-0.1g) was added. Samples (40µl) were taken at regular intervals, (0, 5, 10, 30, 60, 120, and 180 minutes) diluted and external standard added (n-hexane). The reaction was monitored by GC.

### **2.4.2 Vapour Phase Alcohol Dehydration Procedure**

Catalyst (0.05-0.1g) was loaded into the fused silica reactor and the reactor tube was secured in place with the Cajun Ultra-Torr joints. The flow rate of the helium carrier gas was set to the required rate and the heating tape, heating oven and furnace were set to the operating temperature. Once the temperatures of the heating

tape, heating oven and furnace were stable, the alcohol flow was switched on and the reaction monitored by GC. The first injection was taken after five minutes and the subsequent injections were taken automatically via the GC program, the intervals depended on the reaction being performed.

### 2.4.3 Alcohol calibration and blank tests

To calculate the concentration of alcohol in the vapour phase, the ideal gas laws and Dalton's laws were assumed to hold. Measuring the flow of helium into the saturator leads to a value of  $V$  ( $\text{m}^3$ ). One mole of gas at standard temperature and pressure (s.t.p) occupies  $0.022414 \text{ m}^3$ , therefore, the number of moles of helium is  $V/0.022414$ . Since the number of moles of the alcohol vaporised is mass ( $w$ ) divided by molecular weight of the alcohol ( $M$ ). The helium/alcohol mixture leaves the saturator at a pressure of  $P_s$  with the vapour being at its saturation vapour pressure,  $p_s$ , with the carrier gas making up the balance ( $P_s - p_s$ ). The gas and alcohol must occupy the same volume upon leaving the saturator and their pressures in the mixture must be in the ratio of the number of moles of each.

$$P_g / (P_s - p_s) = (w/M) / V/0.022414$$

By knowing the theoretical vapour pressure,  $p_s$  and the total pressure (atmospheric pressure: 101kPa) it is possible to know the alcohol concentration leaving the saturator. For example, a vapour pressure of 10% Isopropanol in helium would require a vapour pressure of 10kPa, which can be entered into the linear regression equation derived from the CRC Handbook of Chemistry and Physics (78<sup>th</sup> Edition) <sup>(5)</sup>:

$$\ln 10 = -5761.1x + 27.949$$

This gives a temperature of 35°C



### 2.4.4 1,4-butanediol blank tests and calibration

#### Vapour Pressure of 1,4-butanediol

The saturation pressure of 1,4-butanediol was taken from the CRC Handbook of Chemistry and Physics (78<sup>th</sup> Edition) <sup>(5)</sup>. By using a linear regression plot it is possible to calculate desired saturation pressures for 1,4-butanediol.

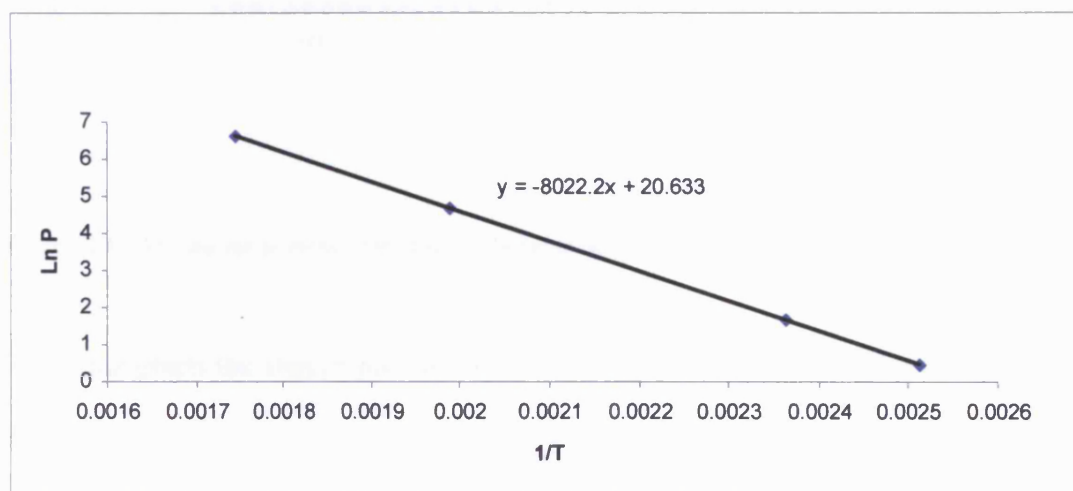


Figure 2.4.4.1 Linear regression plot for 1,4-butanediol

Table 2.4.4.2: 1,4-butanediol vapour pressure against temperature <sup>(5)</sup>.

Temperature (K)	1/T (K <sup>-1</sup> )	Pressure (kPa)	Ln p
398	0.002513	1.61	0.4762
423	0.002364	5.3	1.6677
503	0.001988	108	4.6845
573	0.001745	759	6.6320

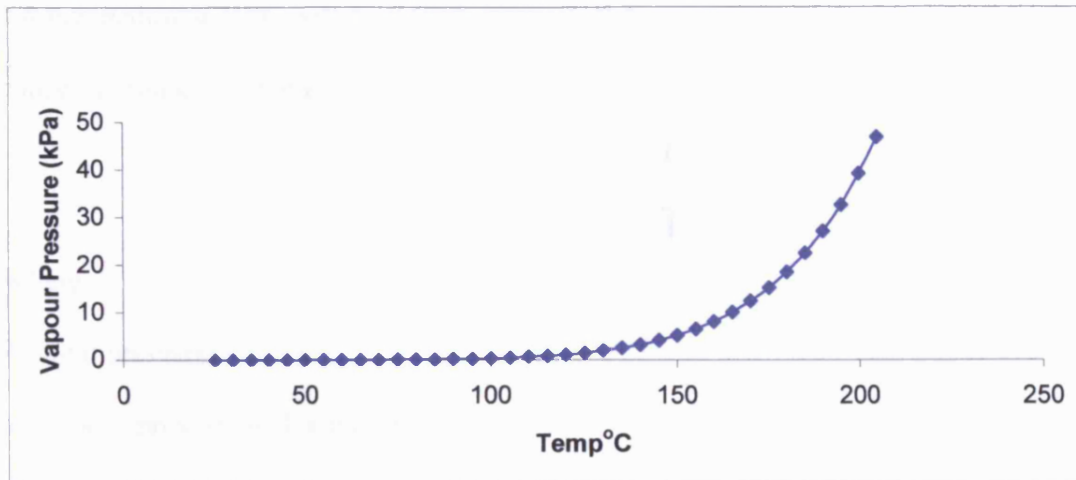


Figure 2.4.4.3: Vapour pressure plot for 1,4-butanediol

From this graph the vapour pressure for the temperature range 25-100°C is shown in table 2.4.4.4

Table 2.4.4.4: Vapour pressure of 1,4-butanediol with temperature CRC Handbook of Chemistry and Physics (78<sup>th</sup> Edition) <sup>(5)</sup>.

Temperature °C	Pressure (kPa)
25	0.001851365
30	0.002887027
35	0.004437566
40	0.006727815
45	0.010067463
50	0.014878071
55	0.021727096
60	0.031370262
65	0.044803835
70	0.063328499
75	0.088626724
80	0.122855668
85	0.168757838
90	0.229791876
95	0.310285987
100	0.41561665

It can be seen that at 60°C the vapour pressure is 0.031 kPa. Under operating conditions the system is at atmospheric pressure, 101 kPa so the concentration of the

1,4-butanediol at 60°C will be 0.03%. This is an over simplification. To calculate the concentration of 1,4-butanediol the following equation is used:

$$\frac{p}{(P - p)} = \frac{(w / RMM)}{(V - 0.022414)}$$

Where:

P= total pressure

p= vapour pressure of 1,4-butanediol

w= weight of 1,4-butanediol

RMM= relative molecular mass of 1,4-butanediol

V= volume of He flowing into the saturator

0.022414= molar volume of gas

Since the carrier gas and 1,4-butanediol occupy the same volume passing out of the saturator, the pressures of each will equal the ratio of moles of each. Knowing the total pressure (atmospheric pressure, 101kPa) and the vapour pressure of 1,4-butanediol it is therefore possible to calculate the 1,4-butanediol concentration exiting the saturator.

For a He flow rate of 30ml/min at a temperature of 60°C, the alcohol concentration is as follows:

$$\frac{P_{\text{sat}}}{P_{\text{tot}} - P_{\text{sat}}} = \frac{0.03}{101 - 0.03}$$

$$0.03 / 101 - 0.03 = 0.0003\%$$

From this equation, the mass vaporised can be calculated, as all the other variables are known.

$$\text{Molar gas flow} = 0.0803 \text{ mole/hour}$$

$$\text{Moles 1,4-butanediol/hour} = 0.0803 \times 0.0003 = 2.49 \times 10^{-5}$$

$$\text{Weight vaporised} = 2.49 \times 10^{-5} \times 90 = 2.2 \times 10^{-3} \text{ g/hour}$$

To estimate the partial pressure for condensation as a function of pore radius the Kelvin equation will be used

$$\ln(p/p^0) = -2\gamma v_l / rRT$$

Where:

$r$  = meniscus radius

$v_l$  = molar volume of liquid

$\gamma$  = surface tension of the liquid

$p$  = vapour pressure in a pore

$p^0$  = atmospheric pressure

The density of 1,4-butanediol is 1.017g/ml therefore the molar volume is  $88.49 \times 10^{-6} \text{ m}^3 \text{ mol}^{-1}$  and the surface tension is  $37.4 \text{ mN m}^{-1}$

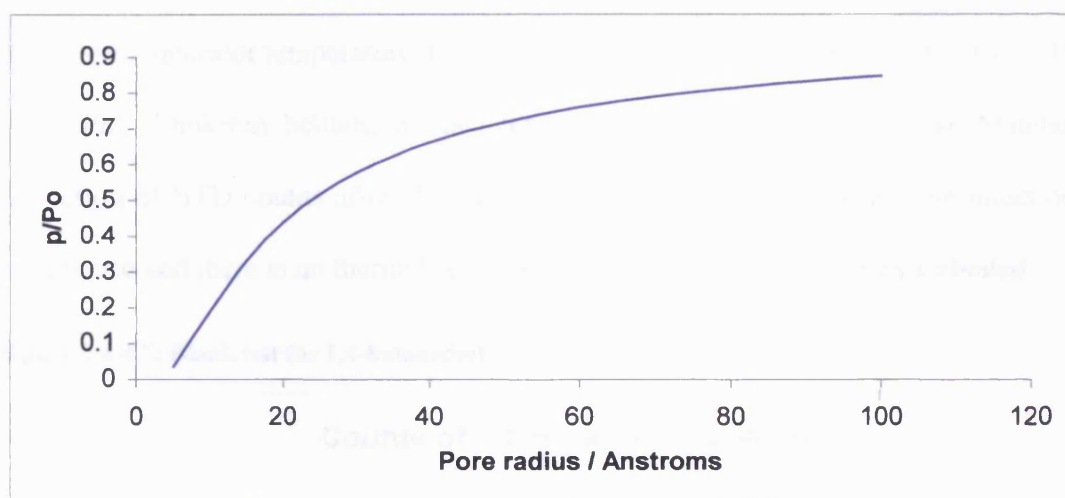
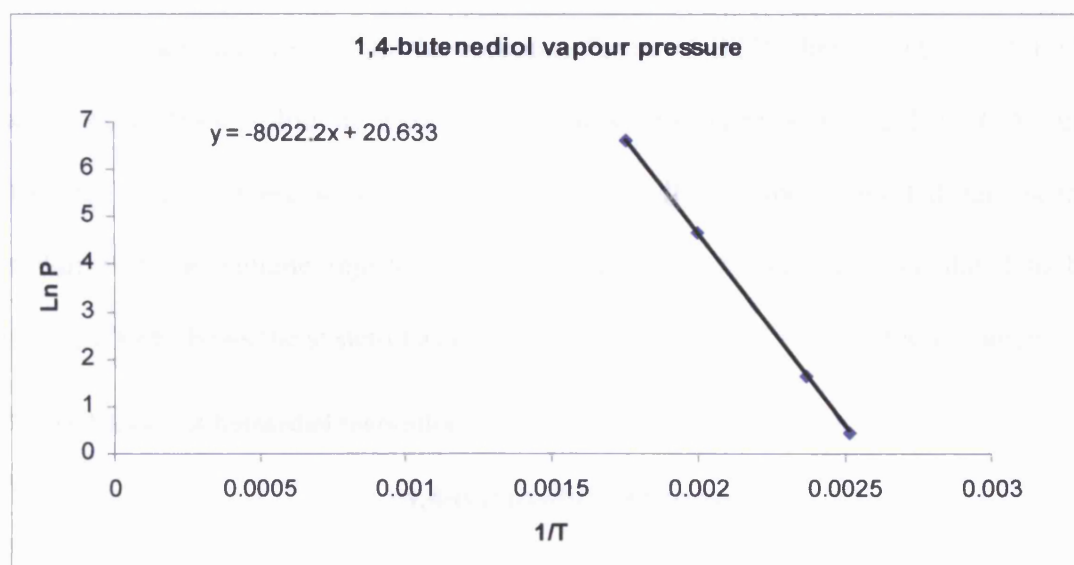


Figure 2.4.4.2: Kelvin equation plot for 1,4-butanediol

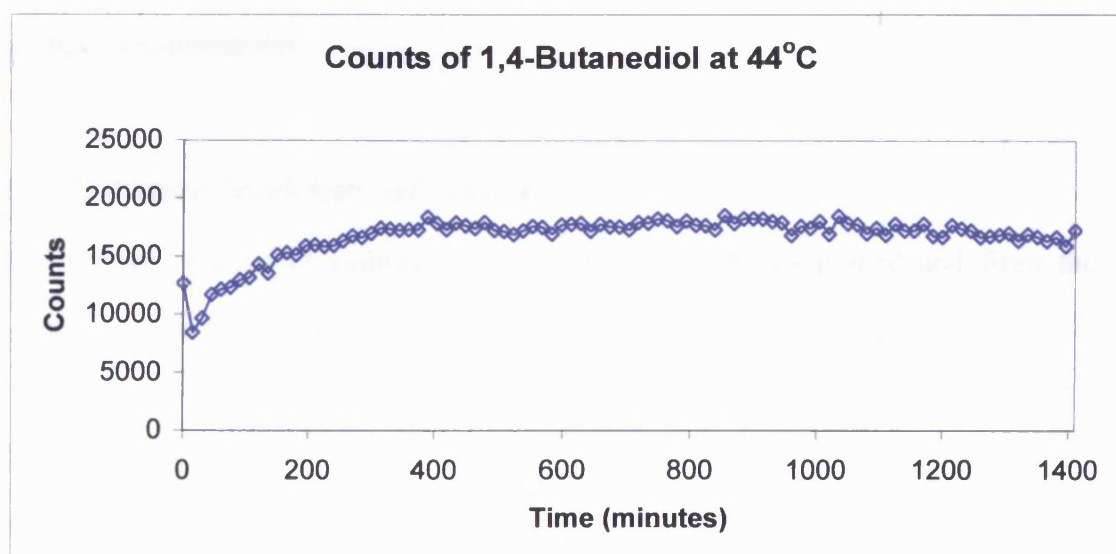
Under reaction conditions of  $p/p^0 = 0.3 \times 10^{-3}$  at  $60^\circ\text{C}$  this is lower than the  $p/p^0$  for a pore size of 5 Angstroms. This shows that the reactions carried out above  $60^\circ\text{C}$  will be happening at the gas/solid interface where the pore size is greater than 5 Angstroms, below this pore size 1,4-butanediol will condense and reactions will take place in the liquid/solid interface instead.

Figure 2.4.4.6: Linear regression plot for 1,4-butanediol



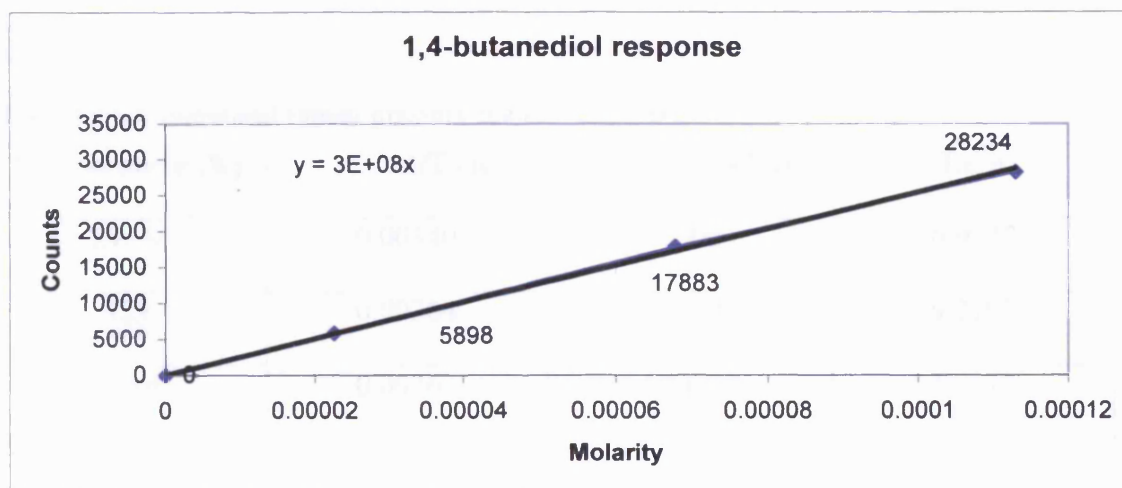
Blank tests were carried out to determine if thermal reactions take place in the reactor tube when no catalyst is present. Experimental conditions used in the blank tests were: Saturator temperature 44°C. The calculated BTD concentration was 0.01% (0.01kPa), 30ml/min helium, furnace temperature of 120°C. % Relative Standard Deviation of BTD counts after 390 minutes was 3% which shows that the injections are precise and there is no thermal reaction once the BTD vapour has equilibrated.

Figure 2.4.4.7: Blank test for 1,4-butanediol



To calibrate the GC to the response factor of BTD, three solutions of BTD were made. These solutions were of the following molarities: 0.022M, 0.067M and 0.113M. 0.5 $\mu$ l of these solutions were injected and the response plotted against the molarity of the volume injected. The correlation coefficient was calculated to be 0.999, which shows the system has a linear response over this concentration range.

Figure 2.4.4.8: 1,4-butanediol calibration

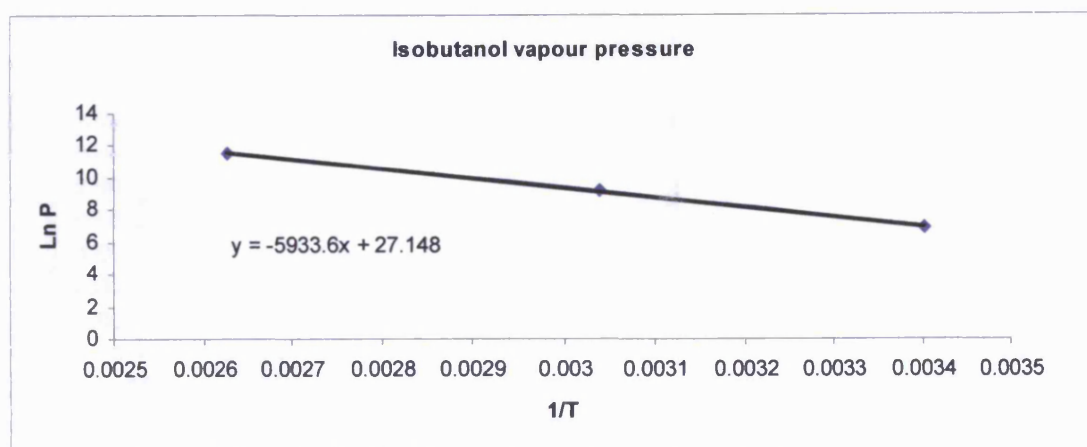


The vapour pressure of isopropanol was plotted against temperature with the resulting graph enabling the concentration of isopropanol in helium to be known over a range of temperatures.

#### 2.4.5 Isobutanol blank tests and calibration

The vapour pressure of isobutanol against temperature was plotted and from the resulting graph the concentration of isobutanol in helium can be known.

Figure 2.4.5.1: Linear regression plot of isobutanol

Table 2.4.5.2: Isobutanol vapour pressure against temperature <sup>(5)</sup>.

Temperature (K)	1/T (K)	Pressure (kPa)	Ln p
293.9	0.00340	1000	6.9077
329	0.00304	10000	9.2103
380.6	0.00262	100000	11.512

Blank reactions with no catalyst in the reactor tube were carried out to determine if there was any thermal reaction. The reaction conditions were: Furnace temperature, 120°C, flow rate of helium 30ml/min and concentration of isobutanol 5.8% (48°C) %RSD of the blank reactions were 2% showing the system is precise and not undergoing any thermal reactions. Due to the higher vapour pressure of isobutanol when compared to 1,4-butanediol at any given temperature, the isobutanol system equilibrates faster under reaction conditions.

Figure 2.4.5.3: Blank test of isobutanol

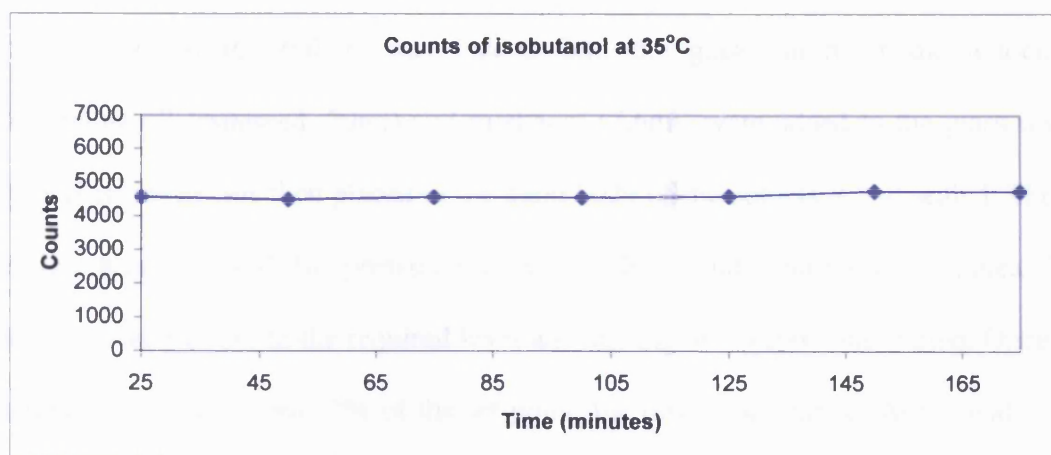
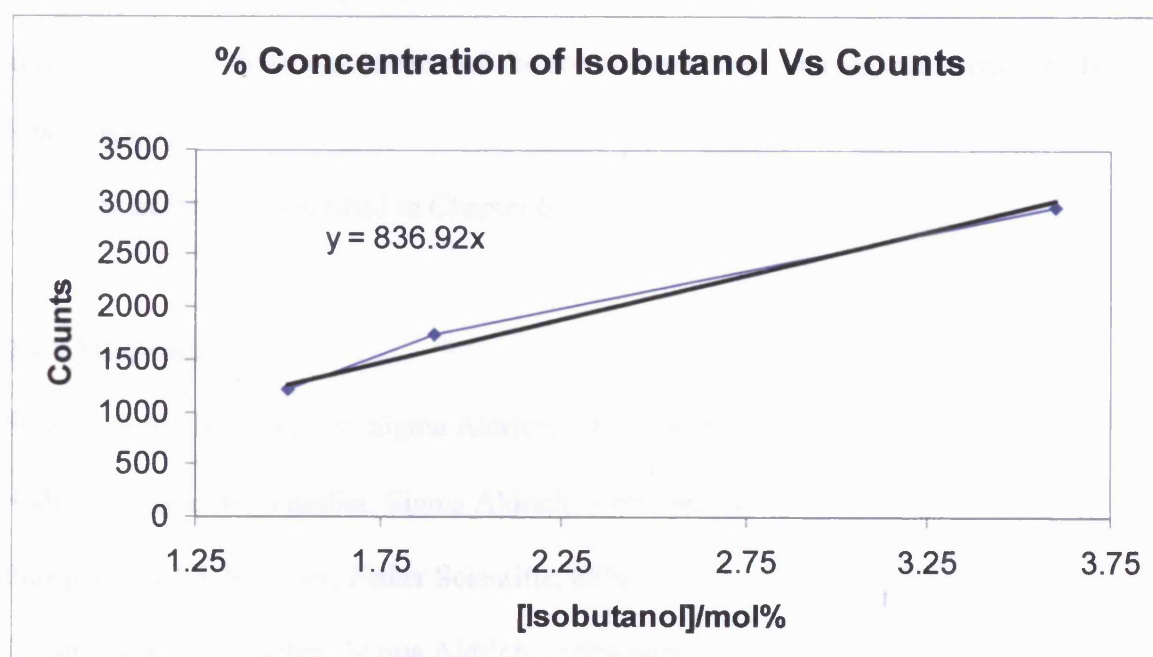


Figure 2.4.5.4: Calibration of isobutanol



In the calibration of isobutanol the saturator was set at 26°C to give a concentration of 1.5%, 30°C to give a concentration of 1.9% and 40°C to give a concentration of 3.6%. The correlation coefficient was calculated at 0.993, which shows the response is linear over the concentration range.



#### 2.4.6 Vegetable Oil Transesterification Experimental Procedure

Catalyst (0.1-0.05g) was loaded into the glass insert of the autoclave. Vegetable oil (rapeseed, 20ml) and methanol (7.6ml) were added to the glass insert. The glass insert was then placed in the main body of the autoclave and sealed. The air inside was removed by pressurising with helium and venting three times. The temperature was set to the required level and stirring at 500rpm was started. Once the temperature was within 10% of the set point, the timer was started. At the end of the reaction, the heating jacket was removed and a beaker of ice-cold water was placed around the autoclave body to arrest the reaction. The contents of the autoclave were allowed to settle before a portion of the lower layer was removed and sent for  $^1\text{H}$  NMR analysis <sup>(6)</sup>.

$^1\text{H}$  NMR analysis is described in Chapter 6

#### 2.4.7 Materials Used

Sodium tungstate, Supplier: Sigma Aldrich,  $\geq 99\%$  purity

Sodium molybdate, Supplier: Sigma Aldrich,  $\geq 99\%$  purity

Phosphoric acid, Supplier: Fisher Scientific, 85%

Caesium nitrate, Supplier: Sigma Aldrich,  $\geq 99\%$  purity

Silicotungstic Acid, Supplier: Sigma Aldrich,  $>99\%$  purity

Silica powder, Supplier: Johnson Matthey

Base treated alumina, Supplier: Johnson Matthey

Alumina beads Supplier: Johnson Matthey

Carbon coated silica, Supplier: Johnson Matthey

Carbon coated alumina, Supplier: Johnson Matthey

1,4-butanediol, Supplier: Sigma Aldrich, 99% purity

Isobutanol, Supplier: Sigma Aldrich, 99% purity

### References

1. H. Wu, *Journal of Biological Chemistry*, 43 (1920) 189-220
2. F. Cavani, *Catalysis Today* 41 (1998) 73-86
3. Z. Ma, W. Hua, Y. Ren, H. He, Z. Gao *Applied Catalysis A: General* 256 (2003) 243–250
4. P. Atkins, *Physical Chemistry*, Sixth Edition Oxford University Press 1998
5. D. R. Lide, *CRC Handbook of Chemistry and Physics* (75<sup>th</sup> Edition) CRC Press, Taylor & Francis Group 1994
6. L.C. Meher D. Vidya Sagar, S.N. Naik *Renewable and Sustainable Energy Reviews* 10 (2006) 248-268

# Chapter Three: Catalyst Characterisation

## 3.1 Catalyst Characterisations

In this chapter the catalysts used in the experiments were characterised by BET surface area measurements, Raman spectroscopy, powder XRD and TGA in order to determine the extent of HPA on the surface of the supports and what change the HPA or the support underwent.

### 3.1.1 BET isotherms

HPA	Surface area m <sup>2</sup> /g
STA	4
CsSTA	4
Cs <sub>2</sub> STA	43
Cs <sub>3</sub> STA	147
Cs <sub>4</sub> STA	86
SMA	6
CsSMA	28
Cs <sub>2</sub> SMA	122
Cs <sub>3</sub> SMA	50
Cs <sub>4</sub> SMA	14
CsPMA	5
Cs <sub>2</sub> PMA	107
CsPTA	22
Cs <sub>2</sub> PTA	83
Cs <sub>3</sub> PTA	132
silica support	249
26% STA on carbon coated alumina	102
26% STA on alumina powder	236
26% STA on carbon coated silica	172
JM supplied silica 20R950	168
26% STA on silica powder	297

Table 3.1.1.1 Surface areas of bulk catalysts, supported catalysts and support

The type of cation has found to influence the properties of the HPA salt. HPAs partially neutralised with small cations such as  $\text{Na}^+$ ,  $\text{Fe}^{3+}$ ,  $\text{Co}^{3+}$ , and  $\text{Ni}^{2+}$  have been found to be highly soluble in polar solvents and water and have a low surface area, while HPA salts of large cations like  $\text{Cs}^+$  have higher surface areas and are largely insoluble in water<sup>(1,2)</sup>. Surface area measurements show that supporting the HPAs on silica decreases the total surface area when compared to the silica alone<sup>(3)</sup>. Substituting a proton for a caesium cation increases the surface area when compared to the unsubstituted HPA and increases the dispersion of the HPA on the surface of the catalyst<sup>(4)</sup>. The surface area reaches a maximum when three of four protons are substituted, in the case of silica containing HPAs, before decreasing when all protons are substituted. This is in agreement with the literature<sup>(5,6)</sup> where the free acid and mono substituted acids have low surface areas compared to the di and tertiary substituted HPAs. Increasing the loading of HPA on a silica support does decrease the overall surface area as well as the average pore volume and size, indicating that most of the pores are filled with solid HPA<sup>(7)</sup>. The surface acidity has been found to increase with successive addition of Cs as an estimation of the concentration of protons bound to the anion and the surface area.<sup>(8)</sup>

### 3.1.2 Raman Spectroscopy

The Raman spectra of the Keggin-type heteropoly acids supported on silica and alumina are shown in figure 3.1.2.1 Raman spectroscopy of the supported catalysts shows the same characteristic peaks associated with HPAs. The most noticeable is the peak at around  $986\text{cm}^{-1}$ , which can be assigned to asymmetric stretching of  $\nu(\text{W}=\text{O})$  while a small peak at  $927\text{cm}^{-1}$  in the silica supported STA can be assigned to the asymmetric stretch  $\nu(\text{Si}-\text{O})$ . This is in agreement with literature

values<sup>(9, 10, 11, 25)</sup>. The main peak is shifted towards  $1000\text{cm}^{-1}$ , possibly as a result of interaction with the support. Other peaks in the  $870\text{cm}^{-1}$  to  $980\text{cm}^{-1}$  region are obscured by a broad shoulder. These would be assigned to the inter W-O-W bonds<sup>(12)</sup>. This broadening is most apparent in the alumina supported STA samples. The blank silica support was also analysed by Raman as a comparison. The support itself did not show any of the peaks observed with the STA impregnated supports. This suggests that the primary and secondary structure of the Keggin HPA is intact on the surface of the supports. This supports the XRD data that the Keggin structure is intact on the surface of the supports and has not decomposed on the surface of the supports.

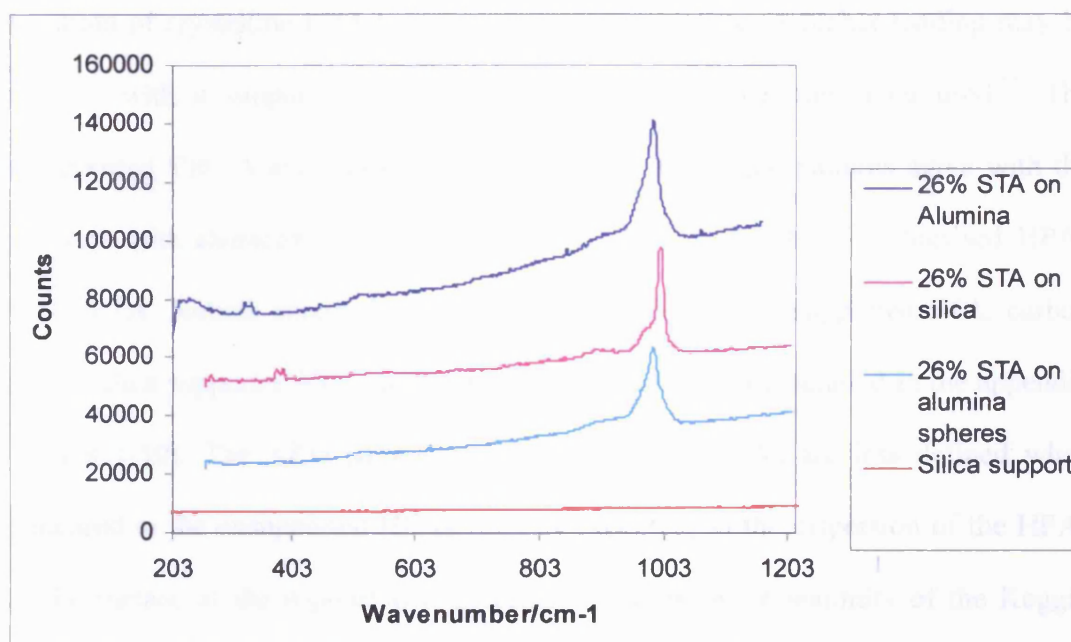


Figure 3.1.2.1: Raman spectroscopy of STA supported on silica and alumina spheres

### 3.1.3 Powder X-ray Diffraction

Powder XRD of Keggin-type heteropoly acids have been performed and show a crystalline structure, the XRD patterns can be compared to a known reference sample. Powder XRD of the supported HPAs was performed and there is correlation between the different supported HPA. While there are some differences that can be

attributed to the supports themselves, it is clear that parts of the XRD patterns are identifiable as the Keggin-type HPA. The XRD spectra agree with similar supported HPAs in the literature<sup>(7)</sup> This indicates that the STA is at least physically present with the supports. This is in agreement with the Raman data. At the loading levels of HPA on the supports it can be shown that the HPA does not undergo structural rearrangement, but has most likely present as bulk HPA on the surface of the support. It has been reported<sup>(11)</sup> that the characteristic diffraction peaks of HPA supported on silica become apparent at loadings above 20 wt.%. Since the catalysts under investigation are around 26 wt.%, then the XRD pattern obtained is within the threshold of crystalline HPA being present on the surface. A higher loading may be possible with a support with a higher surface area than the silica used.<sup>(7)</sup> The unsupported CsSTA and supported CsSTA XRD diffraction patterns agree with the literature with characteristic peaks at  $2\theta = 23^\circ$  <sup>(20, 21)</sup>. XRDs of synthesised HPAs PMA, PTA, Aldrich supplied PTA, Aldrich supplied, silica supported STA, carbon coated silica supported STA and alumina supported STA are detailed in the appendix (figures 1-10). The XRD patterns for the supported HPAs are less defined when compared to the unsupported HPAs. This is expected, as the dispersion of the HPAs on the surface of the support will decrease the apparent crystallinity of the Keggin units.

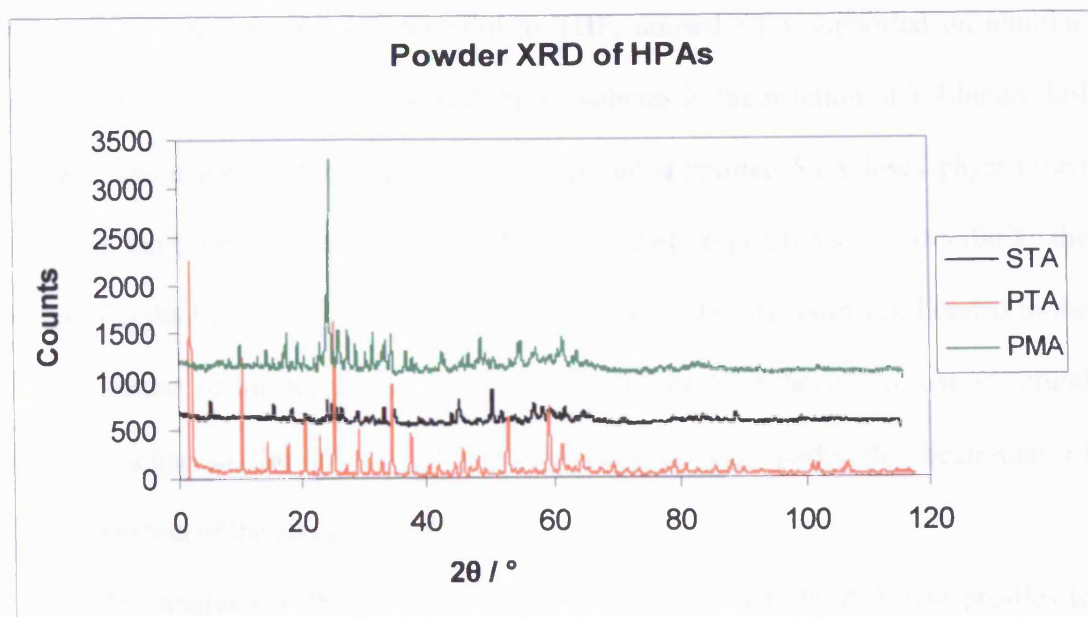


Figure 3.1.3.1 Powder XRD data for Unsupported HPAs

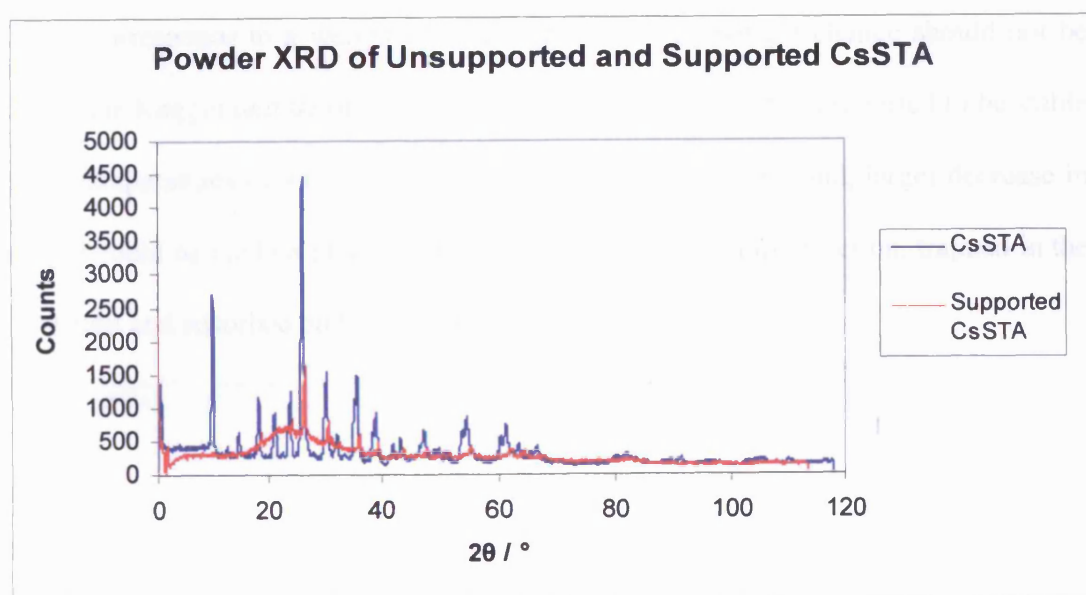


Figure 3.1.3.2 Powder XRD of supported and unsupported CsSTA

### 3.1.4 Thermal Gravimetric Analysis (TGA)

TGA of the HPA catalysts have been carried out in air at temperatures of up to 500°C. The samples were unused STA supported on silica, used STA supported on

silica in the reaction of 1,4-butanediol to THF, unused STA supported on alumina spheres and used STA supported on alumina spheres in the reaction of 1,4-butanediol to THF. From the TGA experiments, the unused supported STA loses physisorbed water at temperatures below 100°C. Between the temperatures of 100-300°C the water of crystallisation is lost.<sup>(14)</sup> These water molecules are hydrogen bonded to the acidic protons of the Keggin unit. At 300-500°C the STA begins to lose structural water relating to the loss of the acidic protons and marks the beginning of decomposition of the Keggin unit.<sup>(15)</sup>

The analysis of the used catalysts revealed substantially different profiles to the unused catalysts. In each of the samples, there were two distinct steps, one for the loss of water and a second, larger decrease in weight appears between 276-425°C, which corresponds to a weight decrease of 5-7%. The weight change should not be due to the Keggin unit thermally decomposing as they have been reported to be stable up to temperatures of 445°C<sup>(16)</sup>. A possible reason for the second, larger decrease in weight could be the loss of adsorbed reactant/product from the reaction, trapped in the HPA unit and adsorbed on the support.

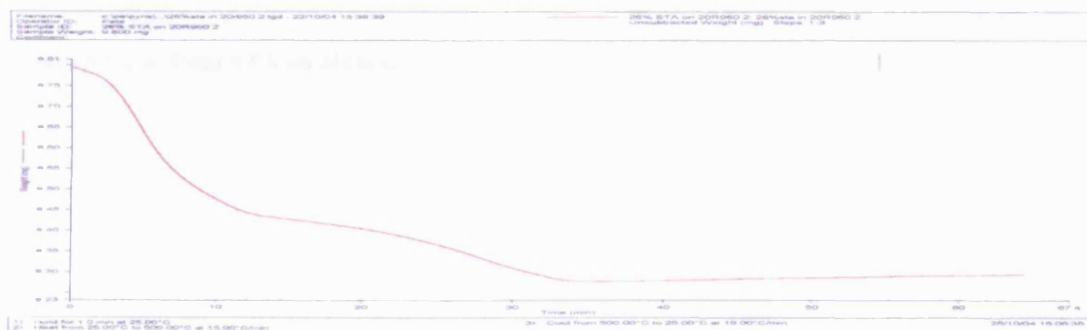


Figure 3.1.4.1 Unused STA on silica



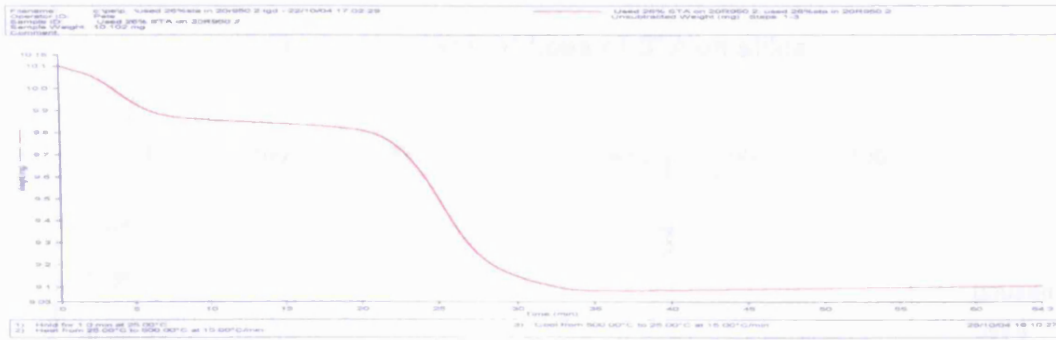


Figure 3.1.4.2: Used STA on silica

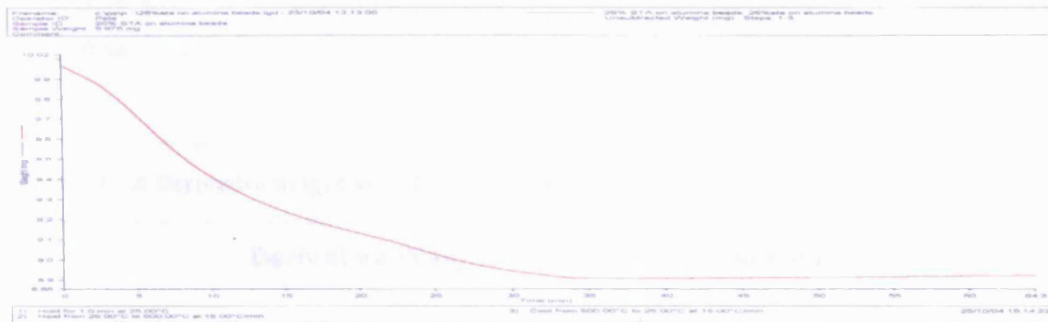


Figure 3.1.5.3 Unused STA on alumina spheres

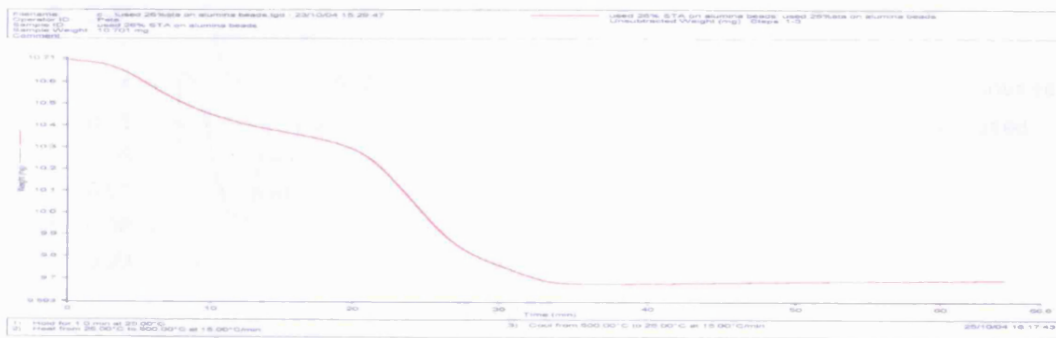


Figure 3.1.6.4: Used STA on alumina spheres

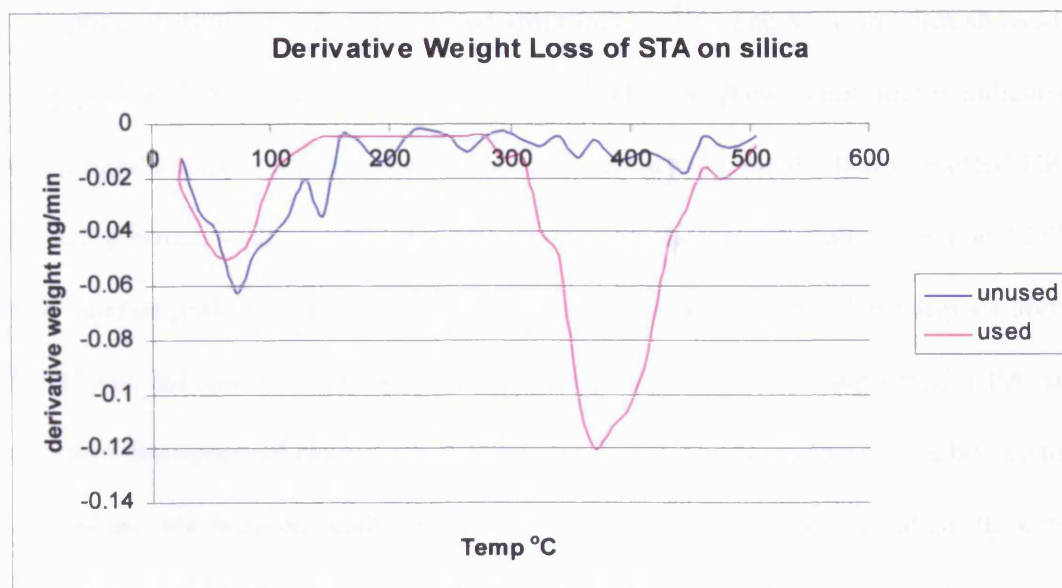


Figure 3.1.7.5 Derivative weight loss of STA on silica

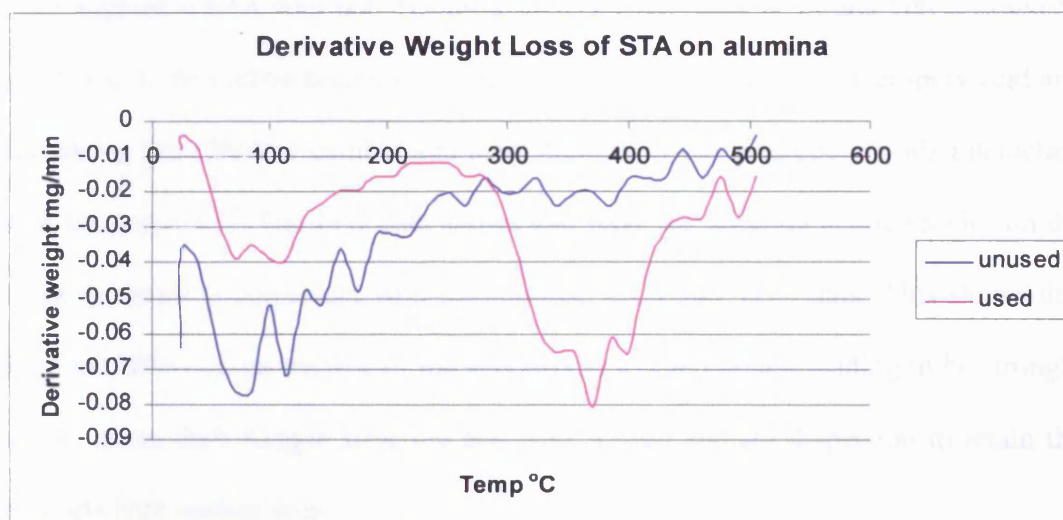


Figure 3.1.8.6 Derivative weight loss of STA on alumina

### 3.1.5 Ammonia Temperature Programmed Desorption (TPD)

The TPD profile for each of the supported HPAs showed a marked difference in the signal produced. (It must also be noted that the TCD signal is incorrectly labelled as  $\text{NH}_3$  absorption, it should read desorption.) All the samples produced an initial broad peak in the range of 175-225°C, except for the silica supported STA, which has an initial signal at around 125°C. These initial signals correspond to

desorption of weakly held, physisorbed ammonia<sup>(17,18,22)</sup>. The STA on silica showed a sharp peak at 225°C while the other supported STA samples do not, this is indicative of stronger acidity and less reducibility<sup>(19)</sup>. The carbon coated silica supported HPA showed a broad, shallow peak at 500°C with a another broad shallow peak at 525°C with another peak appearing at 575°C before the analysis ends. These signals above 225°C are indicative of the acid sites present with the silica supported HPA and represent desorption of chemisorbed ammonia. It can be shown that the carbon coated alumina and the alumina beads have very similar behaviour, while the silica supported STA has a very definite maxima of ammonia desorption while the carbon coated silica supported STA does not. The absence of a sharp peak at around 500°C could be indicative of the carbon coated silica strongly interacting with the heteropoly acid and decreasing the effective number and acid strength of the heteropoly acids interacting with the support.<sup>(23)</sup> The TPD data shows that there are strongly acidic species on the supports which is agreement with the Raman, XRD and TGA data. This shows that there are HPAs on the surface of the supports at a high enough loading to be strongly acidic, retain their Keggin structure and have a high enough dispersion to retain the supports high surface area.

It has been reported<sup>(24)</sup> that the interaction between HPAs and the OH groups present on the surface of silica will decrease the acid strength by forming  $-\text{OH}_2^+$  and  $\text{HPA}^-$  thereby removing an acidic proton from the HPA anion. It is also noted that ammonia will interact with the OH groups present on the surface of silica and with the Lewis acid sites present on the surface of alumina, this would also account for the broad peak seen at lower temperatures in the TPD data.

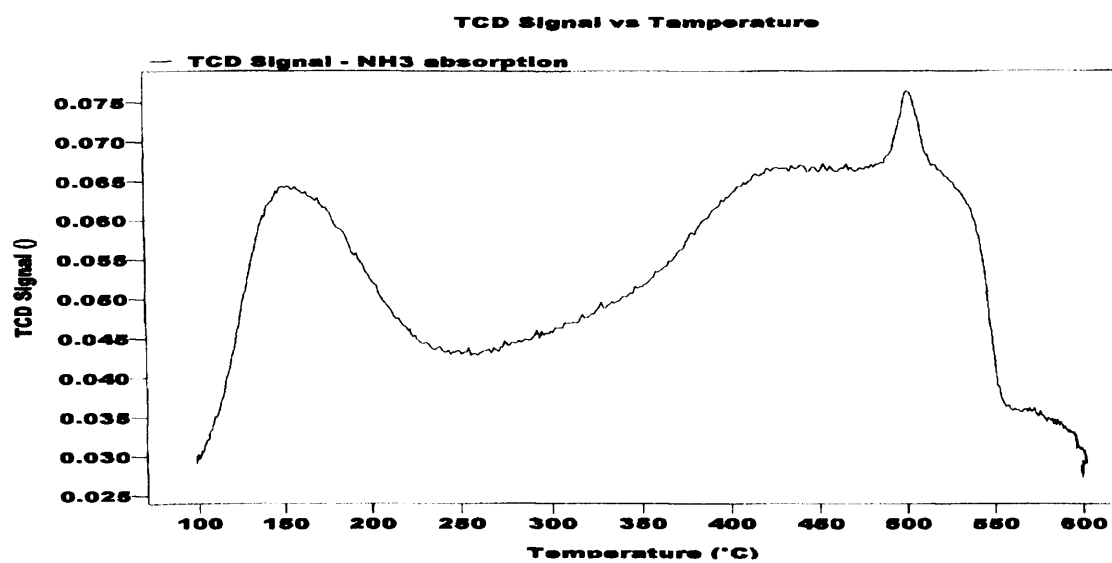


Figure 3.1.5.1: Ammonia TPD of Silica supported STA

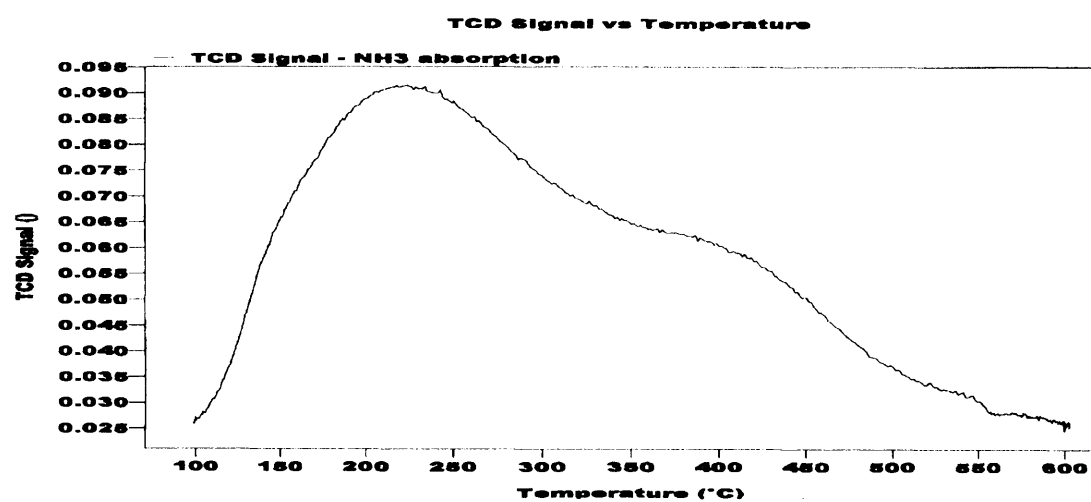


Figure 3.1.5.2: Ammonia TPD of alumina sphere supported STA

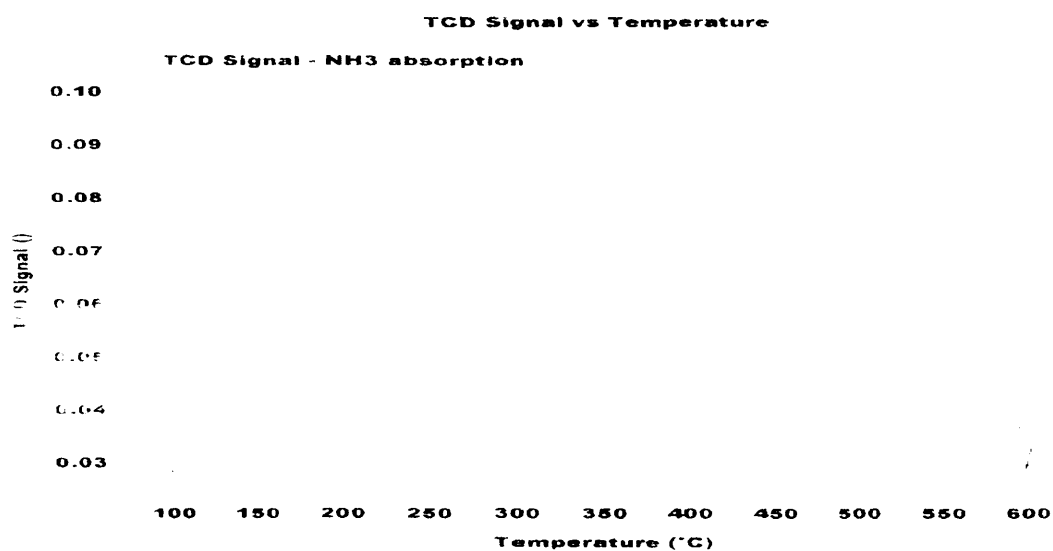


Figure 3.1.5.3: Ammonia TPD of carbon coated alumina powder supported STA

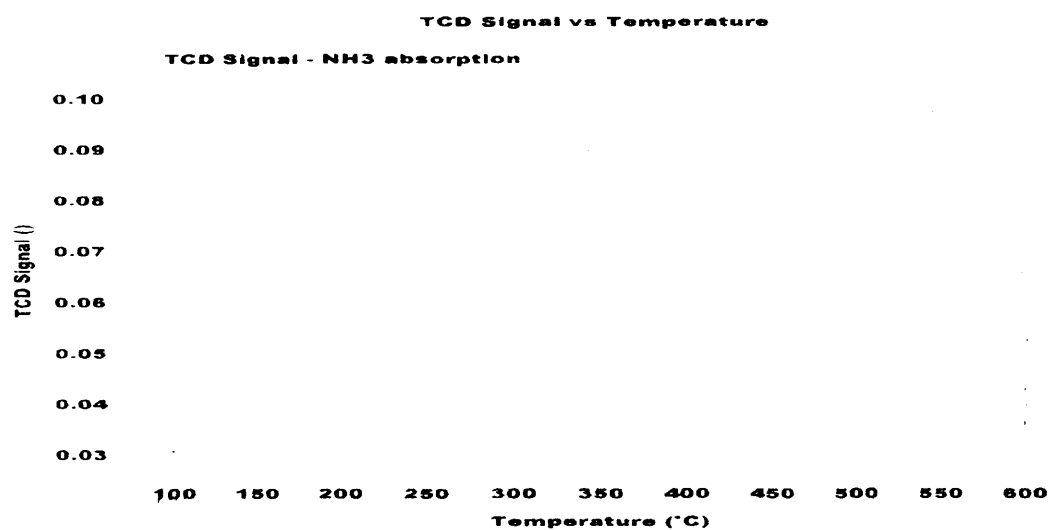


Figure 3.1.5.14: Ammonia TPD of carbon coated silica supported STA

## References

1. S. Soled, S. Miseo, G. McVicker, W.E. Gates, A. Gutierrez, J. Paes The Chemical Engineering Journal 64 (1996) 247-254
2. G. P. Romanelli, J. C. Autino, M. N. Blanco, L. R. Pizzio Applied Catalysis A: General 295 (2005) 209–215
3. C. Yuan, F. Zhang, J. Wang, X. Ren, Catalysis Communications 6 (2005) 721–724

4. L.R. Pizzio, P. G. Vazquez, C.V Caceres, M.N, Alesso, M.I. Erlich, R. Torviso, L. Finkielsztejn, B. Lantano, G.Y. Moltrasio *Catalyst Letters* 93, 1-2 (2004) 67-73
5. J. Pozniczek, A. Lubanska, D. Muchaa, A. Bielanski *Journal of Molecular Catalysis A: Chemical* 257 (2006) 99–104
6. J.A. Dias, E. Caliman, S.C.L. Dias, *Microporous and Mesoporous Materials* 76 (2004) 221-232
7. Y. Zhang, Z. Du, E. Min *Catalysis Today* 93-95 (2004) 327-332
8. T. Okuhara, *Applied Catalysis A: General* 256 (2003) 213-224
9. W. Kuang, A. Rives, B. Ouled B. Tayeb, M. Fournier, R. Hubaut *Journal of Colloid and Interface Science* 248 (2002) 123-129
10. B. M. Devassy, S.B. Halligudi *Journal of Catalysis* 236 (2006) 313-323
11. B. M. Devassy, S.B. Halligudi *Journal of Molecular Catalysis A: Chemical* 253 (2006) 8-15
12. H. Liu and E. Iglesia, *Journal of Catalysis* 223 (2004) 161–169
13. W. Kuang, A. Rives, M. Fournier, R. Hubaut *Applied Catalysis A: General* 250 (2003) 221-229
14. N. Essayem, Y.Y. Tong, H. Jobic, J.C. Vedrine *Applied Catalysis A: General* 194-195 (2000) 109-122
15. J. Kaur, K. Griffin, B. Harrison, I. V. Kozhevnikov, *Journal of Catalysis* 208, (2002) 448-455
16. I.V. Kozhevnikov *Chem. Rev.* 98 (1998) 171-198
17. E. F. Kozhevnikova, I. V. Kozhevnikov *Journal of Catalysis* 224 (2004) 164–169

18. Á. Molnár, C. Keresszegi, B. Török *Applied Catalysis A: General* 189 (1999) 217–224
19. N. Dimitratos, J. C. Védrine *Catalysis Communications* 7 (2006) 811–818
20. H. Jin, Q. Wu, W. Pang *Material Letters* 58 (2004) 3657-3660
21. L. Pesaresi, D. R. Brown, A. F. Lee, J. M. Montero, H. Williams, K. Wilson *Applied Catalysis A: General* 360 (2009) 50-58
22. K. M. Reddy, N. Lingaiah, K. N. Rao, N. Rahman, P.S.S. Prasad, I. Suryanarayana *Applied Catalysis: General* 296 (2005) 108-113
23. Q. Y. Liu, W. L. Wu, J. Wang, X. Q. Ren, Y. R. Wang, *Microporous and Mesoporous Materials* 76 (2004) 51-60
24. A. Miyaji, T. Echizen, K. Nagata, Y. Yoshinaga, T. Okuhara *Journal of Molecular Catalysis A: Chemical* 201 (2003) 145-153
25. E. Ortiz-Islas, T. Lopez, R. Gomez, J. Navarrete, D.H Aguilar, P. Quintana, M. Picquart *Applied Surface Science* 252 (2005) 839-846

# Chapter Four: Gas Phase Alcohol Dehydration

## 4.1 Introduction

Alcohol dehydration can occur by heating the alcohol and using an acid as a catalyst, typical acidic compound used are sulphuric acid or phosphoric acid in liquid phase reactions or sulphated zirconia <sup>(1)</sup> or alumina <sup>(2)</sup> in gas phase reactions. The various classes of alcohols differ in their ease of reaction, the order of reactivity being: tertiary > secondary > primary.

For the dehydration of secondary and tertiary alcohols the mechanism is generally accepted as below:

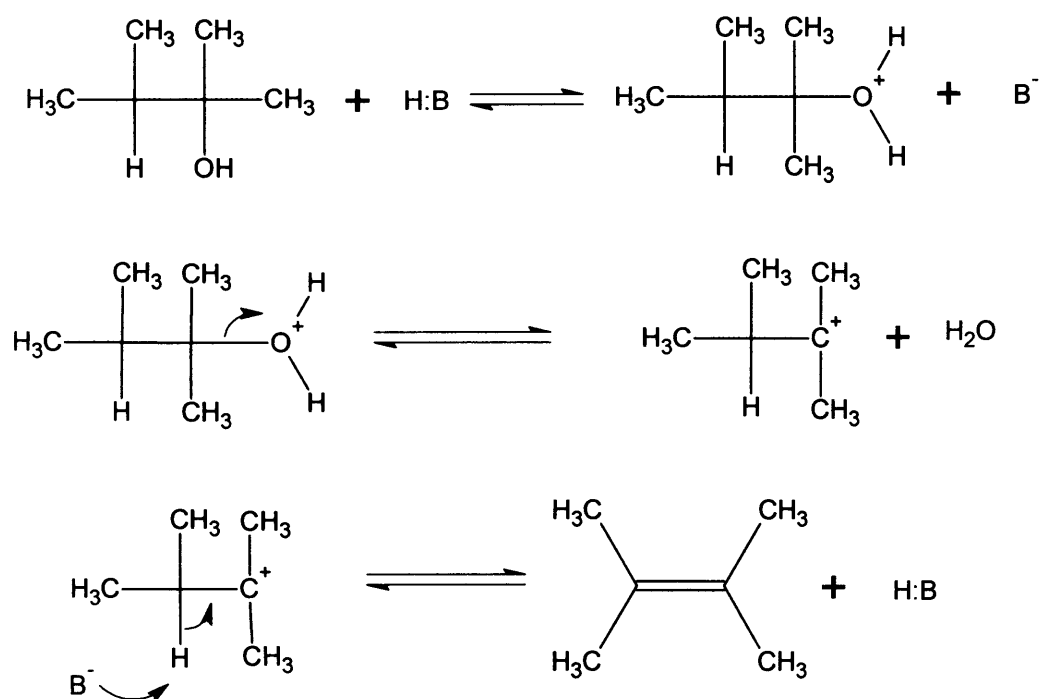


Figure 4.1.1: Dehydration mechanism of a secondary or tertiary HB is a Brønsted acid <sup>(3)</sup>

Keggin type heteropoly acids possess strong Brønsted acidity <sup>(4)</sup>, which is important in the first step of the mechanism of protonating the alcohol.



## 4.2 Cyclodehydration of 1,4-butanediol

### 4.2.1 Introduction

The cyclodehydration of 1,4-butanediol (BTD) to tetrahydrofuran (THF) was chosen as the current method uses the Reppe process which involves a reaction between acetylene and formaldehyde to give 2-butyne-1,4-diol, with subsequent hydrogenation to 1,4-butanediol. The catalyst most commonly used for this process is a silica supported copper(II) oxide, with bismuth oxide added<sup>(5,6)</sup>. The saturated diol is cyclodehydrated to THF with elimination of water by acid catalysis above 100°C. Using a supported heteropoly acid (HPA) would eliminate the need for the neutralisation of the above-mentioned acids and reduce the cost of disposal for the waste generated.

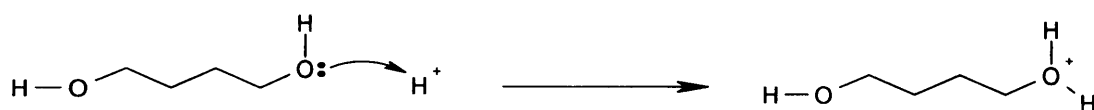
THF is an important and versatile chemical with many uses in industry. Uses include use as a reaction solvent and it is used in pharmaceutical synthetic procedures. Another use is as an intermediate in making polytetramethylene ether glycol for use in the manufacture of urethane elastomers and fibres<sup>(7)</sup>. By using a solid catalyst Envirocat E PZ G, instead of  $\text{AlCl}_3$  the synthesis of *para*-chlorobenzophenone, the problem of an aqueous quench is solved and HCl emissions are decreased by 75% and decreasing the weight of the catalysts used by a factor of ten<sup>(8)</sup>. Legislation makes creating liquid effluent waste an expensive mode of operation, making heterogeneous catalysis a more favoured approach. The fine chemical and pharmaceutical sectors of the chemical industry produce more by-products than usable products. Solid heteropoly acids offer safer working conditions and more eco-friendly approach to acid catalysis than traditional soluble acid catalysts.

Zirconia catalysts have been used in the synthesis of the vapour-phase dehydration of 1,4-butanediol <sup>(9)</sup>. The dehydration of 1,4-butanediol to 3-buten-1-ol and THF was investigated over zirconia at temperatures of 275–425°C. At 325–350°C, 3-buten-1-ol and THF were competitively produced from 1,4-butanediol at a ratio of around 1:1 over zirconia, and the combined selectivities exceeded 90 mol%. The by-products formed from 3-buten-1-ol, such as 1,3-butadiene, 2-buten-1-ol, 2-butenal and 1-butanol, which had been observed in the dehydration of 1,4-butanediol over pure ceria, were suppressed over zirconia at 325°C.

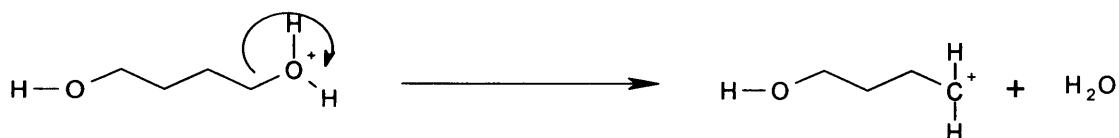
#### 4.2.2 Reaction of 1,4-butanediol

The proposed mechanism for the cyclodehydration reaction proceeds by four steps to yield THF.

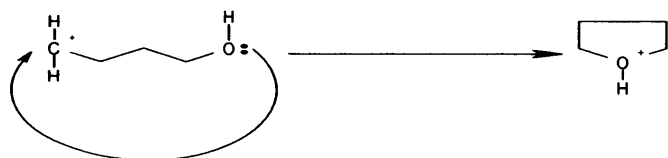
Step one: Protonation of 1,4-butanediol



Step two: Elimination of H<sub>2</sub>O



Step three: Ring formation



Step four: Regeneration of H<sup>+</sup>

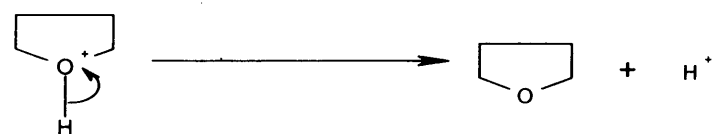


Figure 4.2.2.1 Mechanism of 1,4-butanediol cyclodehydration

### 4.2.3 Initial Reactions

The initial reaction yields and selectivities of 1,4-butanediol to THF at different temperatures using STA on silica powder were investigated. The results appeared to be very encouraging with very high yields and selectivity to THF. The level of conversion obtained for BTD was stable over many hours of reaction time. The contact time for the feedstock to pass over the catalyst was 0.04 seconds and the gas hourly space velocity (GHSV) for the reaction was  $96000 \text{ hr}^{-1}$ . The Yield was calculated by multiplying the conversion by selectivity.

150°C

Time (min)	Conversion (%)	Yield (%)	Selectivity (%)
60	99.3	98.6	99.3
120	99.7	99.4	99.7
180	99.7	99.4	99.7
240	99.7	99.4	99.7
300	99.4	98.8	99.4

175°C

Time (min)	Conversion (%)	Yield (%)	Selectivity (%)
60	99.0	98.0	99.0
120	99.5	99.0	99.5
180	99.5	99.0	99.5

200°C

Time (min)	Conversion (%)	Yield (%)	Selectivity (%)
60	98.1	94.4	98.1
120	99.2	98.4	99.2
180	99.7	99.4	99.7
240	99.1	98.2	99.1
300	95.1	88.5	93.1

225°C

Time (min)	Conversion (%)	Yield (%)	Selectivity (%)
60	99.0	98.0	99.0
120	99.5	99.0	99.5
180	99.5	99.0	99.5
240	99.5	99.0	99.5
300	99.6	99.2	99.6

Time (min)	Conversion (%)	Yield (%)	Selectivity (%)
60	32.0	32.0	99.9
120	33.0	32.2	97.5
210	64.0	60.7	94.9
270	53.0	51.2	97.7
330	48.0	44.0	91.7

Blank with glass wool at 175°C

Figure 4.2.3.1 Selectivities of 1,4-BTD to THF using STA on silica powder

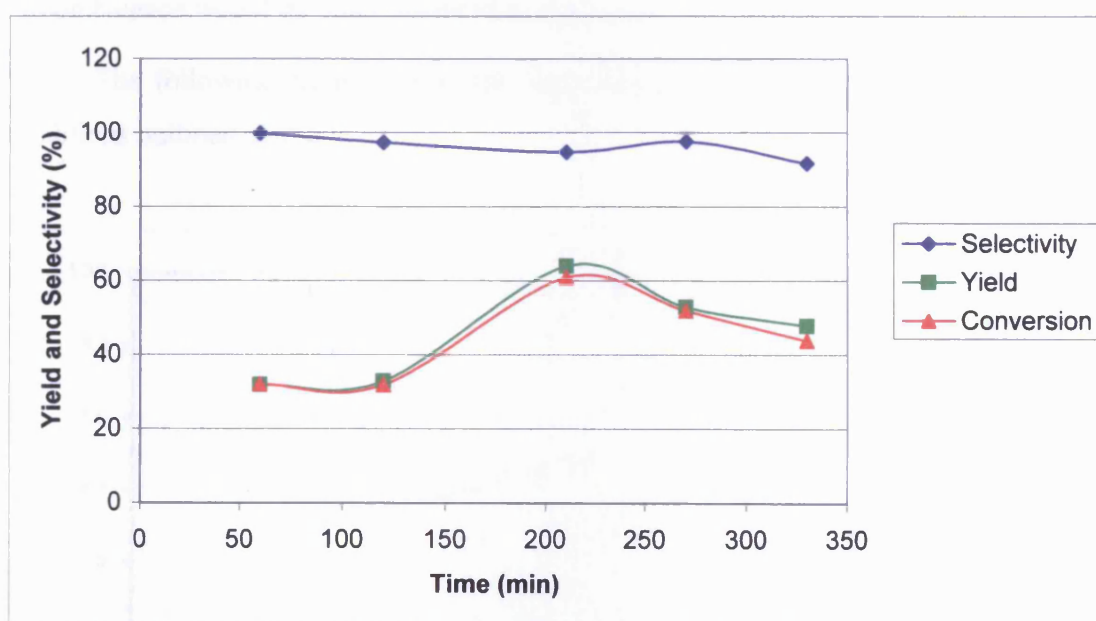


Figure 4.2.3.2: Yield and selectivity of glass wool, 175°C, 80ml/min He flow

In this experimental set up of the reactor, the BTD was not being vaporised in the heating oven. Instead, it was flooding the glass reactor tube containing the catalyst. Since any THF produced in the reaction would have boiled off into the collecting bottle, this would account for the very high conversion and selectivity to THF observed. In light of the technical limitations of the experimental set up, the apparatus was modified to ensure the vaporisation of BTD and stop the flooding of the reactor tube. The modified apparatus is described in Chapter Two, the heating

oven was replaced by a 500ml steel bomb and the HPLC pump was replaced by a peristaltic pump.

Reactions run at 80°C with 0.05g of STA on silica gave high selectivity to THF but suffered from irreproducibility since none of the results obtained agreed with each other (see figures 4.2.3.3 to 4.2.3.5). Other difficulties were that the lines leading from the glass reactor tube would block, resulting in abandoned experiments. This makes the results obtained unrepresentative of the reaction performed since the carbon balance would be much lower than expected.

The following figures show the irreproducibility of the reaction under the conditions outlined above.

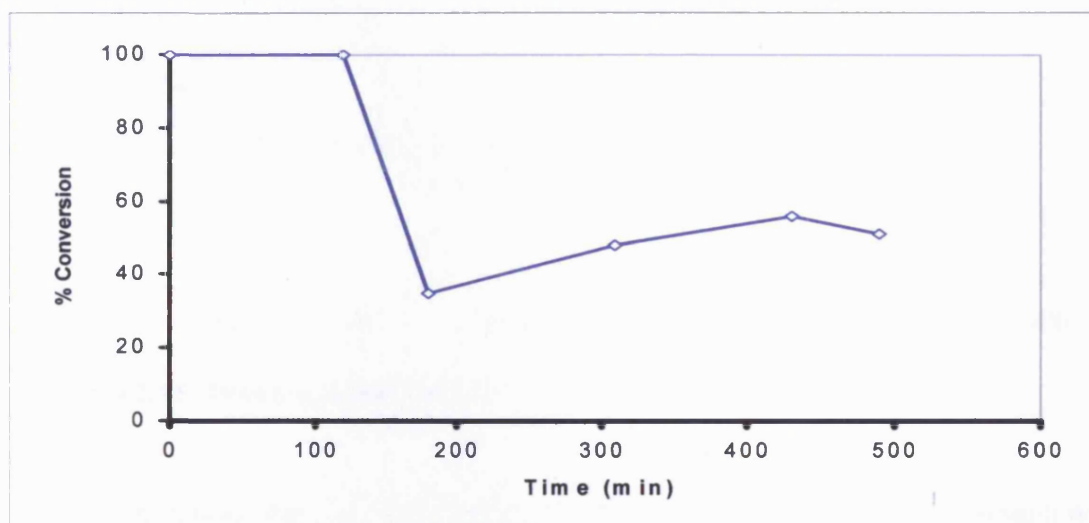


Figure 4.2.3.3: First vapour phase run at 80ml/min, 70°C

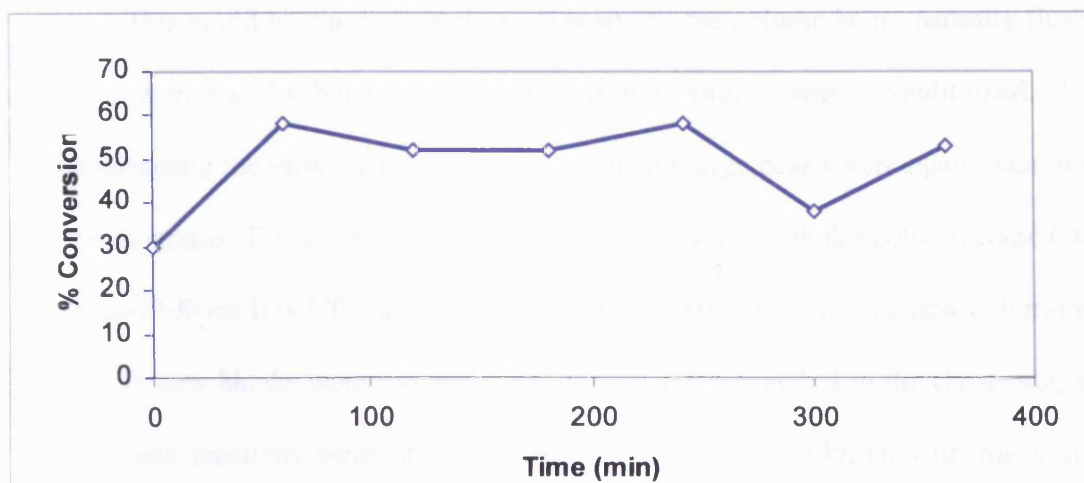


Figure 4.2.3.4: Second vapour phase run at 80ml/min, 70°C

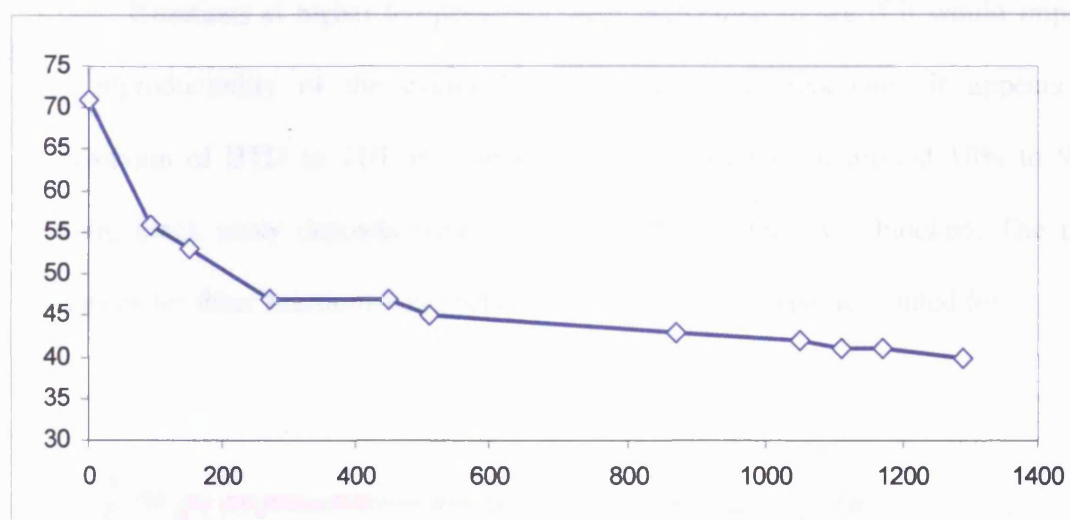


Figure 4.2.3.5: Third run at 80ml/min, 70°C

Reactions were run again under similar conditions and none of the results were reproducible. Several experiments were run with the heating cylinder at higher temperatures (70-115°C) and none of these results were reproducible, while reactions at lower temperatures encountered problems of signal to noise due to the low concentration of 1,4-butanediol in the vapour phase. Blanks (no catalyst) were run to determine flow of 1,4-butanediol through the system and very large, broad peaks were found to be present in the chromatograms along with the 1,4-butanediol peak.

This could be due to polymeric deposits on the column being partially flushed though with the 1,4-butanediol stream, so the column was reconditioned. After reconditioning the same blanks were run again and large peaks were again seen in the chromatograms. The column was replaced with a six-foot tubular column coated with 10% sp-2100 on 100/120 supelcoport and blanks were run. Once the new column was installed, new blanks were run and showed only 1,4-butanediol in the chromatogram. Subsequent reactions were run with the flow of He at 90ml/min, with the heating cylinder at 120°C to provide a vapour concentration of around 1.2%.

Reactions at higher temperatures were performed to see if it would improve the reproducibility of the cyclodehydration. In these reactions, it appears the conversion of BTD to THF is dramatically fluctuating from around 10% to 90%. Again, black sooty deposits were found after the system was blocked. The mass balances for these reactions were between 40-50% of the mass accounted for.

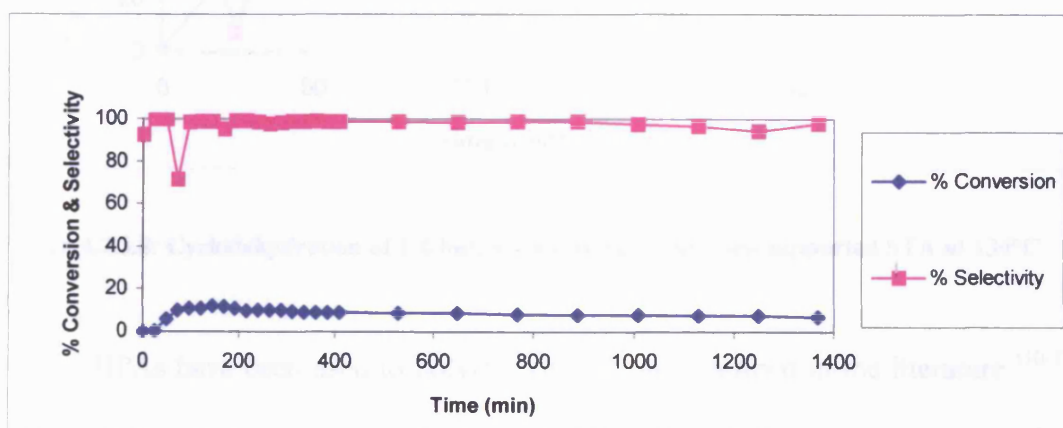


Figure 4.2.3.6: Cyclodehydration of 1,4-butanediol using 0.05g silica supported STA at 134°C

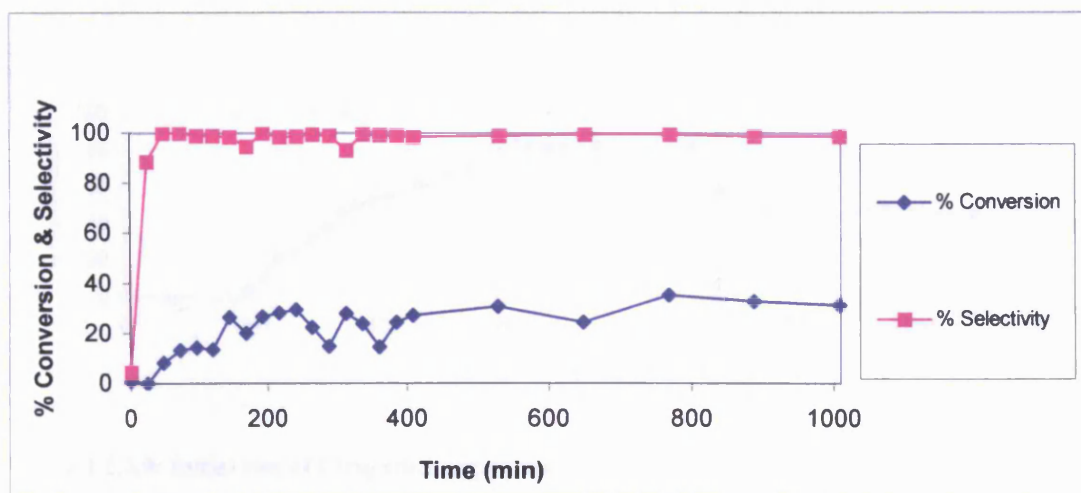


Figure 4.2.3.7: Cyclodehydration of 1,4-butanediol using 0.05g silica supported STA at 134°C

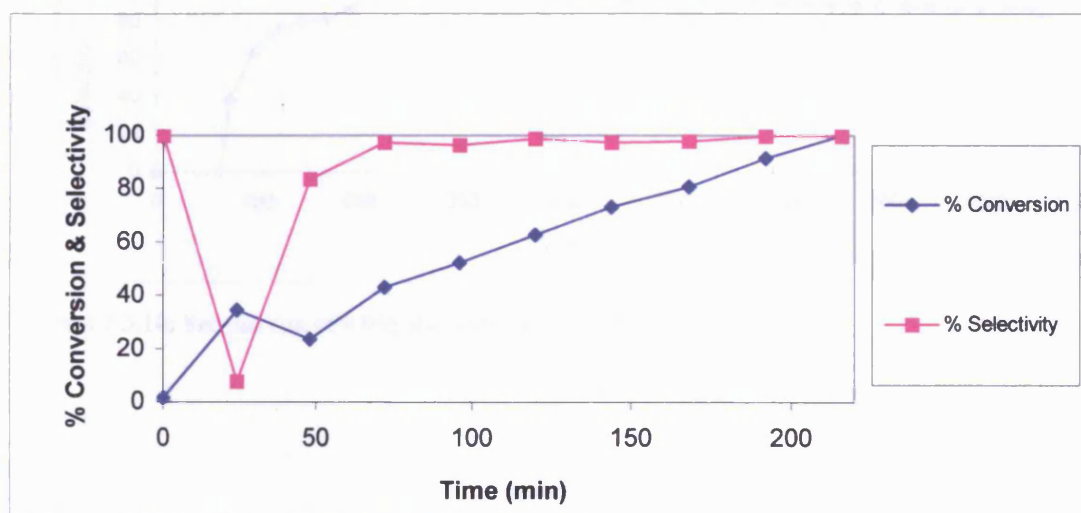


Figure 4.2.3.8: Cyclodehydration of 1,4-butanediol using 0.05g silica supported STA at 134°C

HPAs have been used to polymerise THF as described in the literature<sup>(10-12)</sup>, in an attempt to decrease the polymerisation of THF in the reactor tube, reactions were performed at a low temperature to see if that would increase the carbon mass balance and inhibit the polymerisation of THF.



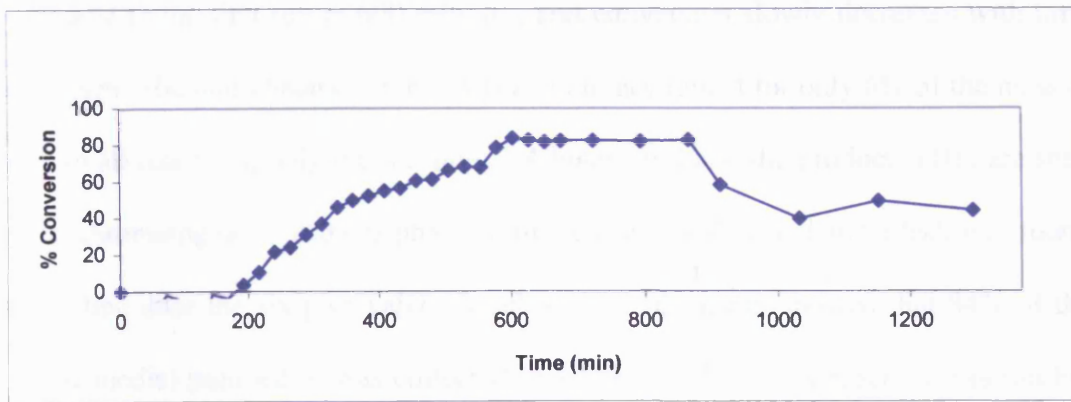


Figure 4.2.3.9: Initial run of 0.05g silica supported STA at 55°C

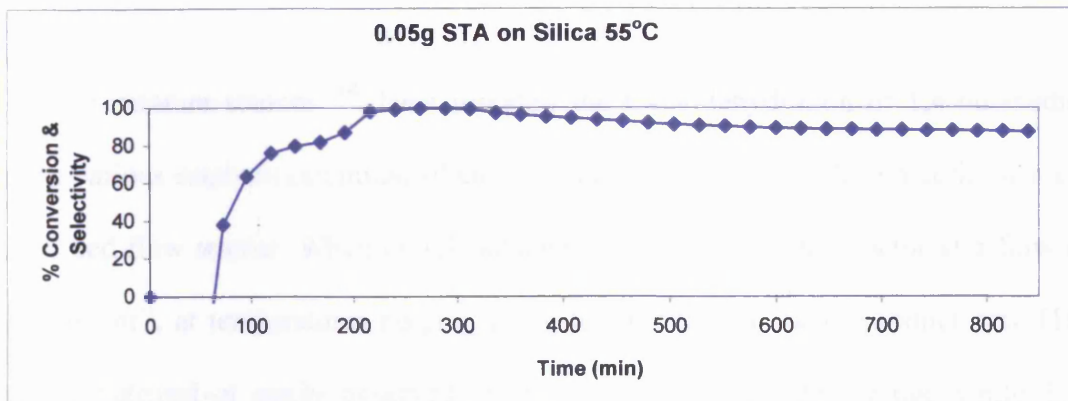


Figure 4.2.3.10: Second run of 0.05g silica supported STA at 55°C

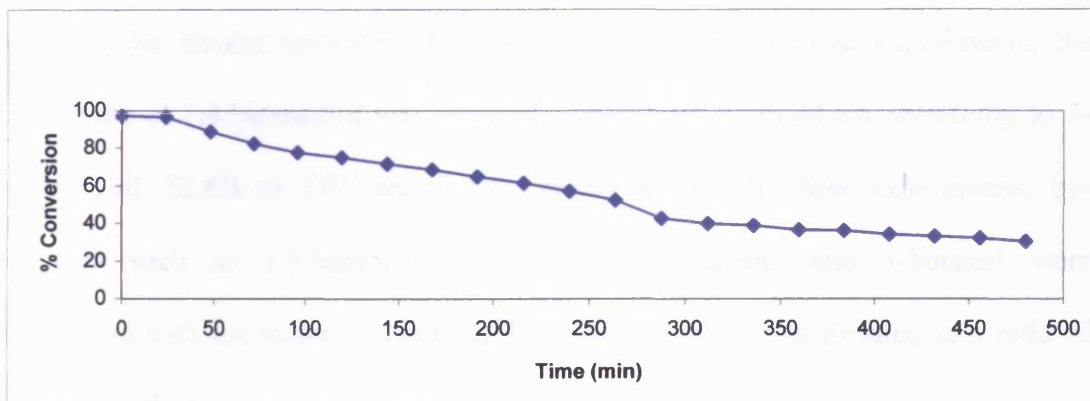


Figure 4.2.3.11: Third run of 0.05g silica supported STA at 55°C

In the vapour phase, conversion of 1,4-butanediol peaks at 83% at 600 minutes and stays constant at 82% for nearly four and a half hours. After this time the conversion decreases to 44% after 21 hours on-stream. The results from the third run are different to the first run. The conversion reaches a plateau at 216 minutes,

compared to the first run at 600 minutes, and conversion slowly decreases with time on-stream. The mass balances when worked out accounted for only 6% of the mass at best. In all reactions, only the reactant, 1,4-butanediol and the product, THF, are seen in the chromatograms. The gas phase equipment was leak tested and a leak was found in the line after the six-port valve. A subsequent blank run showed that 84% of the 1,4-butanediol pumped in was collected in a Dreschel bottle. A reaction was run but was abandoned due to coking at the bottom of the reactor tube contaminating the GC traces.

Literature sources <sup>(14)</sup> have reported the Cyclodehydration of 1,4-butanediol using various catalysts (alumina, silica, zirconia, magnesium oxide and ceria) using a fixed bed flow reactor. When 1,4-butanediol was fed into the reactor at a flow of  $1.77\text{cm}^3\text{ hr}^{-1}$ , at temperatures ranging from 200-425°C, the major product was THF with 3-butene-1-ol rarely observed at this reaction temperature range while 1,3-butadiene was observed as a major product at 200°C and as a minor product at temperatures above 200°C. The cyclodehydration of 1,4-butanediol over zirconia at 325°C under similar conditions has been reported <sup>(15)</sup>. In these experiments, the conversion of 1,4-butanediol was reported to be 39.9% with 44.6% selectivity to 3-butene-1-ol, 52.8% to THF and 0.2%  $\gamma$ -butyrolactone. In these experiments, by-products such as 1,3-butadiene, 2-butan-1-ol, 2-butenal and 1-butanol were suppressed with the major products of THF and 3-butene-1-ol forming at a ratio of approximately 1:1.

The prevention of coke formation in propene oligomerisation over PTA supported on silica (40% loading) at 150°C, has been reported by introducing nucleophiles such as water and methanol into the reaction mixture at (7% volume) <sup>(17)</sup>. Water was found to be the most effective inhibitor of coke formation by reacting

with carbenium ion intermediates decreased the amount of coke deposited by seven when compared to the background reaction.

It was noticed that all the vapour phase reaction results were not reproducible. A test mixture of 0.5ml 1,4-butanediol and 0.5ml 1,4-dioxane was diluted with 100ml of acetone and injected into a Varian 3400CX GC and the ratio recorded. (see appendix: Tables 1 - 5) The same mixture was then injected into Varian 3800 GC to compare the results. After fifty separate injections on each GC, the ratio of BTD to dioxane is not reproducible and for the on-line experiments the mass balances are between 0.8-6.1%. There is no correlation between the mass loss and temperature the reaction was run at. The method of analysis is therefore not appropriate for this reaction.

### **4.3 Dehydration of Isobutanol**

The dehydration of isobutanol to isobutene was investigated as a test reaction in order to determine the activity of the heteropoly acids in reaction conditions. The heteropoly acid catalysts were tested against solid phosphoric acid, zinc chloride impregnated montmorillonite K10 clay and nafion on silica. The reactor was designed to minimise the catalyst being washed out by liquid reactant in the event of the saturator becoming flooded during the reaction, as heteropoly acids are soluble in alcohols and other polar liquids. A heated saturator was used to give control over the vapour pressure and therefore the concentration of the alcohol in the vapour phase.

#### **4.3.1 Activity over time**

Gas phase reactions with isobutanol were performed with silica supported STA and CsSTA and solid phosphoric acid (SPA). The SPA did not show any

conversion at the same temperature investigated. In these experiments, it is apparent that the silica supported CsSTA deactivates at a slower rate than that of the silica supported STA. The silica supported CsSTA does have a lower conversion of isobutanol than the silica supported STA, this could be attributed to the decreased acidity of the CsSTA due to the partial neutralisation of the HPA as the most acidic proton is substituted during synthesis of the salt.

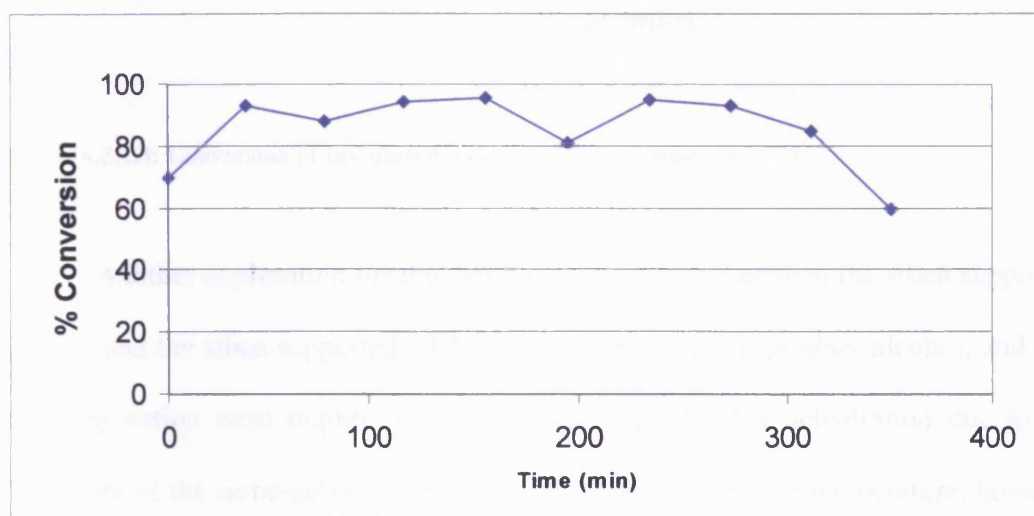


Figure 4.3.2.1: Conversion of isobutanol with 0.1g STA on silica 165°C reaction temperature

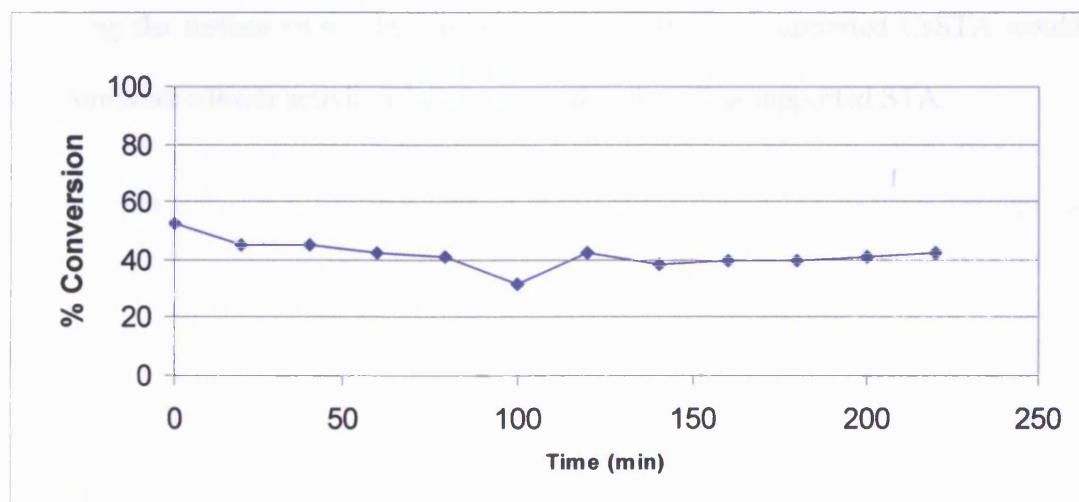


Figure 4.3.2.2: Conversion of isobutanol with 0.1g CsSTA on silica at 165°C reaction temperature

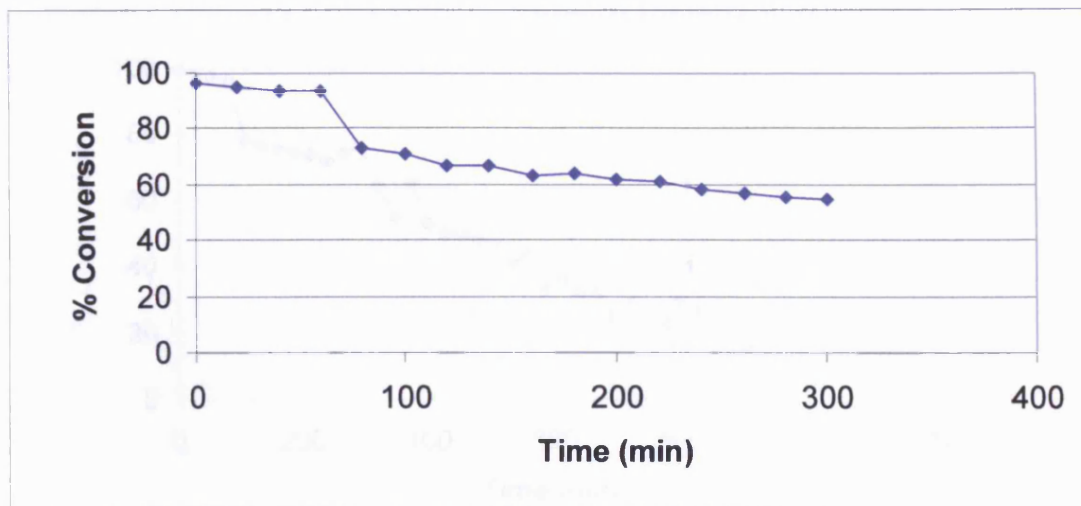


Figure 4.3.2.3: Conversion of isobutanol with 0.1g STA on silica at 175°C

Another explanation for the difference in activity between the silica supported CsSTA and the silica supported STA is that isobutanol is a primary alcohol, and that the dehydration must require a higher temperature for the dehydration due to the instability of the carbo-cations formed in the reaction. A higher temperature, however would not favour the adsorption of isobutanol into the bulk of the HPA, thus favouring the surface sites. The partially neutralised silica supported CsSTA would therefore have a lower activity when compared to the silica supported STA.

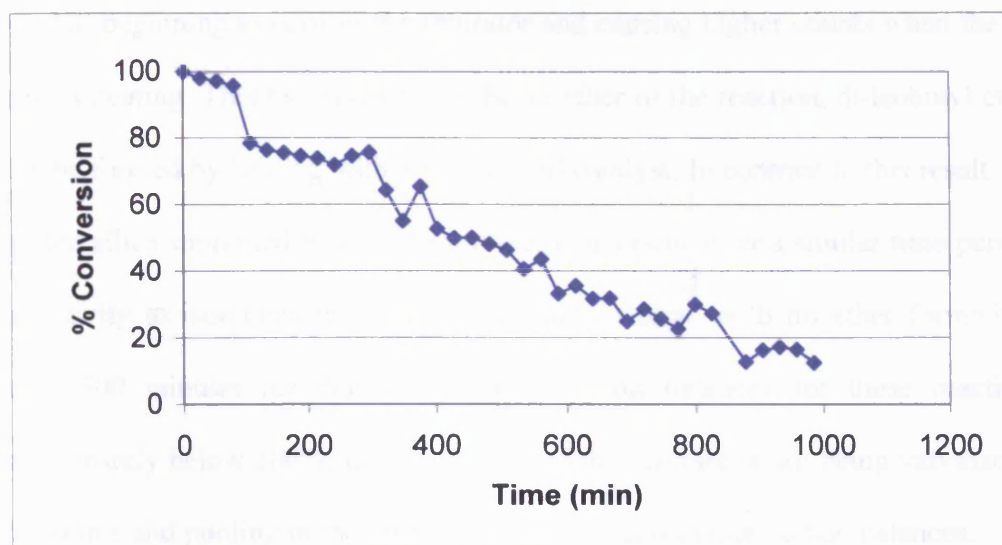


Figure 4.3.2.4: Conversion of isobutanol with 0.1g silica supported STA at 175°C, 30ml/min He, 3ml/hr isobutanol

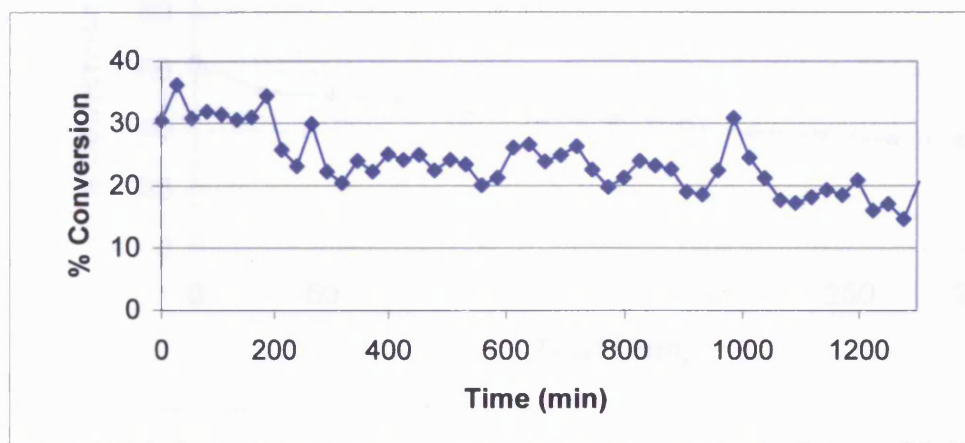


Figure 4.3.2.5: Conversion of isobutanol with 0.1g STA supported on carbon coated silica at 165°C, 30ml/min He, 3ml/hr isobutanol

Reactions with 0.1g of STA supported on silica at 175°C show the conversion steadily decreasing from nearly 100% conversion to 12% after 1000 minutes on stream. The %RSD of the twenty blank (no catalyst) injections before the reaction was run was 8%. The yield and selectivity to isobutene also decreases, while the selectivity to a by-product increases. The scatter of data points can be attributed to the

alcohol beginning to pool in the saturator and causing higher counts when the heating tape is heating. This by-product may be an ether of the reaction, di-isobutyl ether that can be formed by heating with a strong acid catalyst. In contrast to this result, carbon-coated silica supported STA gives a lower conversion over a similar time period. The selectivity to isobutene increases with reaction time, with no ether formation seen after 500 minutes reaction time. The carbon balances for these reactions are significantly below 100%, meaning some of the reactant is not being vaporised in the apparatus and pooling in the saturator leading to inaccurate carbon balances.

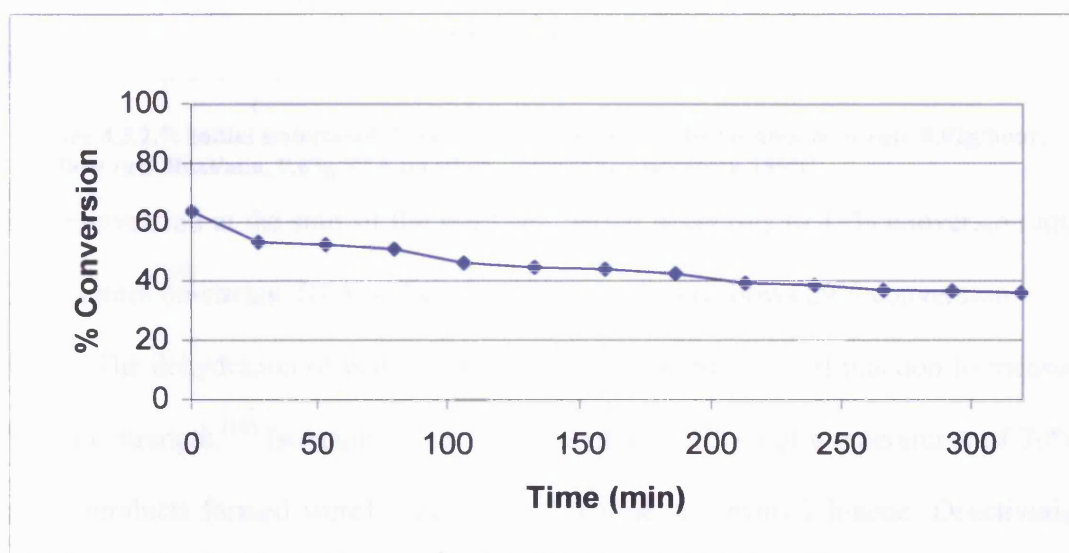
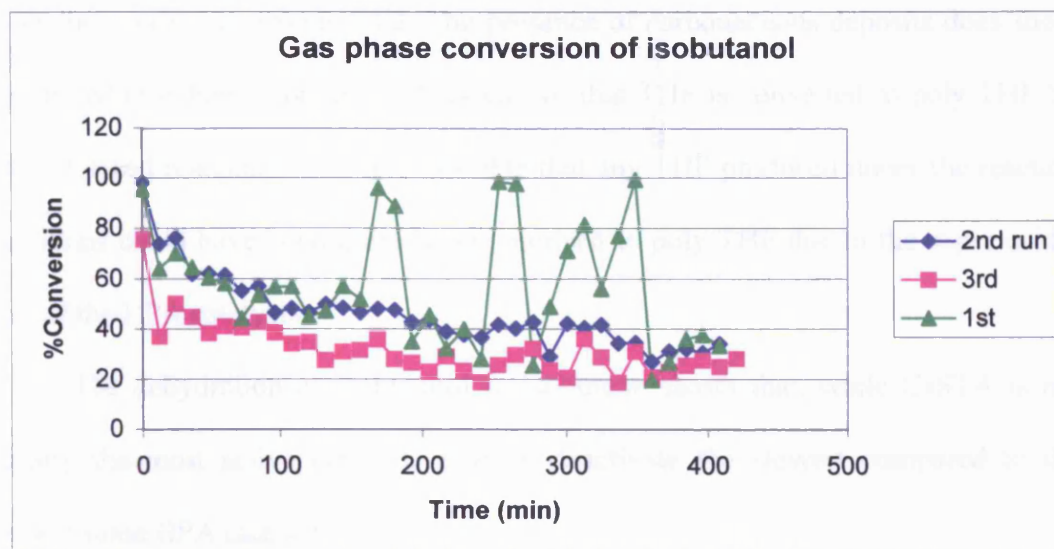


Figure 4.3.2.6: Conversion of isobutanol with 0.05g silica supported STA at 165°C, 30ml/min He, 3ml/hr isobutanol

STA supported on carbon-coated alumina appeared to be inactive for this reaction at the same reaction temperatures investigated. Lowering the reaction temperature to 100°C had an adverse effect on the reaction as none of the previously active catalysts gave any conversion.

Reactions with silica supported STA and silica supported CsSTA with a helium flow rate of 30ml/min show that the STA on silica deactivates rapidly from 93% conversion at the start of the reaction to 15% at 450 minutes on-stream. This is

in agreement with studies on HPA coking and regeneration <sup>(13)</sup> CsSTA on silica shows



**Figure 4.3.2.7: Initial isobutanol dehydration experiments** Isobutanol flow rate 0.92g/hour, He flow rate 30ml/min, 0.05g STA on silica, reactor temperature 155°C

55% conversion at the start of the reaction, which decreases to 43% conversion after 220 minutes on-stream. STA at the same time on stream shows 29% conversion.

The dehydration of isobutanol has been reported as a test reaction to measure catalytic strength.<sup>(16)</sup> Isobutanol was dehydrated with HPAs at temperatures of 70°C, major products formed were 1-butene, *cis*-2-butene and *trans*-2-butene. Deactivation by oligomerisation was not observed. The rate of 2-butanol dehydration decreased with increasing 2-butanol pressure, the mechanism proceeds by adsorption of 2-butanol onto the Brønsted sites by hydrogen bonds. The hydrogen bonded 2-butanol irreversibly decomposed by E1 type pathways, the dehydration is complete when the adsorbed reactants deprotonate to form the alkene.

#### 4.4 Conclusions

The analysis of BTD employed was unable to accurately determine the ratio of BTD to an internal standard, which is why the results were irreproducible. Also the



reoccurring problem of the reactor lines becoming blocked with a carbonaceous deposit showed that vapour phase cyclodehydration of BTM to THF is not feasible under the conditions investigated. The presence of carbonaceous deposits does show that the BTM is being converted. It is known that THF is converted to poly-THF by acid catalysed reactions<sup>(10-12)</sup>. It is possible that any THF produced under the reaction conditions could have been quickly polymerised to poly-THF due to the super acidic sites of the HPA catalysts.

The dehydration of isobutanol to isobutene shows that, while CsSTA is not initially the most active catalyst, it does deactivate the slowest compared to the unsubstituted HPA catalysts.

### References

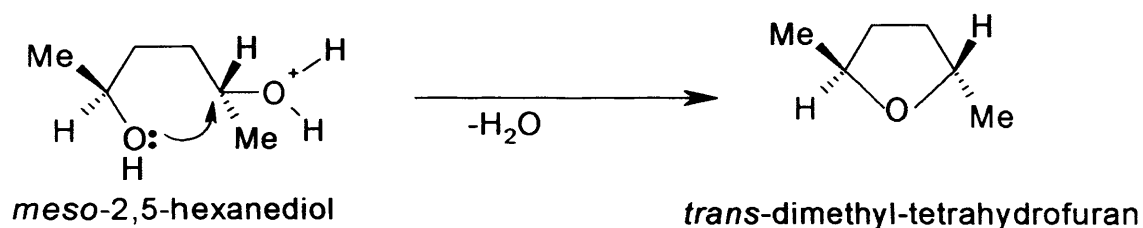
1. T. A. Peters, N. E. Benes, A. Holmen, J T.F. Keurentjes, *Applied Catalysis A: General* 297 (2006) 182–188
2. M.M. Doheim, S.A. Hanafy, G.A. El-Shobaky, *Materials Letters* 55 (2002) 304–311
3. Morrison, Boyd, *Organic Chemistry* 6<sup>th</sup> Edition, 1992, Prentice-Hall
4. A. Bielanski, A. Lubanska, J. Pozniczek, A. Micek-Ilnicka *Applied Catalysis A: General* 256 (2003) 153–171
5. A. Küksal, E. Klemm, G. Emig, *Applied Catalysis A: General* 228 (2002) 237–251
6. T. Haas, B. Jaeger, R. Weber, S.F. Mitchell, C.F. King, *Applied Catalysis A: General* 280 (2005) 83–88
7. V. Pallassana, M. Neurock, G. Coulston *Catalysis Today*, 50, (1999), 589-601
8. <http://www.chemsoc.org/chembytes/ezine/1996/lester.htm>

9. N. Yamamoto, S. Sato, R. Takahashi, K. Inui *Catalysis Communications* 6 (2005) 480–484
10. H. Li, H. Yin, T. Jiang, T. Hu, J. Wu, Y. Wada, *Catalysis Communications* 7 (2006) 778–782
11. I. V. Kozhevnikov, *Chemical Reviews* 98 (1998) 171-198
12. M.N. Timofeeva, *Applied Catalysis A: General* 256 (2003) 19–35
13. I. V. Kozhevnikov, S. Holmes, M.R.H. Siddiqui *Applied Catalysis A: General* 214 (2001) 47–58
14. S. Sato, R. Takahashi, T. Sodesawa, N. Yamamoto *Catalysis Communications* 5 (2004) 397-400
15. N. Yamamoto, S. Sato, R. Takahashi, K. Inui *Catalysis Communications* 6 (2005) 480-484
16. J. Match, R.T. Carr, E. Iglesia *Journal of Catalysis* 264 (2009) 54-66
17. I. V. Kozhevnikov *Journal of Molecular Catalysis A: Chemical* 305 (2009) 104-111

# Chapter Five: Liquid Phase Alcohol Dehydration

## 5.1 Introduction

Diols can readily undergo electrophilic dehydration reactions with a wide range of catalysts in homogeneous and heterogeneous conditions <sup>(1)</sup>. In the homogeneous cyclodehydration reaction of diols <sup>(2)</sup> (1,4-butanediol, 2,5-hexanediol, 2,5-dimethyl-2,5-hexanediol and 1,5-pentanediol) with four unsupported HPAs ( $H_3[PW_{12}O_{40}]$ ,  $H_3[PMo_{12}O_{40}]$ ,  $H_4[SiW_{12}O_{40}]$ ,  $H_4[SiMo_{12}O_{40}]$ ), all the diols were dehydrated to yield the corresponding cyclic ethers with high selectivity.



One diol, 1,6-hexanediol was found to produce oxacyloheptane, and five- and six-membered cyclic ethers. It was found that the weaker acid  $H_4[SiMo_{12}O_{40}]$  gave higher selectivity in this reaction, due to the limited ability to generate ring contraction by carbocationic processes. 2,5-dimethyl-2,5-hexanediol undergoes cyclodehydration with high selectivity with HPAs and is stereospecific, producing *cis*-2,5-dimethyltetrahydrofuran from racemic 2,5-hexanediol and *trans*-2,5-dimethyltetrahydrofuran from *meso*-2,5-hexanediol. The cyclodehydration occurs by an intramolecular  $S_N2$  mechanism. 1,2-diols (1,2-propanediol, isomeric 2,3-butanediols and 2,3-dimethyl-2,3-butanediol) undergo highly selective transformations into the analogous carbonyl compound (propanal, 2-butanone and

3,3-dimethyl-2-butanone). The four HPAs studied were all highly active and selective for this reaction, with highest selectivity from  $H_3[PW_{12}O_{40}]$ .

In the homogeneous dehydration of pentaerythritol (PE) to dipentaerythritol (DPE) at 150°C in a sealed Teflon tube with HPAs<sup>(3)</sup>, water was found to increase the formation of DPE over  $H_3[PW_{12}O_{40}]$ . The yield of the DPE decreased with the increase of water added because of a decrease in conversion. Supported  $H_4[SiW_{12}O_{40}]$  exhibited some activity without water present. The addition of water produced a negative effect on yield.

Product	$H_4[SiMo_{12}O_{40}]$	$H_3[PMo_{12}O_{40}]$	$H_4[SiW_{12}O_{40}]$	$H_3[PW_{12}O_{40}]$
2,3-dimethyl-1-butene	17	10	-	-
2,3-dimethyl-1-butadiene	15	20	29	22
Acetone	15	27	-	-
3,3-dimethyl-2-butanone	44	43	71	78
Unidentified	9	-	-	-

**Table 5.1.1:** selectivity of the dehydration of 2,3-dimethyl-2,3-butanediol at 150°C <sup>(2)</sup>

Supported and bulk form of the caesium salts of PTA have been used to catalyse the dehydration of xylose to furfural<sup>(4)</sup> in water/toluene or DMSO solvent system. It was found that in the water/toluene systems that the activity of the supported caesium salts were comparable to that of using 0.05M sulphuric acid and increasing the caesium salt PTA loading from 15 to 34 wt% or using a support with a larger pore diameter doubles the yield. It was noted that an increase in reaction temperature from 140 to 160°C triples yield.

Phosphotungstic acid and phosphomolybdic acid have been tested in liquid-phase reactions for the esterification of acetic acid with isoamyl alcohol to obtain isoamyl acetate with different supports<sup>(5)</sup>. The supports were silica, functionalised silica, polyvinyl alcohol hydrogel–polyethyleneglycol (PVA-PEG) beads, MCM-41 and functionalised MCM-41. The PVA-PEG beads showed the highest turnover rate out of the supports, this was attributed to the higher maximum acid strength of the PTA on the PVA-PEG beads (640mV) compared to the PTA on the other supports (185mV) when obtained by titration with *n*-butylamine.

1,4-butanediol has been dehydrated to 3-buten-1-ol over ceria catalysts<sup>(6)</sup> at 400°C. Using alumina and silica-alumina catalysts, the major product was THF with a selectivity of 78-99%. Using the ceria catalysts the selectivity to 3-buten-1-ol was increased to 68% at 400°C. It was found that at lower temperatures, the 1,4-butanediol reactant was strongly absorbed, meaning that the reactant was dehydrated further. It was found that the formation of homoallyl alcohol is the initial reaction of the stepwise dehydration of 1,4-butanediol into 1,3-butadiene.

THF has been converted to 1,4-diacetoxybutane by reacting THF with a mixture of acetic acid and acetic anhydride in the presence of an HPA catalyst<sup>(7)</sup>. The reaction conditions were 60°C with 50mg of either silicotungstic acid (STA) or phosphotungstic acid (PTA). In the case of the PTA catalysed reaction, the conversion is 100% at 120 minutes reaction time with a 50:50 mix of acetic acid: acetic anhydride. The high activity observed is probably due to their high acid strength, ability to form complexes with ethers and the HPA anions ability to enhance cationic organic intermediates.

Caesium salts of HPAs have been shown to be water tolerant<sup>(7-10)</sup> and have higher surface areas than their parent acid. This enables them to be in a polar medium,

which would otherwise leach the active catalyst from the support. Other techniques of immobilising HPAs has included the grafting of the acid onto the support <sup>(13,14)</sup> encapsulating the HPA in a zeolite cage <sup>(5, 15-18)</sup>

### 5.2 Geraniol Dehydration

Geraniol is a naturally occurring monoterpenoid and is the primary constituent of oil-of-rose and palmarosa oil. It has a strong rose-like odour and is frequently used in the perfume and cosmetic industries as a result. Geraniol has found use not only as a constituent in perfumes and other personal care products, it has also found to be a natural insect repellent

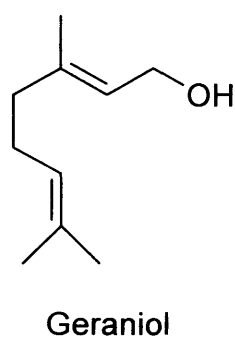
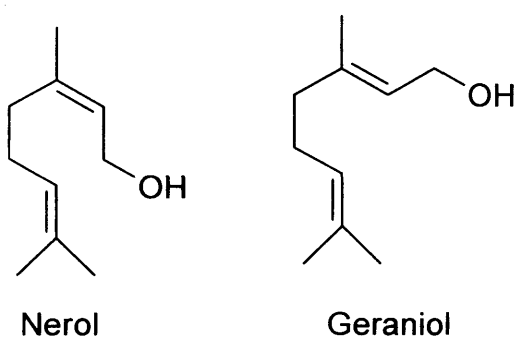


**Figure 5.2.1: Geraniol and its isomer, nerol**

The most common dehydration products of geraniol are geranial, geranic acid, limonene, linalool, citral, pinene oxide, perillyl alcohol and beta-pinene.

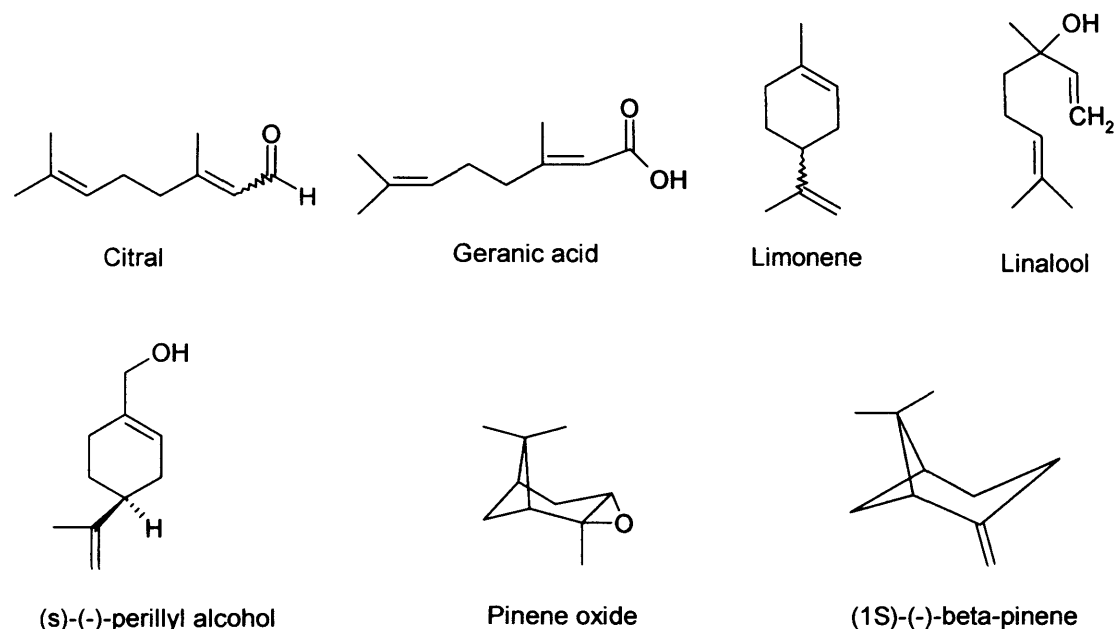


Figure 5.2.2: Possible products for the dehydration of geraniol

The possibility of catalysing the transformation of geraniol to another aroma compound would be of interest to the perfumery and cosmetic industries. One possible target compound is limonene, which is used extensively in the perfume, cosmetic industries. It is also found in some foods as flavouring and has found some use as an environmentally friendly replacement for mineral oils for cleaning machine parts as it is more biodegradable than mineral oils and can come from a renewable source.

### 5.2.1 Initial Reactions

Initial blank reactions were carried out at room temperature with no HPA catalyst present. No reaction was observed when analysed with a Varian 3400 Gas Chromatograph (GC) fitted with a 30-metre Chrompack capillary column coated with CP-Sil 8 CP. The detector used on the GC was an FID. The target compound from the acid catalysed dehydration of geraniol was limonene.

Reactions were carried out with supported and unsupported free HPA and caesium salts of HPAs. Initial reactions with catalyst showed that the conversion of geraniol was greatest with silicotungstic acid when compared to phosphotungstic acid.

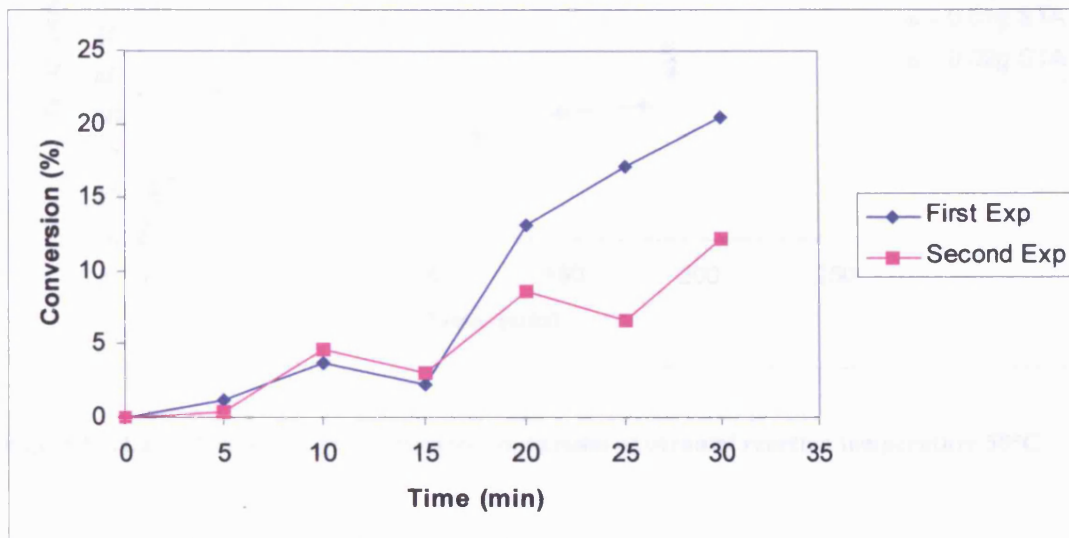


Figure 5.2.1.1: Conversion of geraniol with 0.01g STA at 50°C

The main identifiable products of the reaction as described in figure 5.2.1.1 are limonene and linalool; the selectivities of these products are 6 and 12% respectively.

Initial reactions show good reproducibility under the same conditions but suffer from low conversions and low selectivity to limonene. The main products from the reaction are linalool and limonene with a substantial number of by-products, which do not correspond to the retention times of geraniol, geranic acid, citral, pinene oxide, perillyl alcohol and beta-pinene. These could be other isomers that geraniol and its isomer, nerol, are known to produce on dehydrating:  $\beta$ -myrcene,  $\beta$ -ocimene,  $\alpha$ -terpinene, and terpinene.



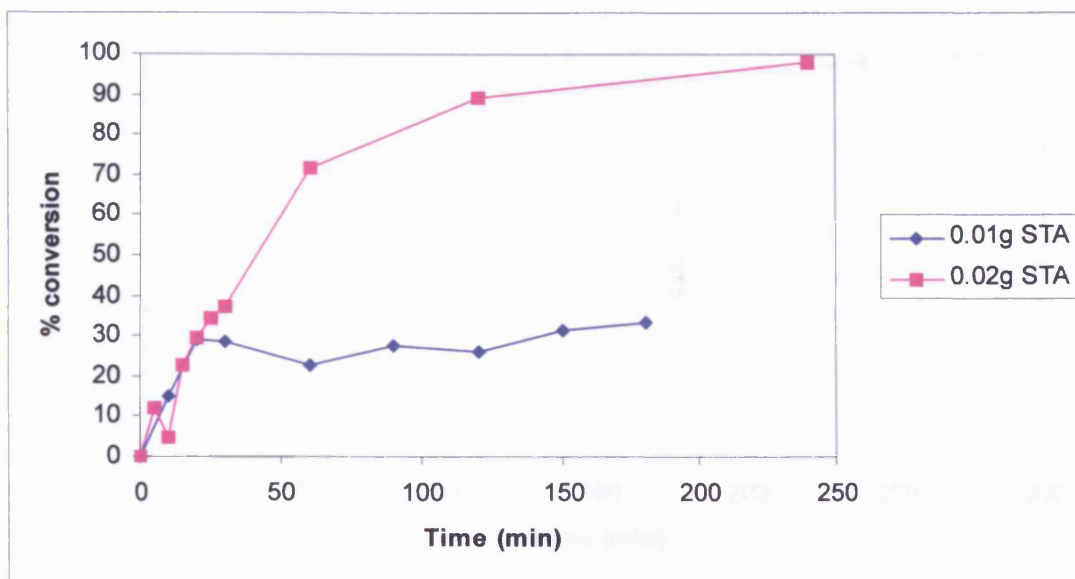


Figure 5.2.1.2: Effect of catalyst weight on conversion of geraniol reaction temperature 50°C

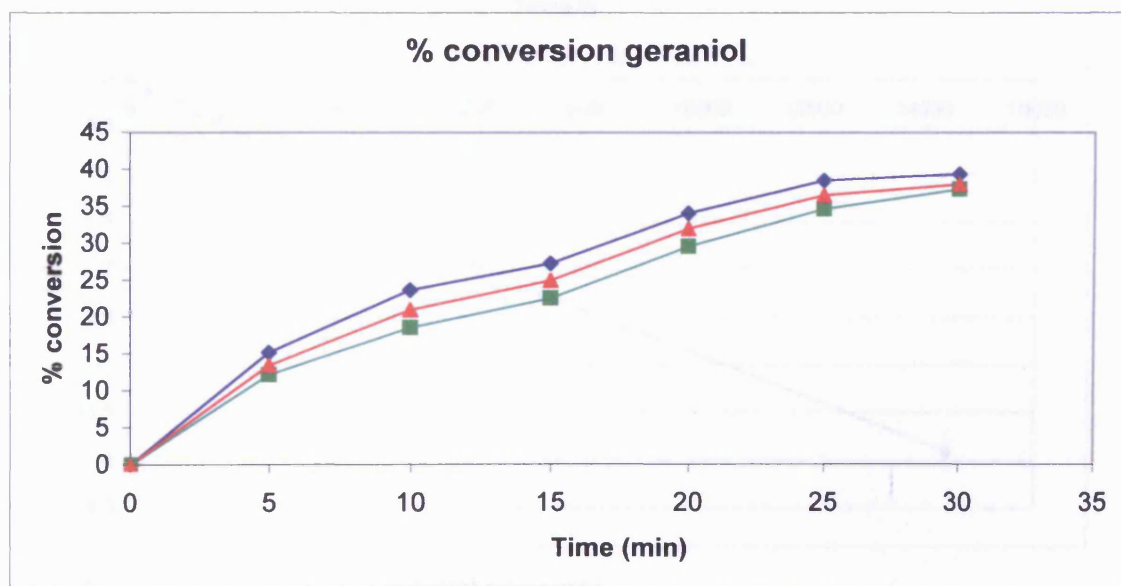


Figure 5.2.1.3: Geraniol conversion at 50°C using 0.02g STA

Figure 5.2.1.3 shows the agreement of results for the dehydration of geraniol using 0.02g of STA. The results agree within a few percent of each other showing that the reaction is reproducible.

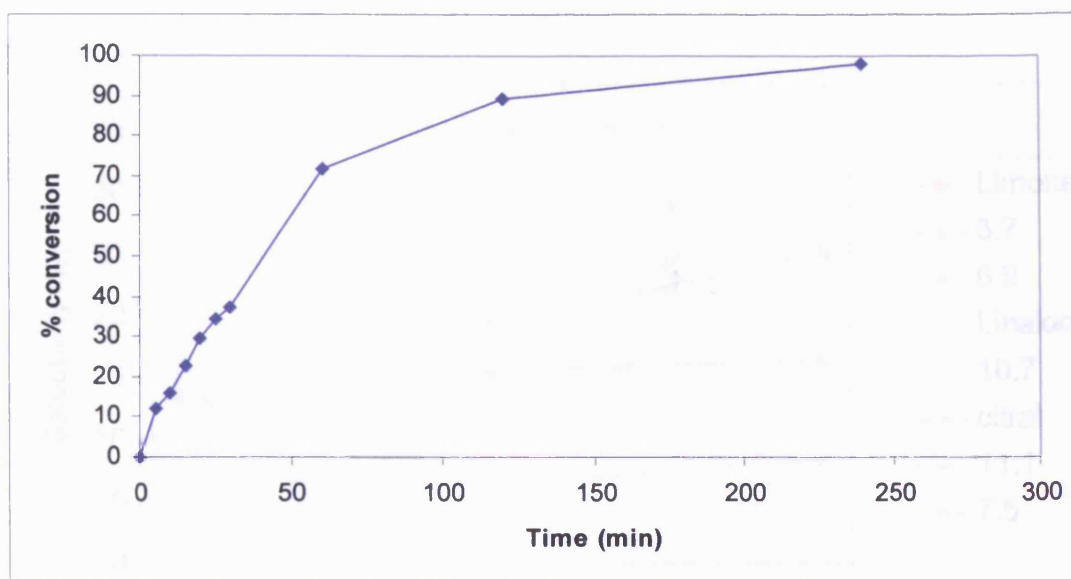


Figure 5.2.1.4: Geraniol conversion at 50°C using 0.02g STA

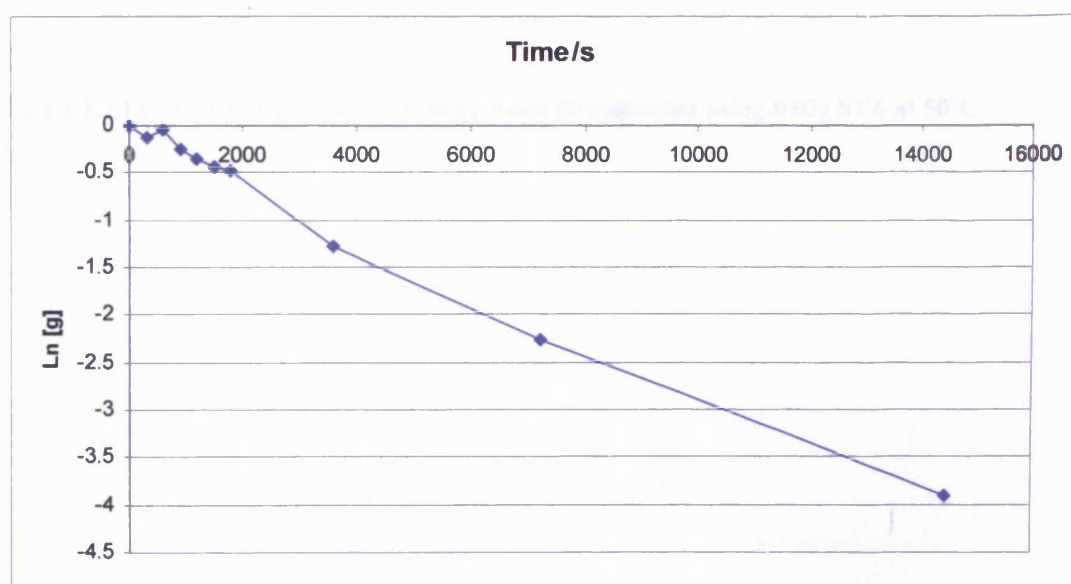


Figure 5.2.1.5: First order plot of geraniol conversion

The reactions with 0.02g of unsupported STA show an increase in conversion of geraniol with increasing reaction time. The major product of the reaction is linalool, until the reaction time reaches 100 minutes. After this time the major product is limonene. There are a number of unidentified products which could be related to any impurities present in the starting material.

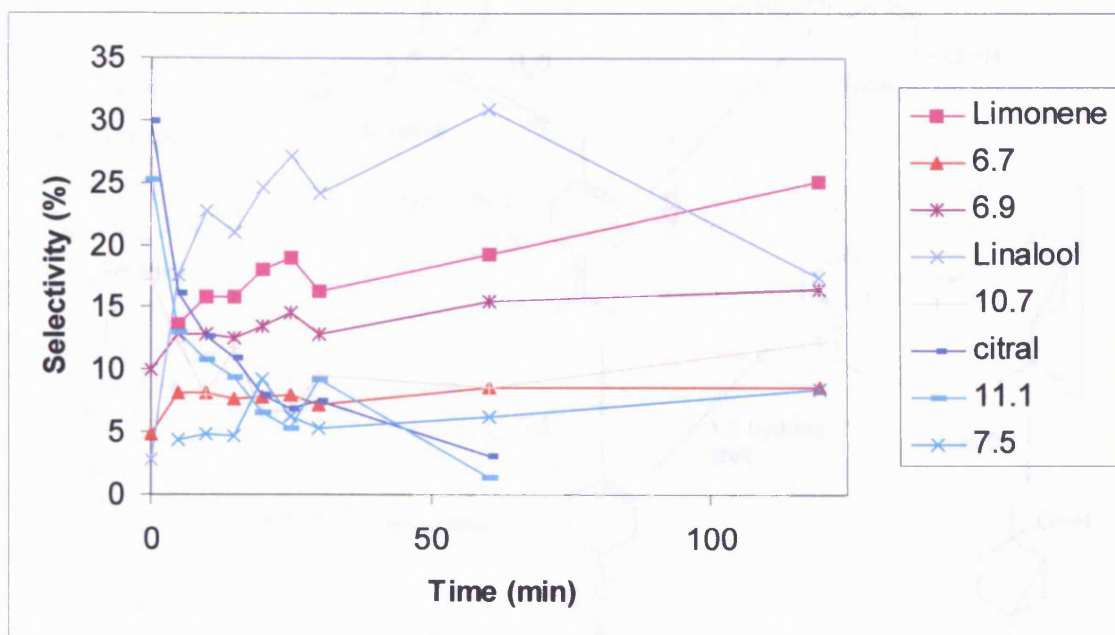


Figure 5.2.1.6: Selectivity of products in geraniol dehydration using 0.02g STA at 50°C

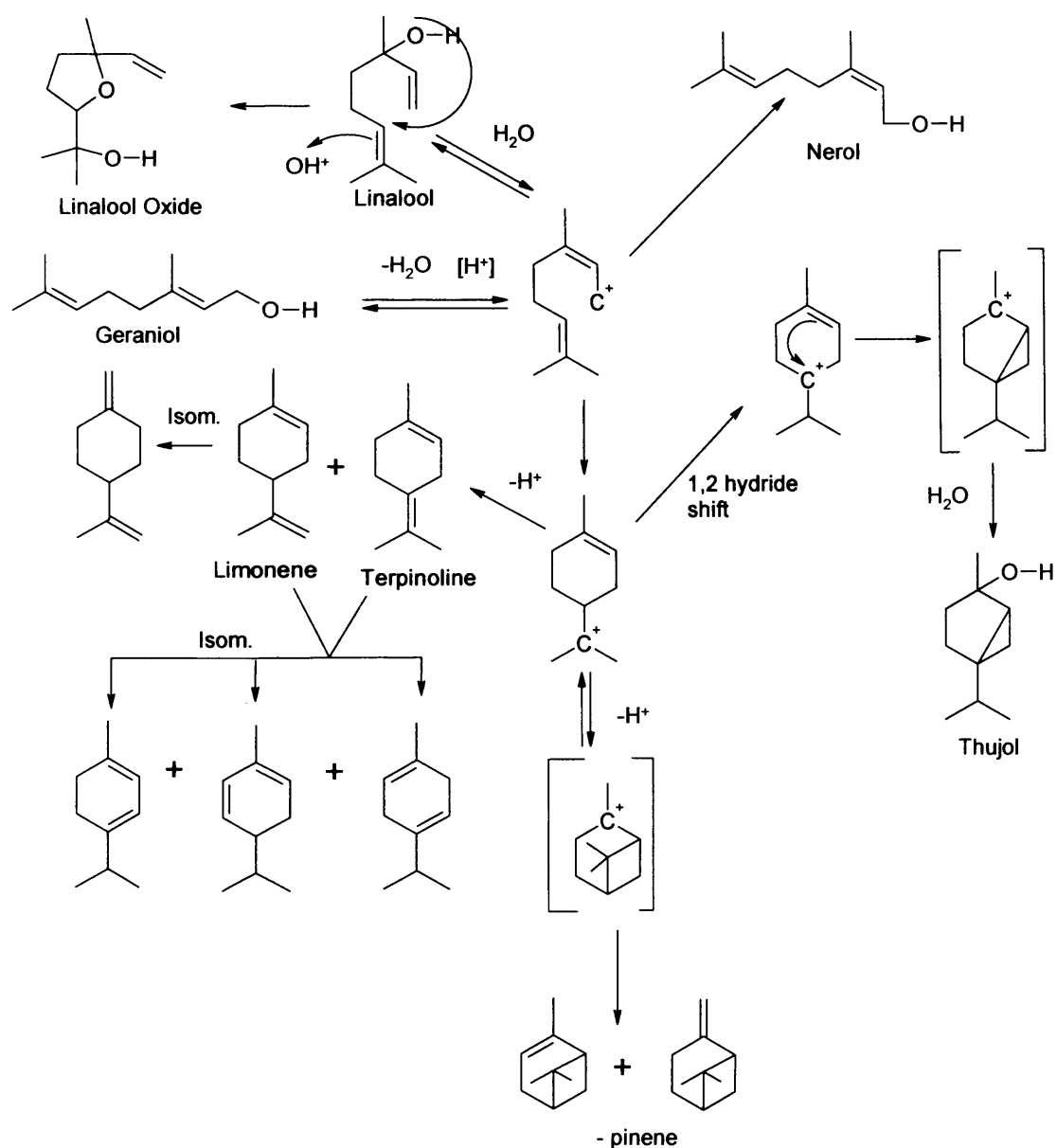
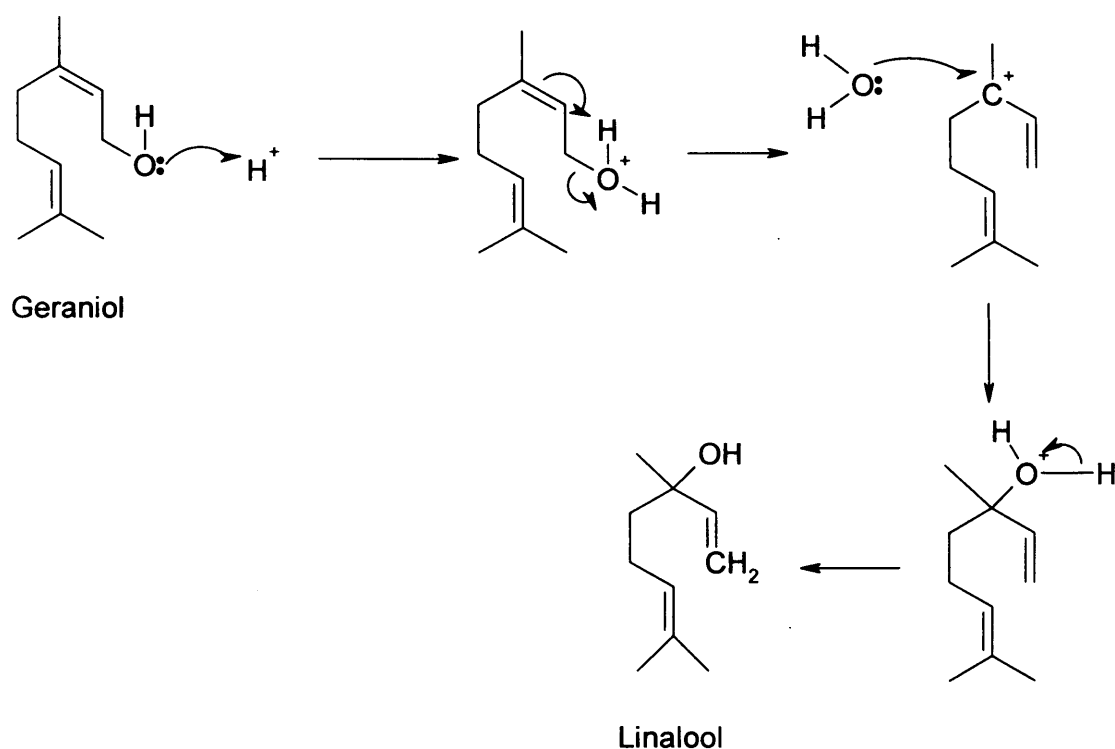


Figure 5.2.1.7 Possible reaction scheme for the acid catalysed reaction of geraniol<sup>(18)</sup>

Limonene is not the major product until the reaction has been proceeding for at least 100 minutes. Linalool, which is the main product, is an isomer of geraniol that is not present in the initial reaction mix, but is observed at five minutes reaction time. A possible mechanism for the rearrangement is shown in figure 5.2.1.8. The hydroxyl group on geraniol is protonated and undergoes internal re-arrangement with the loss of water, leaving a tertiary carbo-cation. This carbo-cation is then attacked by the

water present and undergoes re-arrangement to form linalool with the re-generation of a proton.



**Figure 5.2.1.8: Possible mechanism for the re-arrangement of geraniol to linalool**

### 5.2.2 Caesium Salts of Silicotungstic Acid

The partially neutralised unsupported caesium salt of STA was used in order to assess the stability of the salt under experimental conditions. The substitution of an acidic proton for a caesium cation would have the effect of decreasing the solubility of the HPA in solution. It is the insoluble catalysts, which may be removed and recycled after the reaction is complete, can contribute to more environmentally friendly chemical processes.

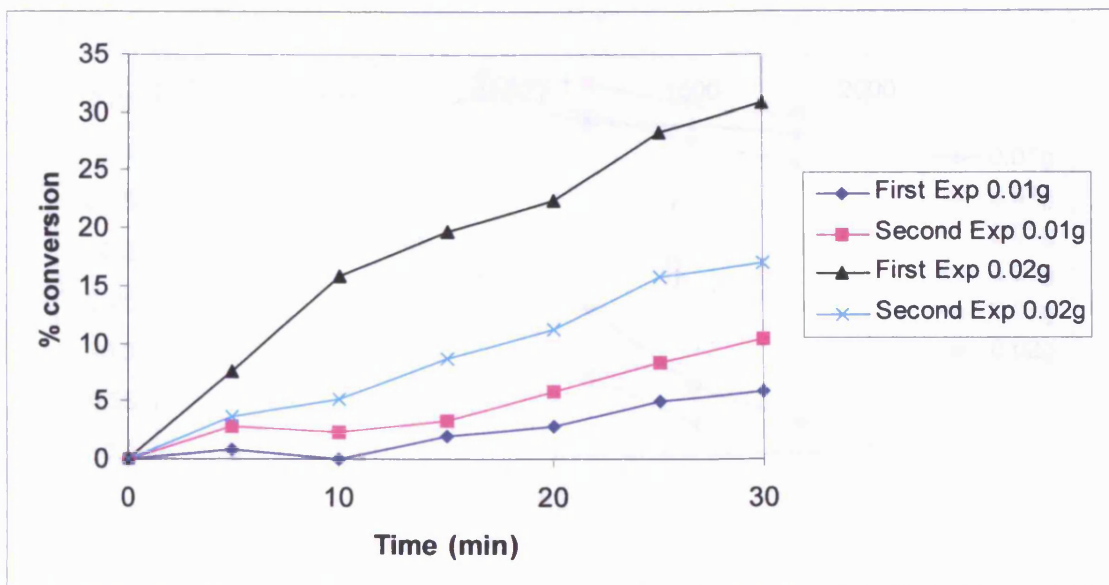


Figure 5.2.2.1: Conversion of geraniol at 50°C using 0.01g and 0.02g CsSTA

As expected, the conversion was lower than the unsupported free salt, due to the neutralisation of the most active proton of the HPA by caesium. The selectivity of the product remains comparable to the free STA after thirty minutes reaction time. Doubling the amount of catalyst in the reaction increases the rate of reaction ( $k$ ) from around  $3.5 \times 10^{-5}$  to around  $2.0 \times 10^{-4}$ . Typically reaction rates are independent of concentration but depend on temperature. However reaction rates can be influenced by an increase of catalyst present, thereby providing an alternate reaction pathway with a greater number of acid sites present.

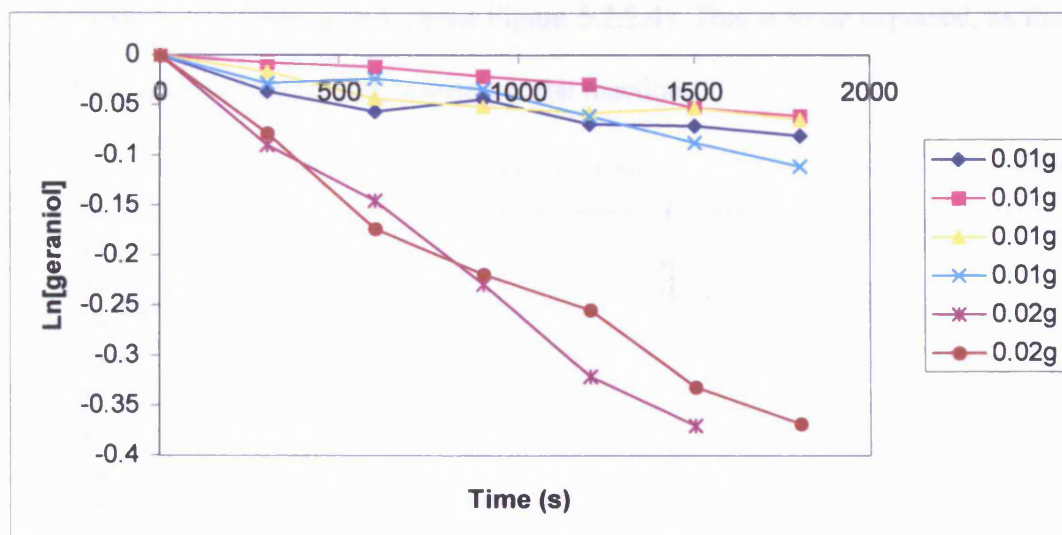


Figure 5.2.2.2: Kinetics of reactions with 0.01g and 0.02g CsSTA

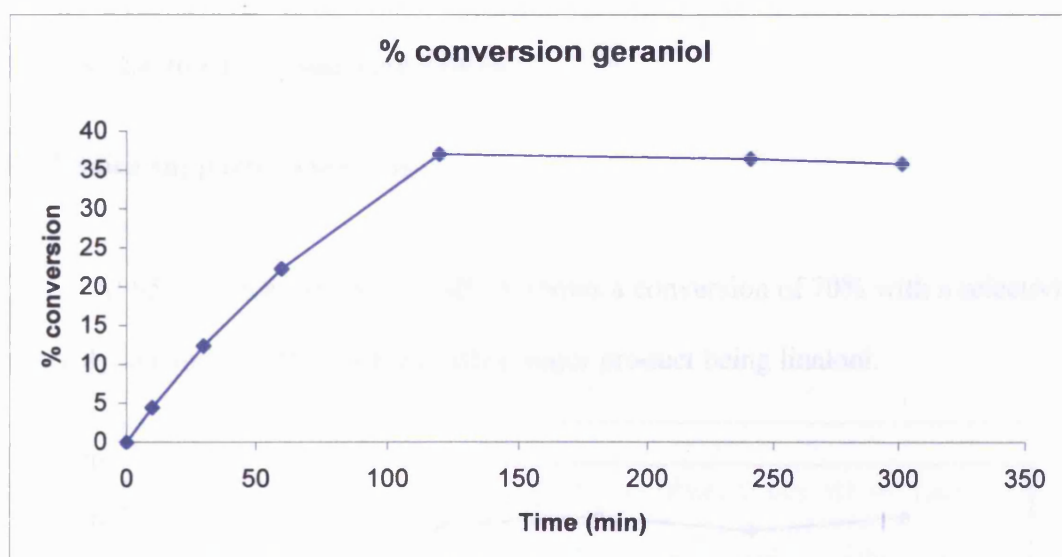


Figure 5.2.2.3: Reaction with 0.01g unsupported CsSTA at 95°C

The major product at 95°C is perillyl alcohol (see figure 5.2.2 for structure) in both the supported and unsupported reactions. Experiments at 50°C show the major product to be linalool. This may be due to the higher temperature enabling the rearrangement of geraniol to perillyl alcohol. Reactions with unsupported

Cs<sub>4</sub>STA show very little activity, (see Figure 5.2.2.4). This is to be expected, as there should be no available protons to catalyse the reaction.

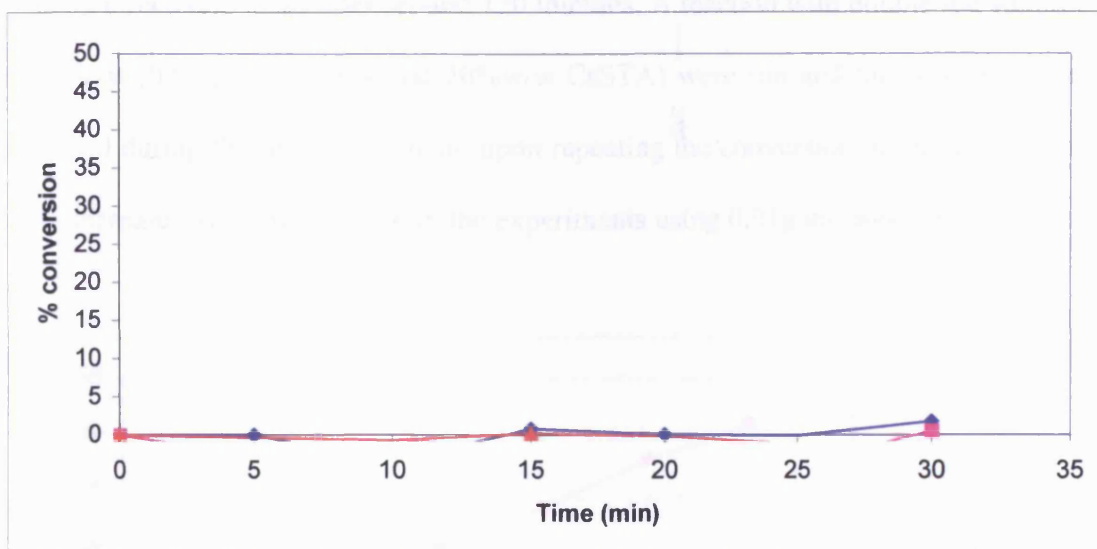


Figure 5.2.2.4: Reactions using 0.01g Cs<sub>4</sub>STA

### 5.2.3 Silica supported catalysis

At 95°C, silica supported CsSTA shows a conversion of 70% with a selectivity to perillyl alcohol of 70% with the other major product being linalool.

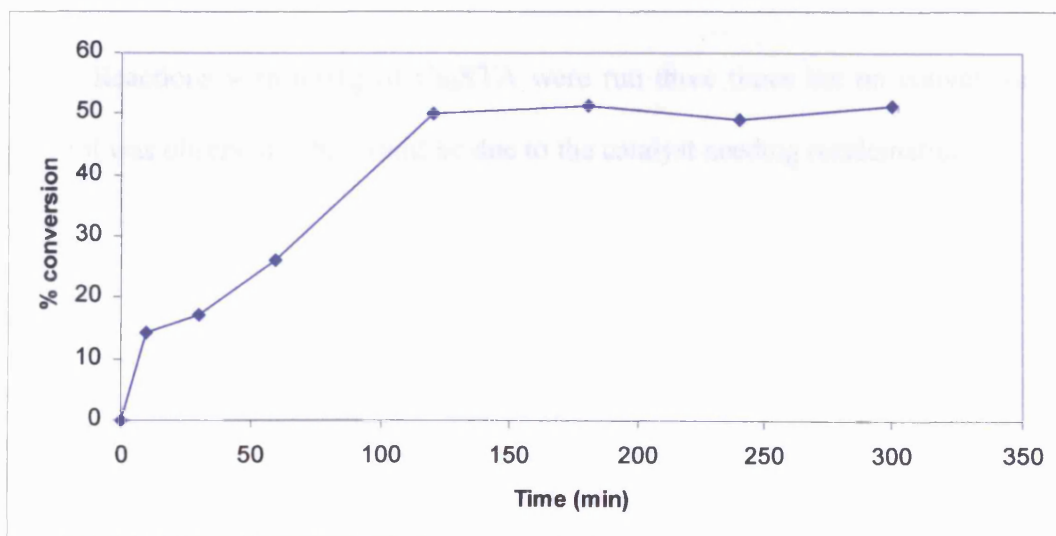


Figure 5.2.3.1: Reaction with 0.1g silica supported CsSTA at 95°C



The silica supported CsSTA gives a higher conversion at 95°C than the unsupported CsSTA, this may be due to the higher surface area of the catalyst. The reaction effectively stops after around 120 minutes. A reaction with double the weight of catalyst (0.02g silica supported 20%w/w CsSTA) were run and the conversion is increased during the first experiment, upon repeating the conversion in the same time scale decreases to the levels seen in the experiments using 0.01g unsupported CsSTA.

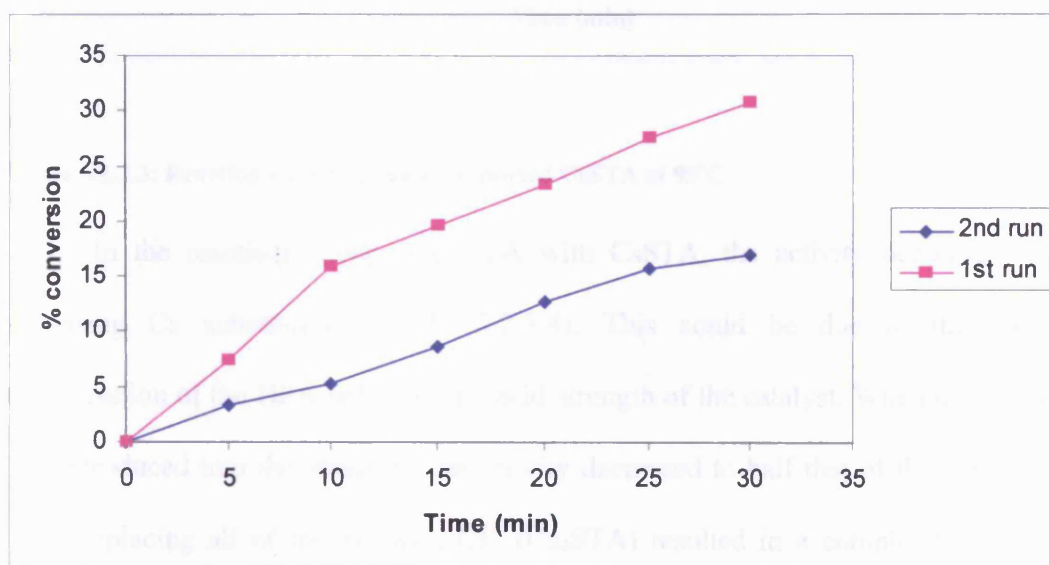


Figure 5.2.3.2: Conversion of geraniol with 0.02g silica supported CsSTA

Reactions with 0.01g of Cs<sub>2</sub>STA were run three times but no conversion of geraniol was observed. This could be due to the catalyst needing recalcination.

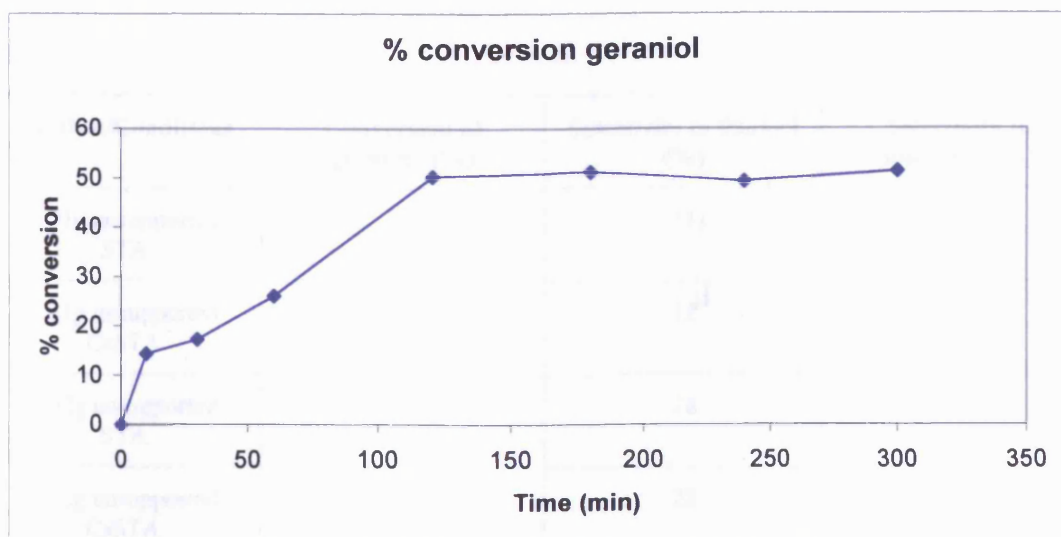


Figure 5.2.3.3: Reaction with 0.1g silica supported CsSTA at 95°C

In the reactions comparing STA with CsSTA, the activity decreases with increasing Cs substitution (Table 5.2.3.4). This could be due to the partial neutralisation of the HPA reducing the acid strength of the catalyst. When one Cs ion was introduced into the structure the activity decreased to half that of the free STA, while replacing all of the  $H^+$  with  $Cs^+$  ( $Cs_4STA$ ) resulted in a completely inactive catalyst. Comparing the HPA catalysts to HCl shows that although the number of moles of protons is comparable, the super acidic nature of the HPAs enables the rearrangement of geraniol.

## Liquid Phase Alcohol Dehydration

Catalyst/Conditions	Conversion of geraniol (%)	Selectivity to linalool (%)	Selectivity to limonene (%)
0.01g unsupported STA	15	12	6
0.01g unsupported CsSTA	7	12	5
0.02g unsupported STA	38	28	17
0.02g unsupported CsSTA	30	28	18
0.01g unsupported Cs <sub>4</sub> STA	0	0	0
HCl	0	0	0

**Table 5.2.3.4: Unsupported free and Cs substituted STA**

Catalyst/Conditions	Conversion of geraniol (%)	Selectivity to linalool (%)	Selectivity to limonene (%)
0.1g Matrex silica supported CsSTA	19	32	26
0.1g Coarse silica supported CsSTA	5	26	17
Reuse of coarse silica supported CsSTA	5	6	7
0.1g Fine silica supported CsSTA	13	21	6
Reuse of fine silica supported CsSTA	8	10	7

**Table 5.2.3.5: Effect of support on conversion and selectivity**

In the supported HPAs, the number of Keggin units is the same as in the unsupported work. Supporting the CsSTA on a high surface area support with a loading of 20% increased the conversion of geraniol and significantly increased the selectivity to limonene and linalool. Experiments with fine grain silica supported HPAs also show another product in the chromatogram, identified as pinene oxide with

a selectivity of 10%. When HPA was supported on coarse grain silica, the conversion was lower than the unsupported HPAs. This may be due to the method of depositing the HPA on the coarse grain silica not achieving the desired level of loading. However the selectivity was higher for both limonene and linalool for the coarse grain silica supported CsSTA than for the unsupported HPAs. Another possible explanation could be that because the fine grain silica has a higher surface area than the coarse grain silica, the reactants may be diffusionally 'trapped' closer to the active sites in the catalyst. The reactants in the coarse grain silica are able to diffuse away from the active sites at a higher rate than in the fine grain silica and therefore do not undergo further reaction to pinene oxide. Another explanation is that the higher surface areas in the fine grain silica act to stabilise cationic intermediates, allowing different product selectivities to be possible. Other supports and solid acids could be used to see how these effect the product distribution.

### **5.2.4 Effect of Water on activity**

The addition of water into the reaction mixture shows retardation in conversion in the same time scale as the previous experiments. This could be attributed to the water in the reaction mixture competing for the acidic sites in the catalyst or shifting the equilibrium of the reaction further from the products, as water is a product from a dehydration reaction and a nucleophile, which would possibly cause the formation of other oxygenated compounds. The amount of water added was 20 $\mu$ l as this was calculated to be enough to poison the acid sites in the catalyst. After 30-minute reaction time the conversion for the CsSTA is between 6-12% and the addition of water does not significantly slow the reaction down under the time scale investigated.

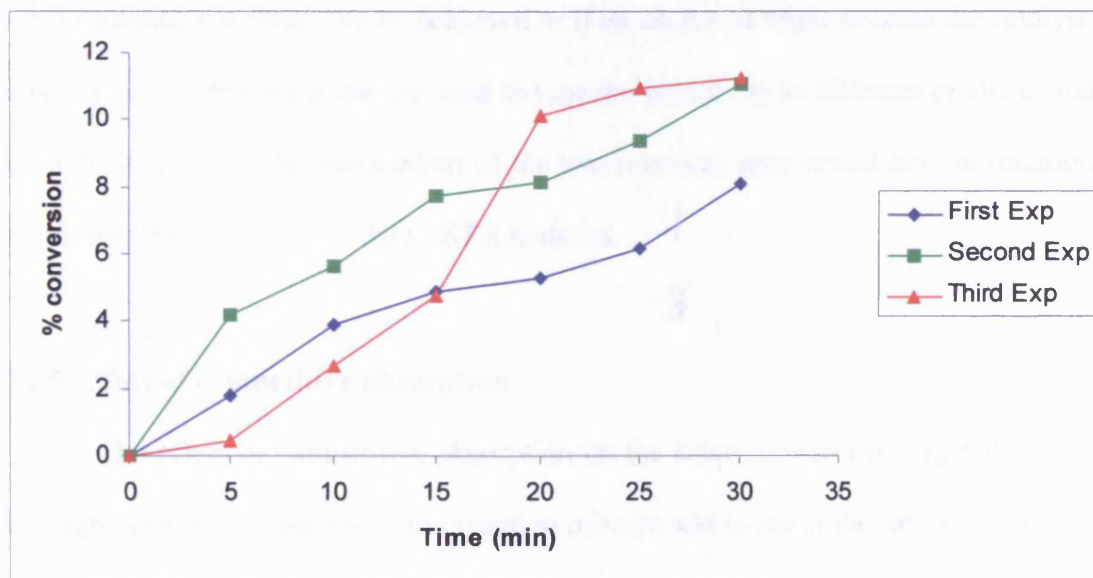


Figure 5.2.4.1: Effect of water addition on geraniol conversion using 0.02g CsSTA

Catalyst/Conditions	Conversion of geraniol (%)	Selectivity to linalool (%)	Selectivity to limonene (%)
0.01g CsSTA	7	12	5
Water added to 0.01g CsSTA	10	6	9
0.01g CsSTA filtered after 5 minutes	5	6	3

Table 5.2.4.2: Effects of water addition and filtering on reaction

The CsSTA catalysts were shown to be tolerant to the addition of 20 $\mu$ l of water. As conversion of geraniol increased from 7% to 10%, it is possible that the added water enhanced the reaction by solvating the CsSTA. This increase in activity was coupled with a change in the selectivity to the two major products. The addition of water could increase the formation of limonene due to the water stabilising the carbocation intermediates, favouring the formation of limonene. By adding increasing amounts of water to the reaction it may be possible to see whether further

enhancements in activity can be achieved or if an excess of water poisons the catalyst.

It is interesting that water can be used to tune the selectivity to different products and an understanding of the mechanism of the two reactions may reveal key information about the effect of water on the CsSTA material.

### 5.2.5 Effect of competitive absorption

The effect of competitive absorption on the catalysts was investigated due to the high number of products in the reaction mixture and to see if the internal standard adversely affected the conversion of geraniol.

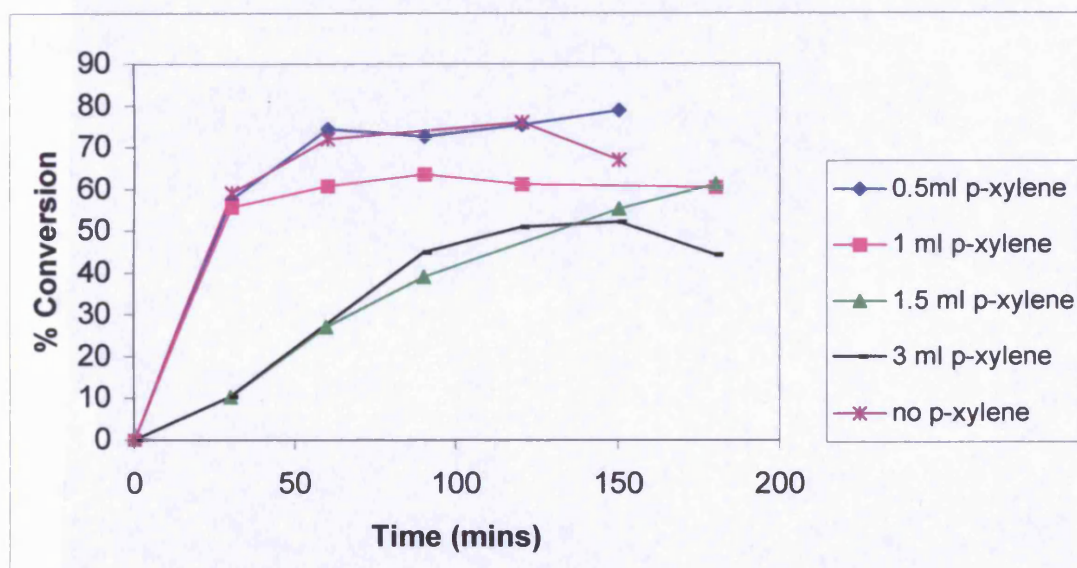


Figure 5.2.5.1: Effect of *p*-xylene addition on geraniol conversion

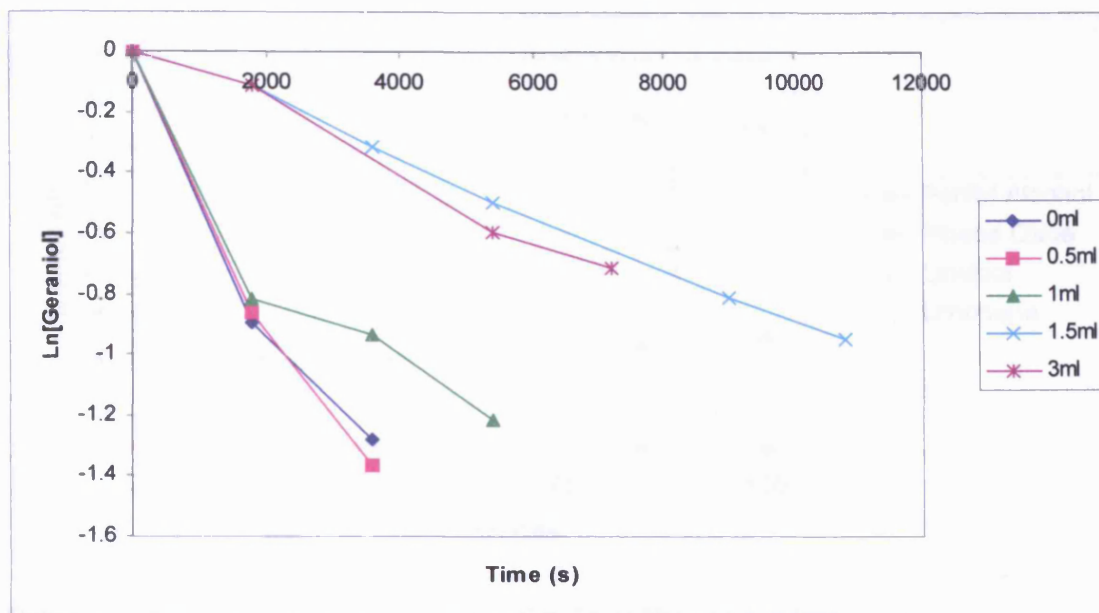


Figure 5.2.5.2: Kinetics of geraniol conversion with differing volumes of *p*-xylene

The liquid phase geraniol reaction with no *p*-xylene in the reaction mixture was repeated three times with similar results, with the final conversion of geraniol around 60-70%. Limonene was the major product in the reactions carried out with no *p*-xylene present in the reaction mixture.

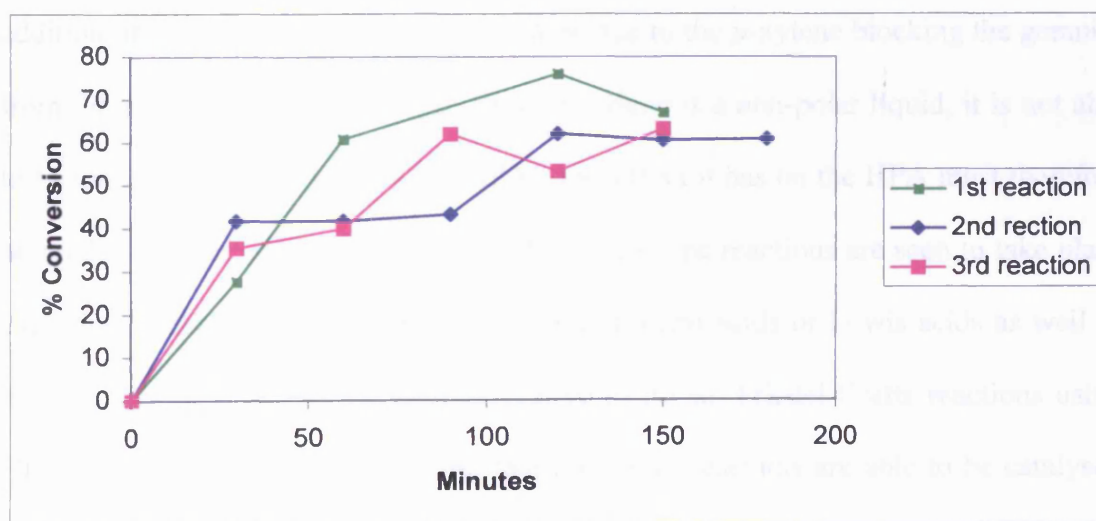


Figure 5.2.5.3: 0.1g CsSTA at 90°C, no *p*-xylene

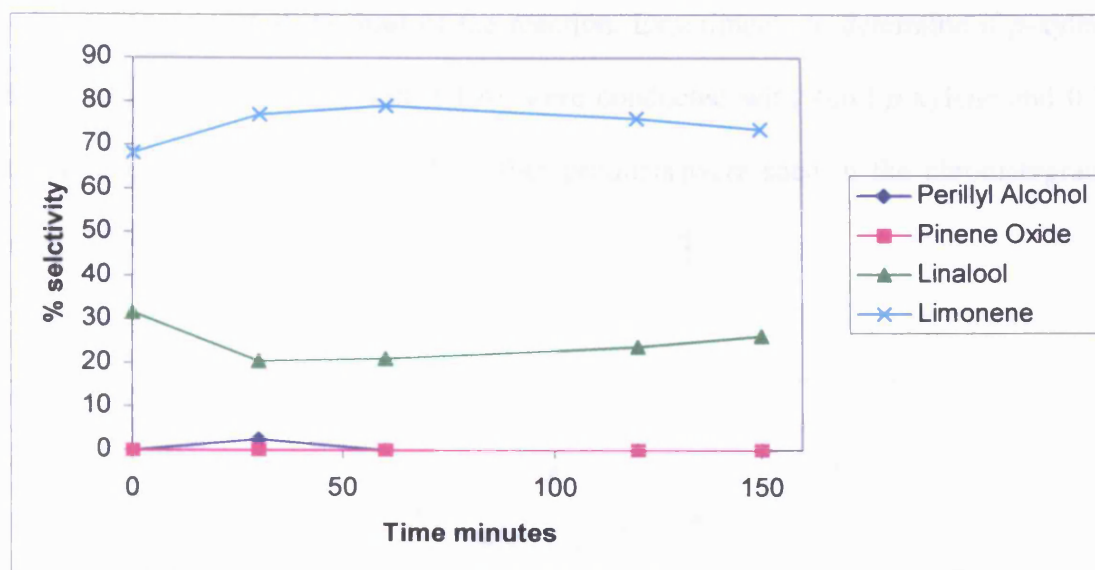


Figure 5.2.5.4: Selectivity of above reaction, CsSTA at 90°C, no *p*-xylene

The CsSTA is sensitive to competitive adsorption, as only 1ml of *p*-xylene in the starting material is enough to decrease the final conversion at 180 minutes from 70 to 60%. Increasing the amount of *p*-xylene effects the conversion, the most noticeable effect is after 1.5ml *p*-xylene, where the initial rate of conversion is significantly lower than that of the experiments with 0.5 and 1ml *p*-xylene. From the kinetic first order plots obtained it also shows that the rate of reaction does decrease with the addition of 1.5ml of *p*-xylene. This could be due to the *p*-xylene blocking the geraniol from the active site of the catalyst. Since *p*-xylene is a non-polar liquid, it is not able to be absorbed into the bulk of the HPA. Any effect it has on the HPA must therefore be on the exterior of the HPA. No Friedel-Crafts type reactions are seen to take place even though these reactions require a strong mineral acids or Lewis acids as well as the presence of a carboxylic acid derivative to do so. Friedel-Crafts reactions using HPAs are well known<sup>(20-23)</sup> showing that non-polar reactants are able to be catalysed by HPAs in Friedel-Crafts type reactions. This may mean that the reaction is very sensitive to competing substrates as 1.5ml *p*-xylene equates to only 3.75% of the



volume of geraniol at the start of the reaction. Experiments to determine if *p*-xylene reacts under the influence with HPAs were conducted with 40ml *p*-xylene and 0.1g silica supported STA at 95°C. No other products were seen in the chromatograms after 1220 minutes' reaction time.

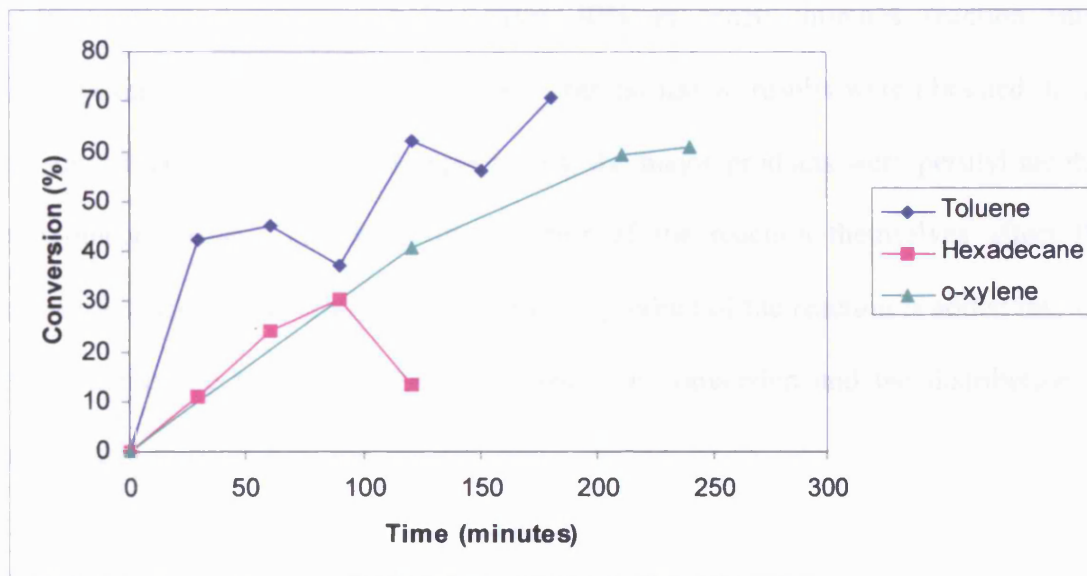


Figure 5.2.5.5: Effect of various compounds on geraniol conversion

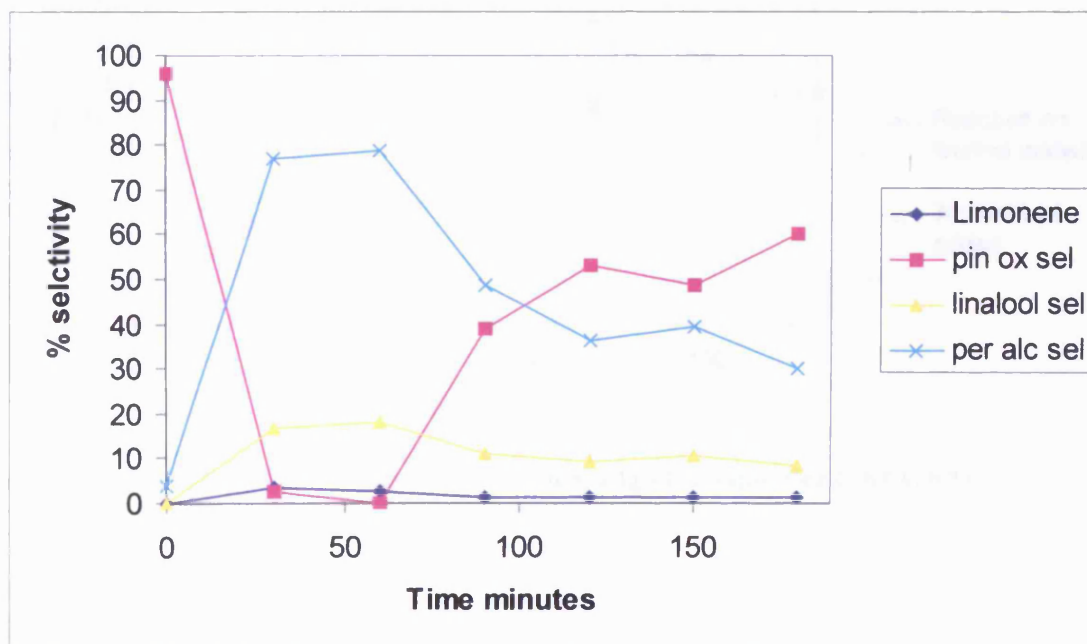


Figure 5.2.5.6: Selectivities of products, 2ml toluene doping

In order to see if any other compounds may block or adsorb on to the active sites of the catalyst, four compounds of similar molecular mass to *p*-xylene were chosen. In the potential poisoning experiments, 1.5ml of the poisons under investigation was added to the reaction mixture prior to the addition of catalyst. Of the poisons investigated, hexadecane had the most significant effect on conversion, as the conversion of geraniol was less than 30% at ninety minutes reaction time. Cyclohexane was also tested as a poison, but no usable results were obtained. In all poison/competitive adsorption experiments, the major products were perillyl alcohol and pinene oxide. To test if the product of the reaction themselves affect the conversion, experiments were run in which a product of the reaction is added into the reaction mixture to see if there is a change in conversion and the distribution of products.

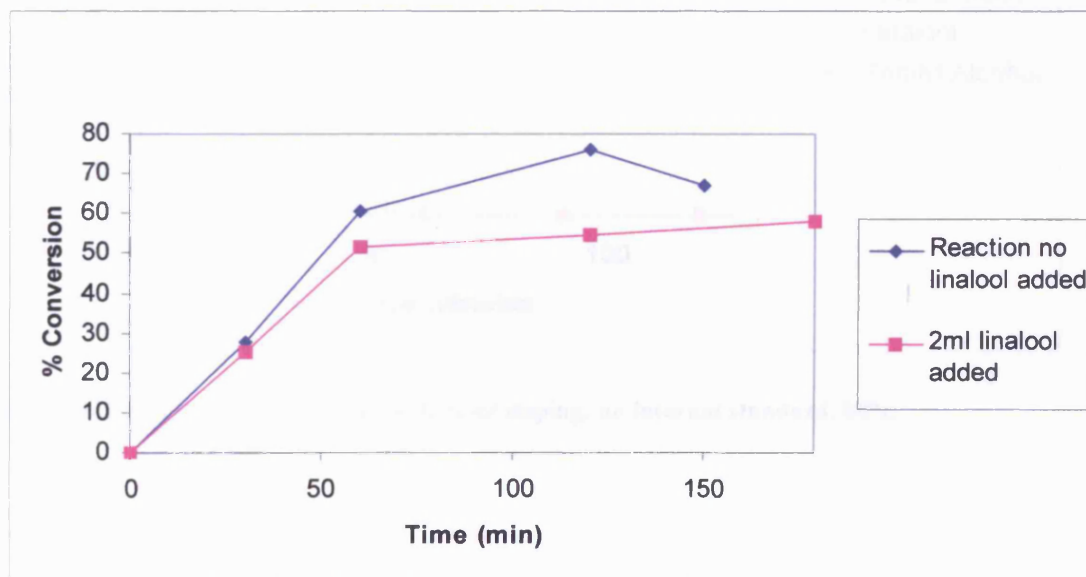


Figure 5.2.5.7: Effect of 2ml linalool on conversion, 0.1g silica supported CsSTA, 80°C

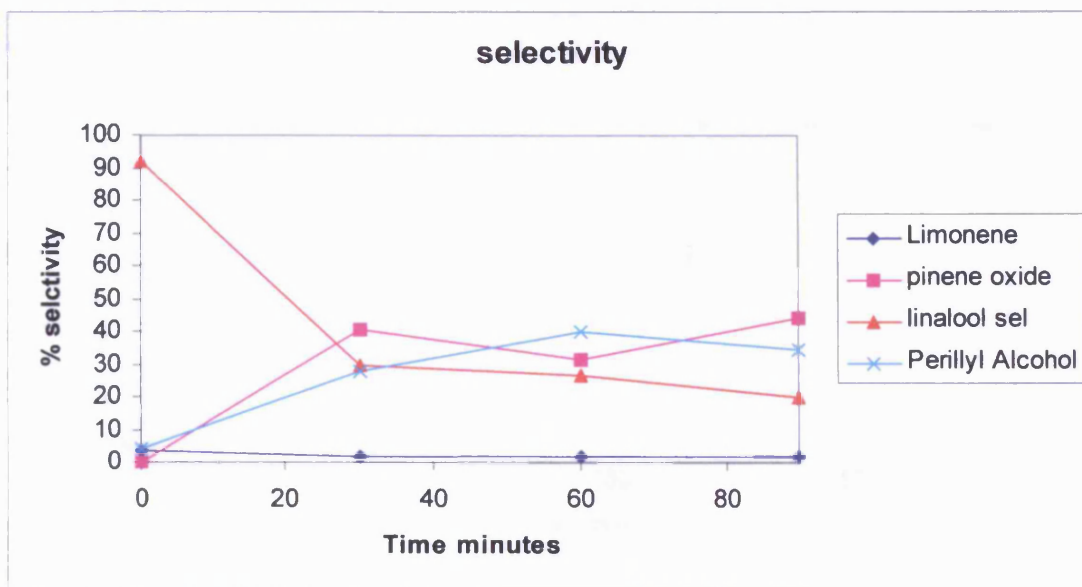


Figure 5.2.5.8: Selectivities of major products with 2ml linalool doping

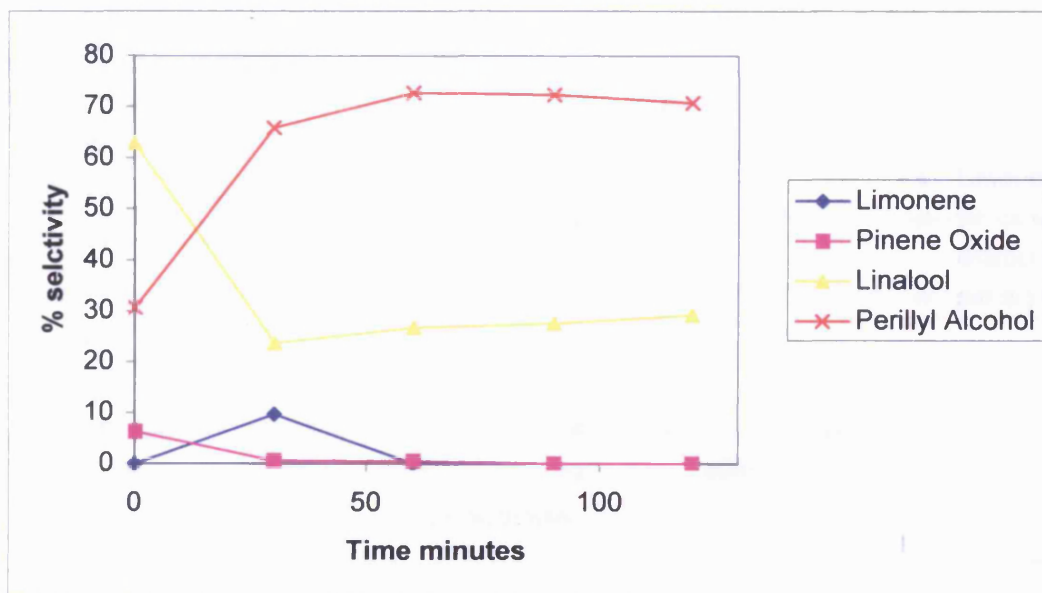


Figure 5.2.5.9: Selectivities without linalool doping, no internal standard, 80°C

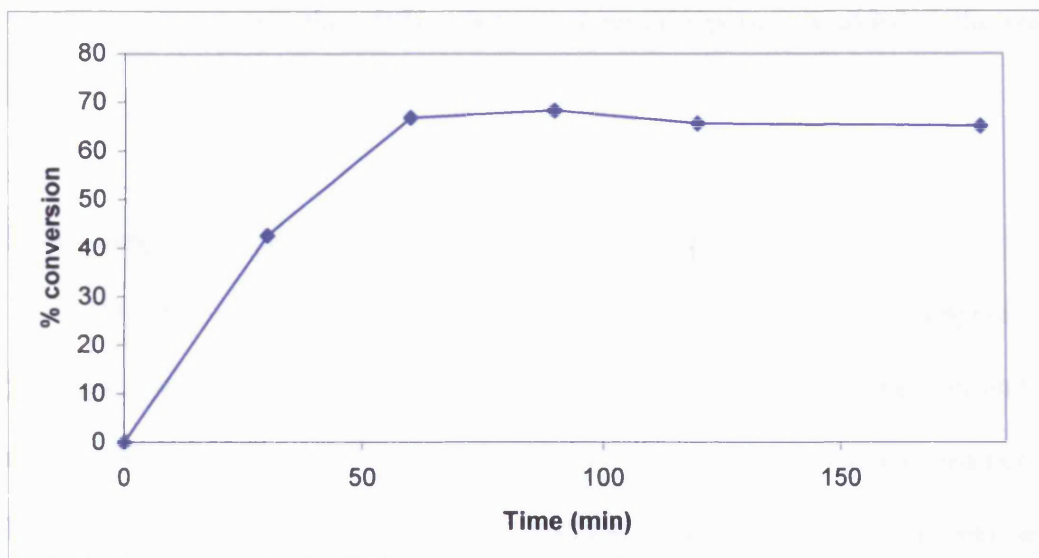


Figure 5.2.5.10: Conversion of geraniol with 1.5ml perillyl alcohol added, 0.1g silica supported CsSTA, no internal standard, 80°C s

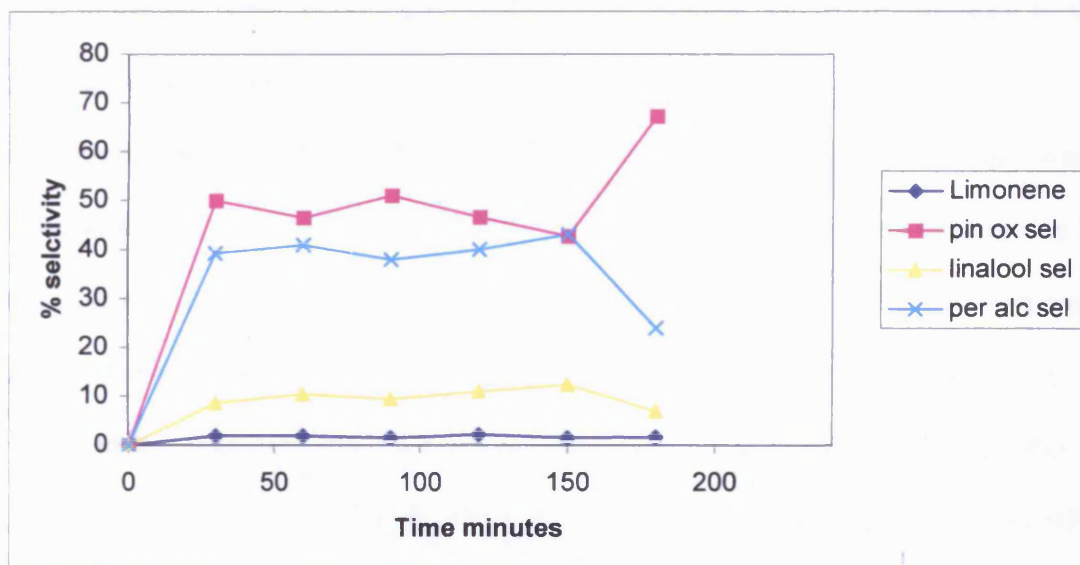


Figure 5.2.5.11: Selectivities with perillyl alcohol doping

In the linalool doping experiment, the selectivity to perillyl alcohol decreases from around 70% in the undoped experiments to 35% at 90minutes reaction time. This, in comparison with the experiments without *p*-xylene in the reaction mixture, gives vastly different product selectivities. The most significant difference is the selectivity to limonene, which decreases from around 75% in experiments with no *p*-

xylene present, to less than 10% when *p*-xylene or a poison is added to the reaction mixture.

### 5.2.6 Comparison with mineral acids

Other acid catalysts, such as solid phosphoric acid (20%w/w), sulphuric acid, hydrogen chloride and aluminium chloride have been used as a comparison under that same conditions (number of acid sites, amount of reactant and reaction temperature). This was determined by GC analysis in which no geraniol conversion was seen by comparing the area ratio of geraniol to an external standard. Due to the relatively large molecular mass of the HPA catalysts (2876g/mol for STA) compared to the mineral acids (98g/mol for sulphuric acid and phosphoric acid, 241g/mol for aluminium chloride hexahydrate), the volume of the sulphuric acid was 0.2ml. When using solid phosphoric acid, two different types were made, one where the number of acidic protons was comparable to the number of acidic protons in the silica supported STA and one where the loading by mass was the same as the silica supported STA.

In the case of aluminium chloride the weight corresponding to the number of mole of acid sites was worked out to be 0.4mg. It was found that the non-HPA catalysts did not catalyse the reaction. This was to be expected of aluminium chloride as this is a Lewis acid and does not have any protons required for Bronsted acidity. For phosphoric and sulphuric acids the results are encouraging as this indicates that the superacidic nature of the HPAs is important in achieving conversion of geraniol.

Catalyst	% Conversion of Geraniol
STA	60
Hydrochloric Acid	0
Sulphuric Acid	0
Phosphoric Acid	1

**Table 5.2.6.1 Comparison between STA and mineral acids on geraniol conversion at 90°C at twenty minutes reaction time**

### 5.2.7 Filtering of the supported catalysts

To determine the extent of the heterogeneous nature of the unsupported CsSTA, experiments in which the catalyst were filtered off after five minutes and the reaction resumed. The reactions were run under the same conditions. Filtering the CsSTA does have an effect on the conversion as the conversion reaches 5% after 30 minutes. The catalyst is not truly heterogeneous as the reaction does not completely stop, therefore some active catalyst must leach into the reaction medium.

When the CsSTA was removed from the reaction mixture after 5 minutes by filtering, reasonable conversion of geraniol is still observed (Figure: 5.3.6.1). After allowing the reaction to run for 30 minutes the conversion was only slightly lower than when the CsSTA was left in the reaction solution. This could be due to the HPA partially dissolving, and a homogeneous catalysed reaction occurring. The conversion is significantly below the results obtained by leaving the catalyst in the reaction vessel for the same time period.

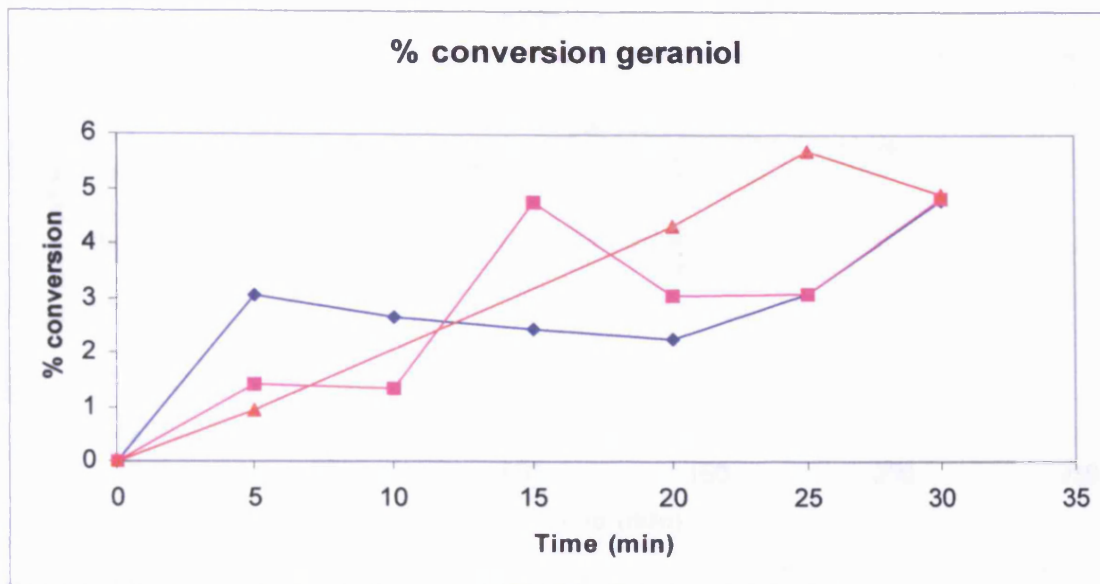


Figure 5.2.7.1: Effect of filtering of 0.01g CsSTA after five minutes

### 5.2.8 Leaching of catalysts

To determine the degree of leaching of the catalyst in the reaction 0.1g of silica supported CsSTA was added to geraniol (40ml). After stirring at room temperature for 15 minutes, the catalyst was filtered off, and fresh geraniol (40ml) added and the reaction run at 80°C

The conversion is far below the 60% conversion seen in comparable experiments where the catalyst has not been immersed in reactant before a reaction is run. The conversion is far higher than the hot filtration experiments showing that at room temperature, the catalyst is not completely washed off the support surface, it is only partially washed off.

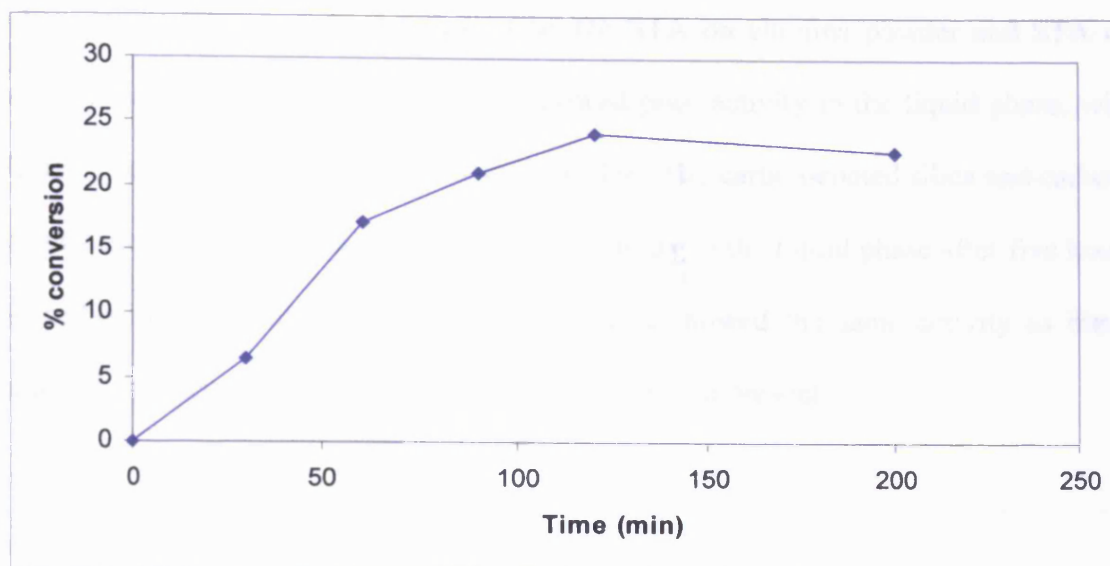


Figure 5.2.8.1: Geraniol conversion after hot filtration

It is known that nerol and geraniol are isomeric about the allylic double bond and that geraniol would favour an acyclic product and that nerol would favour a cyclic product. Experiments using nerol instead of geraniol would see if this would result in higher selectivity to limonene.

### 5.3 Cyclodehydration of 1,4-butanediol

The cyclodehydration of 1,4-butanediol in the liquid phase was investigated using the same catalysts as used in the dehydration of geraniol. The aim of these experiments was to investigate the use of supported and unsupported HPAs in liquid phase and vapour phase reactions. Experimental apparatus details are given in chapter two.

#### 5.3.1 Initial reactions

The liquid phase reactions of 1,4-butanediol were performed as described in Chapter Two. Of the five catalysts made on site at the Johnson Matthey Royston site tested for activity in the cyclodehydration of 1,4-butanediol, only three catalysts tested had moderate activity for the conversion of 1,4-butanediol to THF in the liquid



phase is the STA on silica, followed by the STA on alumina powder and STA on alumina beads. All the other catalysts showed poor activity in the liquid phase, with little or no conversion of 1,4-butanediol to THF. The carbon-coated silica and carbon-coated alumina supported HPA showed no activity in the liquid phase after five hours at reflux. As a comparison, the other catalysts showed the same activity as blank alumina spheres or the blank reaction with no catalyst present.

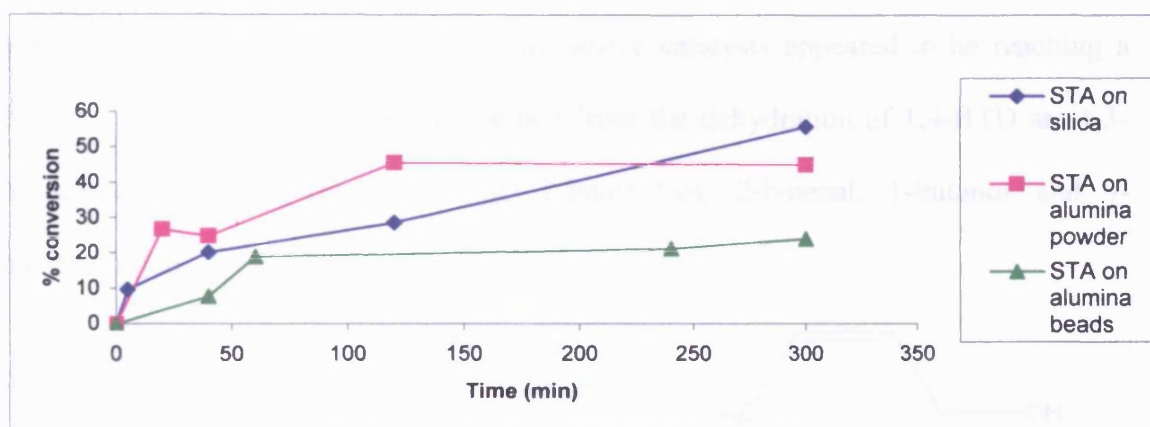


Figure 5.3.1.1: Conversion of 1,4-BTD to THF with STA on various supports

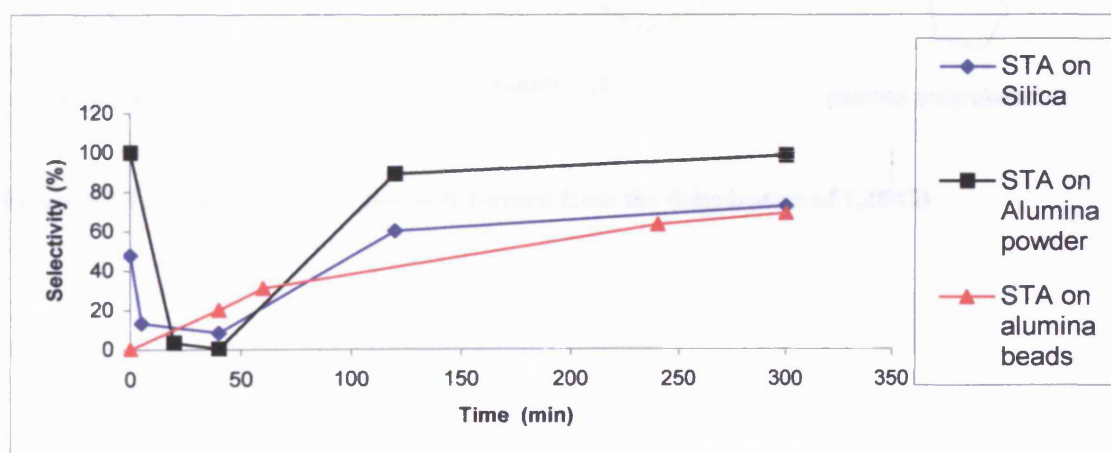
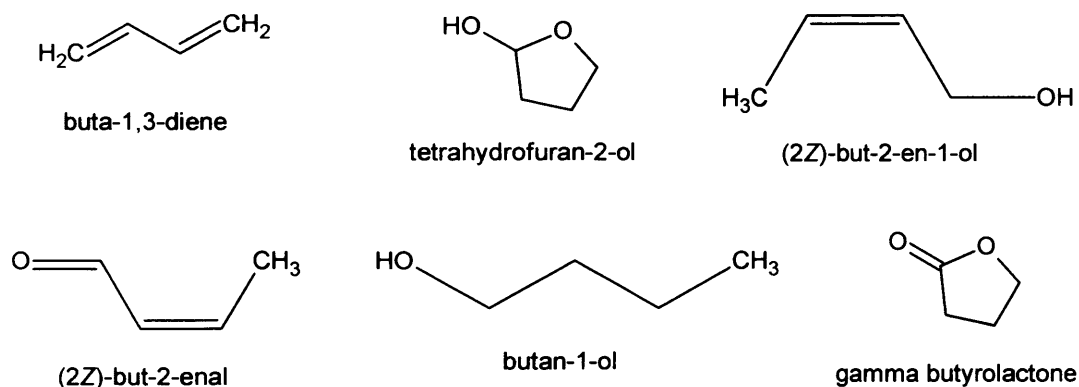


Figure 5.3.1.2: Selectivity to THF with STA on various supports

The selectivity of the catalysts that showed activity after 5 hours showed that the alumina powder was the most selective and the alumina beads were the least

## Liquid Phase Alcohol Dehydration

selective. The STA on silica had the highest conversion after five hours, but at around 240 minutes, the STA on alumina powder has the higher conversion. HPAs in the liquid phase are able to dehydrate 1,4-butanediol with moderate conversion. The conversion of the 1,4-butanediol with the STA supported on alumina powder and alumina beads appeared to be steady after 120 minutes reaction time. In contrast, the STA supported on silica increased the conversion of the reactant in the same time period. The selectivity of the STA on alumina powder was the highest after five hours. The selectivities of the other two active catalysts appeared to be reaching a plateau. The most likely products formed from the dehydration of 1,4-BTD are 1,3-butadiene, 2-hydroxytetrahydrofuran, 2-buten-1-ol, 2-butenal, 1-butanol and  $\gamma$ -butyrolactone.



**Figure 5.3.1.3 The most likely products formed from the dehydration of 1,4BTD**

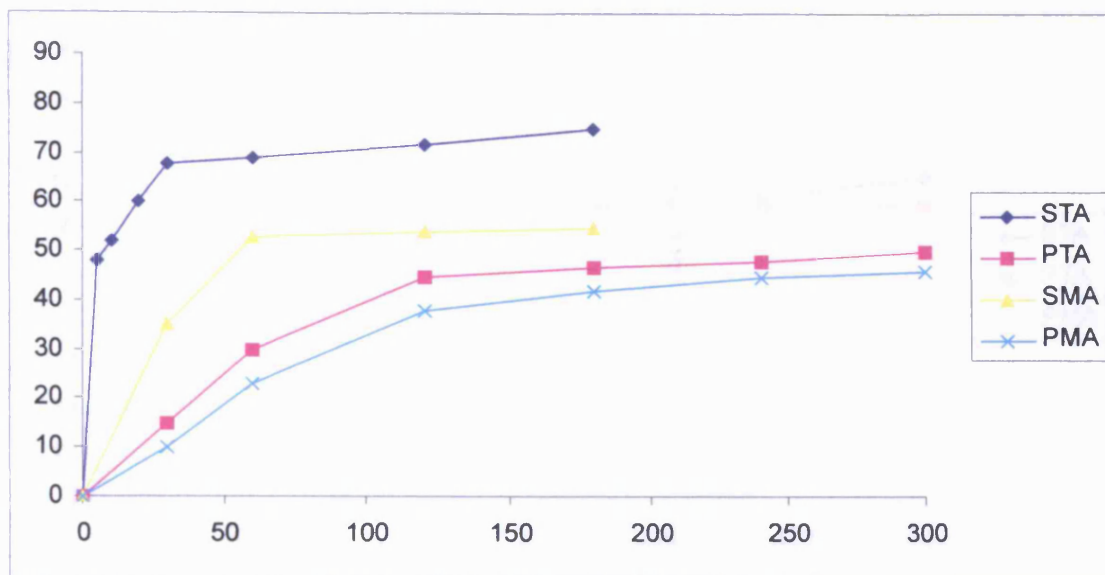


Figure 5.3.1.4: Dehydration of 1,4BTD using unsupported HPAs at room temperature

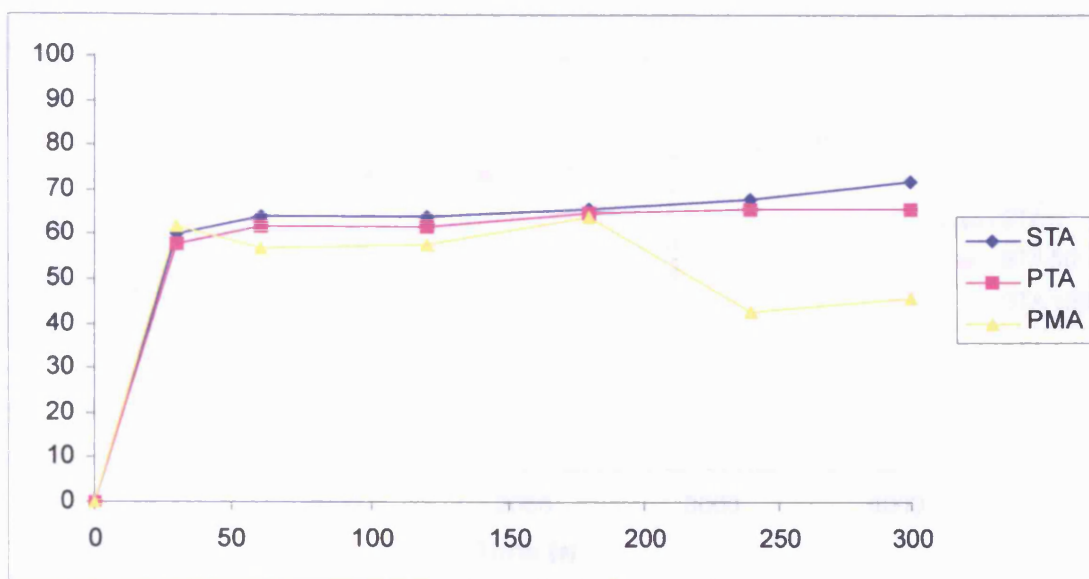


Figure 5.3.1.5: Dehydration of 1,4BTD using unsupported HPAs at 50°C

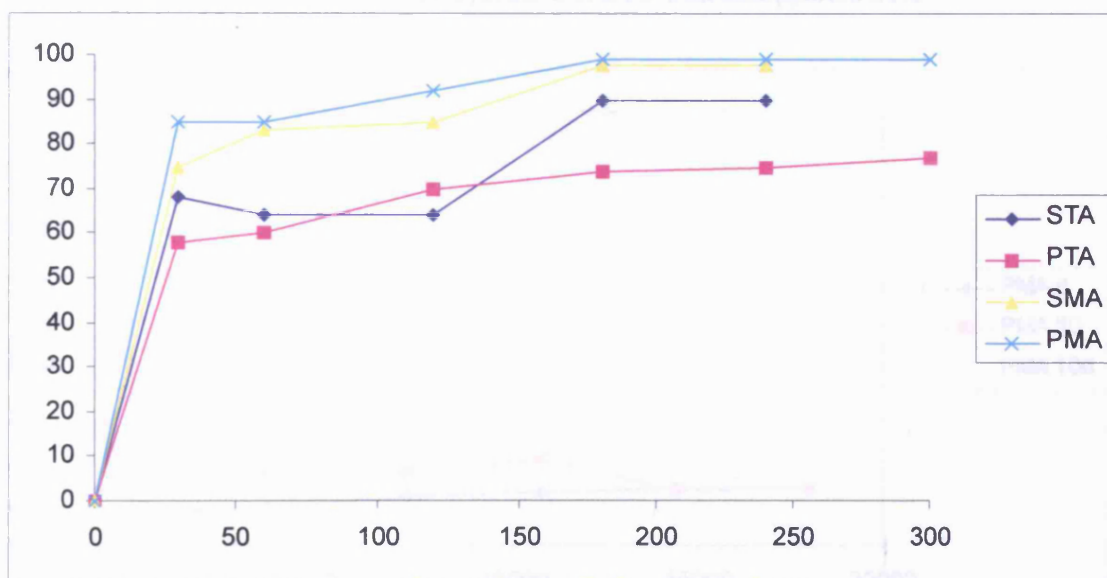


Figure 5.3.1.6: Dehydration of 1,4BTD using unsupported HPAs at 100°C

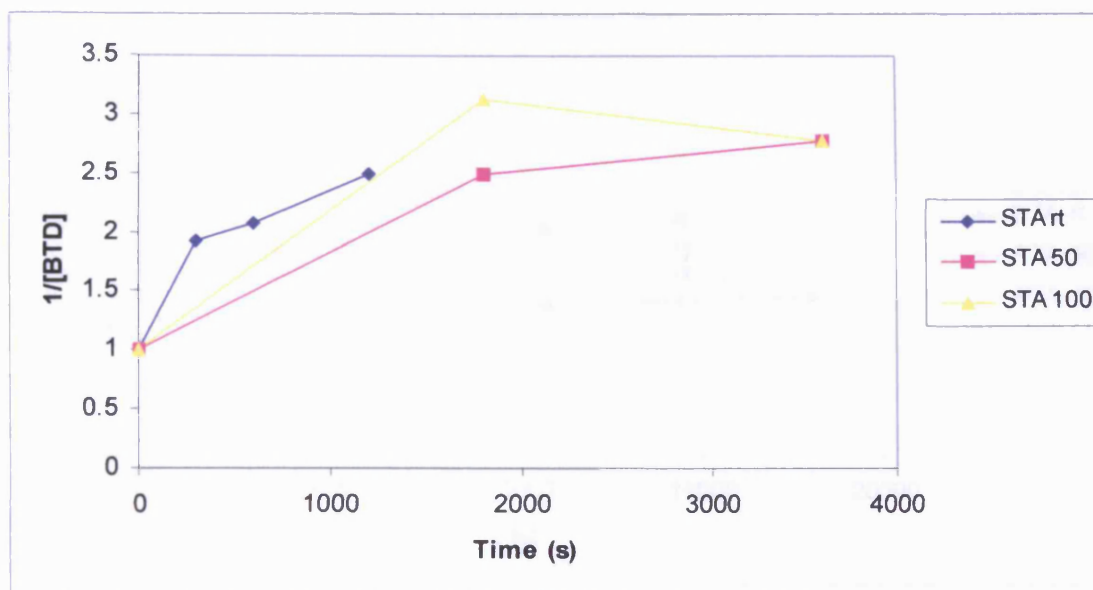


Figure 5.3.1.7 Second Order Plot of Dehydration of BTB with unsupported STA

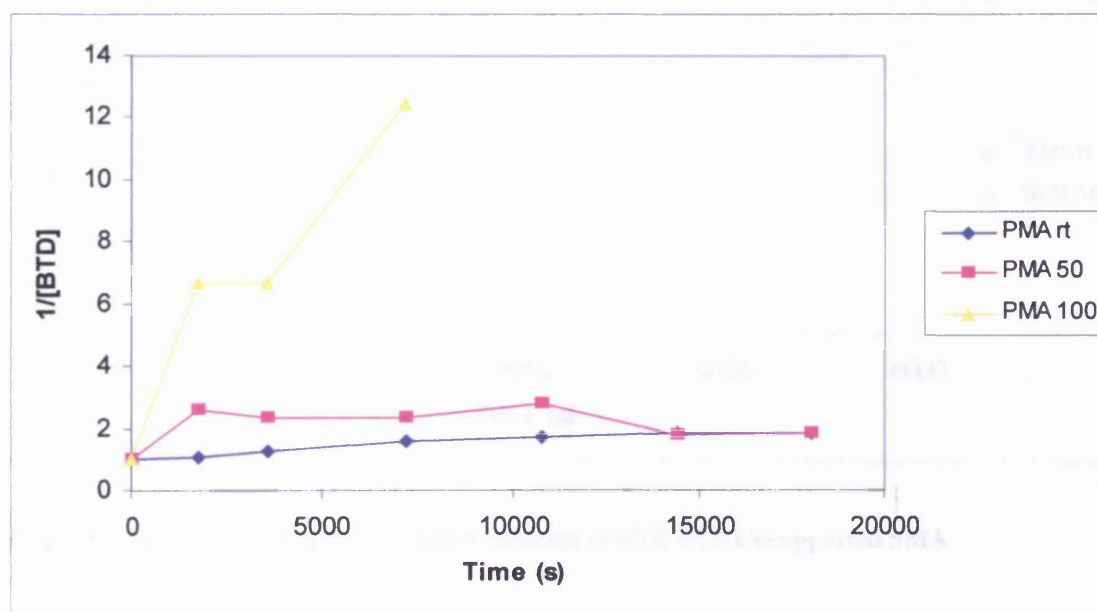


Figure 5.3.1.8 Second Order Plot of Dehydration of BTB with unsupported PMA

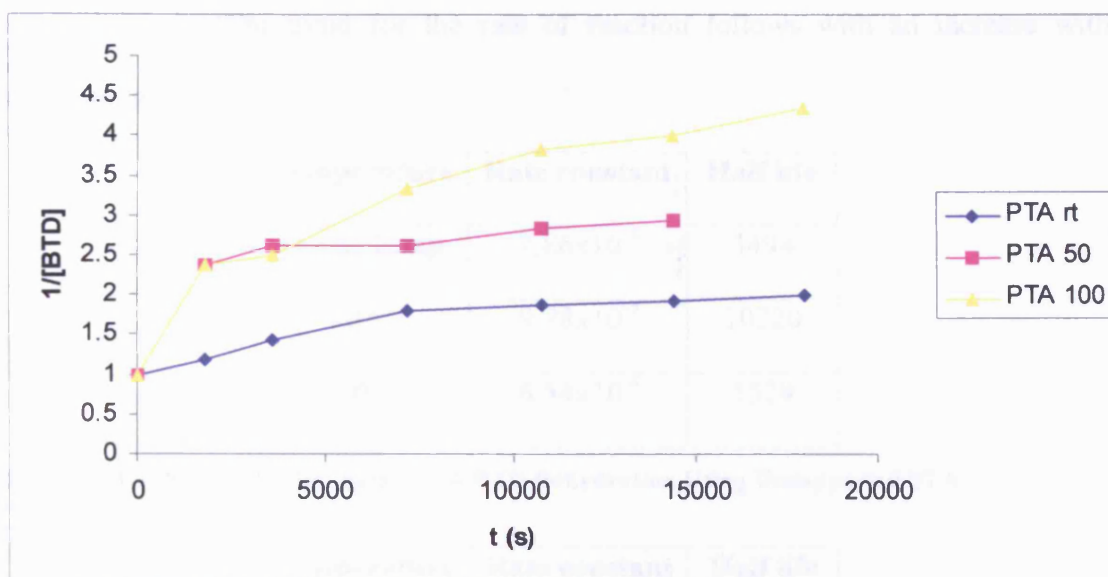


Figure 5.3.1.9 Second Order Plot of Dehydration of BTD with Unsupported PTA

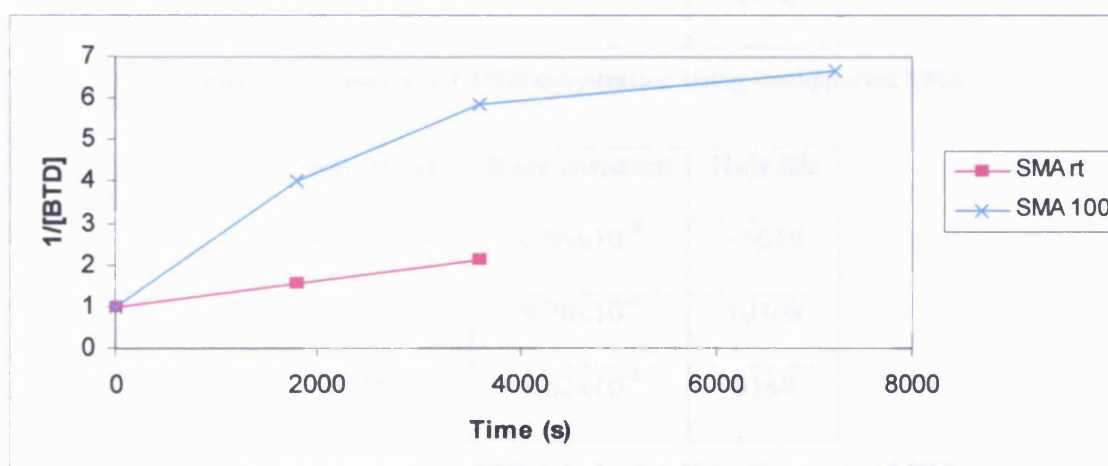


Figure 5.3.1.10 Second Order Plot of Dehydration of BTD with Unsupported SMA

The kinetics shows that the reaction is a second order reaction. Plotting  $\ln[A/A_0]$  versus time does not result in a straight line plot, showing that the reaction is not a first order reaction. The slope of the graph is  $k$ . The rate of reaction for unsupported STA at room temperature is significantly higher than the reactions at 50 and 100°C. This is unrealistic, as the rest of the unsupported catalysts do not exhibit

this behaviour. The trend for the rate of reaction follows with an increase with temperature.

Temperature	Rate constant	Half life
Room Temp	$2.86 \times 10^{-4}$	3494
50°C	$9.78 \times 10^{-5}$	10220
100°C	$6.54 \times 10^{-4}$	1529

**Table 5.3.1.7: Second Order Data of 1,4-BTD Dehydration Using Unsupported STA**

Temperature	Rate constant	Half life
Room Temp	$3.13 \times 10^{-4}$	3192
100°C	$7.44 \times 10^{-4}$	1342

**Table 5.3.1.8: Second Order Data of 1,4-DTD dehydration Using Unsupported SMA**

Temperature	Rate constant	Half life
Room Temp	$6.66 \times 10^{-4}$	15010
50°C	$9.70 \times 10^{-4}$	10308
100°C	$1.62 \times 10^{-4}$	6160

**Table 5.3.1.9: Second Order Data of 1,4-DTD dehydration Using Unsupported PTA**

Temperature	Rate constant	Half life
Room Temp	$4.93 \times 10^{-4}$	20262
50°C	$1.09 \times 10^{-4}$	9134
100°C	$1.46 \times 10^{-4}$	684

**Table 5.3.1.10: Second Order Data of 1,4-DTD dehydration Using Unsupported PMA**

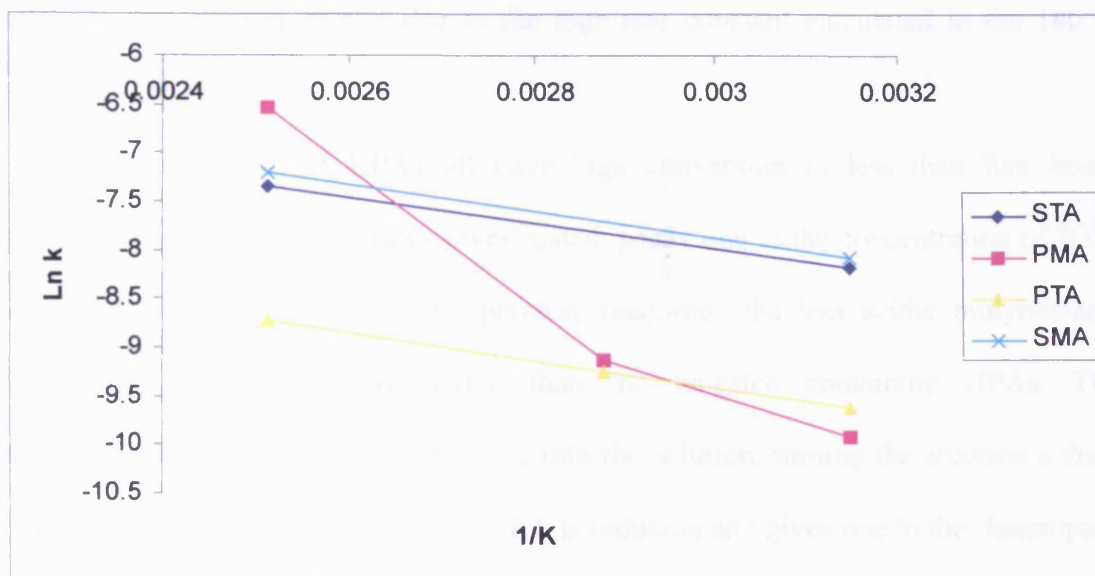


Table 15.1.3.11 Arrhenius Plot for 1,4-BTD Dehydration Reaction

Catalyst	Ea (kJ mol <sup>-1</sup> )	A (L mol <sup>-1</sup> s <sup>-1</sup> )
STA	10.869	0.0017
PMA	45.395	1101.177
PTA	11.724	0.0056
SMA	11.382	0.0232

Table 5.3.1.11: Activation Energies and Pre-Exponential Factors of Dehydration of 1,4-BTD

The Arrhenius plot for the unsupported catalysts shows that the activation energy for three of the four catalysts is not more than 11.7 kJ mol<sup>-1</sup>, unsupported PTA has an apparent activation energy of 45 kJ mol<sup>-1</sup>, around four times of the other HPAs. This is probably not a realistic result even though PTA is considered the most acidic of the four HPAs used in these experiments. The cyclodehydration of 1,4-butanediol using a strong acid cation resin <sup>(24)</sup> (Indion-130) has a reported activation energy of 35.5 kJ mol<sup>-1</sup>. The activation energy shows that the rate of reaction is dependant on temperature. The pre-exponential factor of PMA is significantly higher than the other



catalysts investigated, this is due to the high rate constant calculated in the 100°C reaction with PMA.

The unsupported HPAs all have high conversion in less than five hours reaction time at the temperatures investigated, partly due to the concentration of BTM in the reaction. In the higher temperature reactions, the less acidic molybdenum containing HPAs are more active than the tungsten containing HPAs. The molybdenum containing HPAs dissolve into the solution, turning the solution a deep blue colour. This would indicate the HPA is reducing and gives rise to the 'heteropoly blues' <sup>(19)</sup>. The electron donation would most likely be from the 1,4-dioxane, since it has two oxygen atoms, which could coordinate to the HPA.

The proposed mechanism for the cyclodehydration reaction proceeds by four steps to yield THF (Fig 4.2.2.1.) Where the molybdenum containing HPAs were used, the solution became dark blue after 5 minutes after addition of the HPA. This indicates that the caesium ion has no real effect on the solubility of the molybdenum containing HPAs. No colour changes were observed in the reactions with the tungsten containing HPAs or their salts.

From the graphs (Appendix Figures:20-31), it is clear that the cyclodehydration reaction of BTM to THF is not reproducible. To see if the problem was the GC instead of the BTM a solution of 0.5ml BTM, 0.5ml *p*-xylene and 0.5ml 2-methyl-1-propanol was diluted in acetone and injected 5 times. The ratios between each analyte was recorded and summarised below:

Component	Ratio to 2-methyl-1-propanol	Ratio to <i>p</i> -xylene	Ratio to 1,4-butanediol
2-methyl-1-propanol	1	0.415	0.632
<i>p</i> -xylene	2.40	1	1.522
1,4-butanediol	1.581	0.656	1

Table 5.3.1.12: Ratios of BTD to *p*-xylene and 2-methyl-1-propanol (first injection)

Component	Ratio to 2-methyl-1-propanol	Ratio to <i>p</i> -xylene	Ratio to 1,4-butanediol
2-methyl-1-propanol	1	0.410	0.626
<i>p</i> -xylene	2.438	1	1.52
1,4-butanediol	1.590	0.654	1

Table 5.3.1.12: Ratios of BTD to *p*-xylene and 2-methyl-1-propanol (second injection)

Component	Ratio to 2-methyl-1-propanol	Ratio to <i>p</i> -xylene	Ratio to 1,4-butanediol
2-methyl-1-propanol	1	0.412	0.453
<i>p</i> -xylene	2.420	1	1.099
1,4-butanediol	2.200	0.909	1

Table 5.3.1.13: Ratios of BTD to *p*-xylene and 2-methyl-1-propanol (third injection)

Component	Ratio to 2-methyl-1-propanol	Ratio to <i>p</i> -xylene	Ratio to 1,4-butanediol
2-methyl-1-propanol	1	0.411	0.487
<i>p</i> -xylene	2.430	1	1.185
1,4-butanediol	2.050	0.843	1

Table 5.3.1.14: Ratios of BTD to *p*-xylene and 2-methyl-1-propanol (fourth injection)

Component	Ratio to 2-methyl-1-propanol	Ratio to <i>p</i> -xylene	Ratio to 1,4-butanediol
2-methyl-1-propanol	1	0.415	0.407
<i>p</i> -xylene	2.40	1	0.981
1,4-butanediol	2.43	1.019	1

Table 5.3.1.14: Ratios of BTD to *p*-xylene and 2-methyl-1-propanol (fifth injection)

The ratios of the 2-methyl-1-propanol and *p*-xylene are constant for each injection while the 1,4-butanediol changes after the second injection with the resulting ratios nowhere close to the original values. It is clear from the tables that after five separate injections where the ratios of 2-methyl-1-propanol and *p*-xylene are constant and the ratios of 1,4-butanediol constantly change shows that the analysis of 1,4-butanediol cannot be resolved by the system used.

The same sample was run on a separate Varian 3400 CX gas chromatograph and similar results were obtained with the *p*-xylene and 2-methyl-1-propanol giving similar ratios while the BTD ratios were not constant. The cause for the change of response of BTD are not known. One possible cause could be that the BTD could have been reacting on the column as it was being eluted but since no other peaks were seen in the chromatograms and BTD's boiling point is 230°C, it is unlikely that it would spontaneously decompose on the column.

By using the response factors from off-line calibrations, the mass balances for the liquid phase reactions is at 50 to 60% in all cases.

## 5.4 Conclusions

The main product of the geraniol dehydration was not limonene as was desired. Instead the major product was linalool. Although the reaction does proceed at

temperatures below 100°C the conversion of geraniol into linalool is moderate at best. When CsSTA was tested, the selectivity to limonene increased. Mineral acids and a neutralised salt of STA, Cs<sub>4</sub>STA, were unable to catalyse the reaction under the same reaction conditions as the more effective catalysts. This supports that the super acidic protons of the HPA are needed to catalyse the reaction. The reaction is very sensitive to competitive adsorption by by-products while the CsSTA was mildly enhanced by the addition of water while the catalyst is easily leached of the silica. Tethering the HPA to the support would, in theory, help solve the leaching problem seen in these experiments.

The 1,4-butanediol reactions when using supported HPAs all suffered from irreproducibility and as such no meaningful conclusions can be made about the efficacy of supported STA and CsSTA in the cyclodehydration of BTB under the conditions employed. However, where THF was detected, no other by-products were seen in the chromatograms. It is interesting to note that the ratio of BTB to *p*-xylene and 2-methyl-1-propanol was not stable in a catalyst free mixture, while the ratios of *p*-xylene and 2-methyl-1-propanol were stable.

### References

1. I. Bucsí, Á. Molnár, M. Bartók, G. A. Olah, *Tetrahedron* Vol. 50 No. 27 (1994) 8195-8202
2. B. Torok, I. Bucsí, T. Beregszászi, I. Kapocsi, A. Molnar, *Journal of Molecular Catalysis A: Chemical* 107 (1996) 305-311
3. L. Li, Y. Kamiya, T. Okuhara *Applied Catalysis A: General* 253 (2003) 29-32
4. A.S. Dias, S. Lima, M. Pillinger, A.A. Valente *Carbohydrate Research* 341 (2006) 2946–2953

5. L.R. Pizzio, P.G. Vázquez, C.V. Cáceres, M.N. Blanco *Applied Catalysis A: General* 256 (2003) 125–139
6. S. Sato, R. Takahashi, T. Sodesawa, N. Yamamoto *Catalysis Communications* 5 (2004) 397–400
7. Y. Izumi, K. Iida, K. Usami, T. Nagata *Applied Catalysis A: General* 256 (2003) 199–202
8. Z. Hou, T. Okuhara *Applied Catalysis A: General* 216 (2001) 147–155
9. F. Zhang, C. Yuan, J. Wang, Y. Kong, H. Zhub, C. Wang *Journal of Molecular Catalysis A: Chemical* 247 (2006) 130–137
10. L. Damjanovi, V. Raki, U.B. Mio, A. Auroux *Thermochimica Acta* 434 (2005) 81–87
11. H. Firouzabadi, N. Iranpoor, A. Ali Jafari *Tetrahedron Letters* 46 (2005) 2683–2686
12. P. Madhusudhan Rao, A. Wolfson, M.V. Landau, M. Herskowitz *Catalysis Communications* 5 (2004) 327–331
13. P. Madhusudhan Rao, A. Wolfson, S. Kababya, S. Vega, M.V. Landau *Journal of Catalysis* 232 (2005) 210–225
14. Y. Izumi, M. Ono, M. Kitagawa, M. Yoshida, K. Urabe *Microporous Materials*, Volume 5, Issue 4, (1995) 255–262
15. Á. Kukovecz, Zs. Balogi, Z. Kónya, M. Toba, P. Lentz, S.-I. Niwa, F. Mizukami, Á. Molnár, J.B. Nagy, I. Kiricsi *Applied Catalysis A: General* 228 (2002) 83–94
16. B. Sulikowski, R. Rachwalik *Applied Catalysis A: General* 256 (2003) 173–182
17. A. Molnár, C. Keresszegi, B. Török *Applied Catalysis A: General* 189 (1999) 217–224

18. D.I Enache, D.W Knight, G.J Hutchings *Catalysis Letters* 103 (2005) 43-52
19. I. V Kozhevnikov *Chemical Reviews* 98 (1998) 171-198
20. I. V. Kozhevnikov *Applied Catalysis A: General* 256 (2003) 2-18
21. N. Bhatt, A. Patel *Journal of the Taiwan Institute of Chemical Engineering* 42 (2011) 356-362
22. T. Tagawa, J. Amemiya, S. Goto *Applied Catalysis A: General* 257 (2004) 19-23
23. K. Su, Z. Li, B. Cheng, L. Zhang, M. Zhang, J. Ming *Fuel Processing Technology* 92 (2011) 2011-2015
24. S. H Vaidya, V.M Bhandari, R. V Chaudhari *Applied Catalysis A: General* 242 (2003) 321-328

# Chapter Six: Bio-diesel Synthesis

## 6.1 Introduction

As non-renewable fossil fuels become scarcer, a new source of fuels will be needed to power the transport of the world. Bio-diesel, made from the transesterification of vegetable oils with alcohol, can be used in modern diesel engines with no required modifications to the engine management system. It is known that the inventor of the diesel engine, Rudolf Diesel, ran the first diesel engine on peanut oil. Due to the cheap production of fossil fuels in the early twentieth century, vegetable derived fuels never became commercially competitive <sup>(1)</sup>. Bio-diesel feedstocks are varied in their source, virgin vegetable oils, waste cooking oils, animal fats and algae.

The use cultivation of vegetable oil for food rather than fuel production is an economic and agricultural debate. The decision to plant crops for fuel, rather than for food in a world population which is currently over 6.9 billion, leads to significant loss of arable land. This potential loss of land has led to the development of second-generation bio fuels in which the sources are diverse such as algae, fungi and saltwater crops where traditional crops cannot grow.

Bio-diesel derived from vegetable oils is usually made from the base catalysed transesterification using sodium hydroxide and methanol. Bio-diesel is non-toxic, biodegradable and emits less NO<sub>x</sub> and polycyclic aromatic hydrocarbons than fossil diesel<sup>(8,9,10)</sup>. The CO<sub>2</sub> emitted during the use of bio-diesel as a source of fuel is offset by the CO<sub>2</sub> taken up by the plant during its time growing, making it more attractive to environmentally concerned consumers <sup>(3)</sup>.

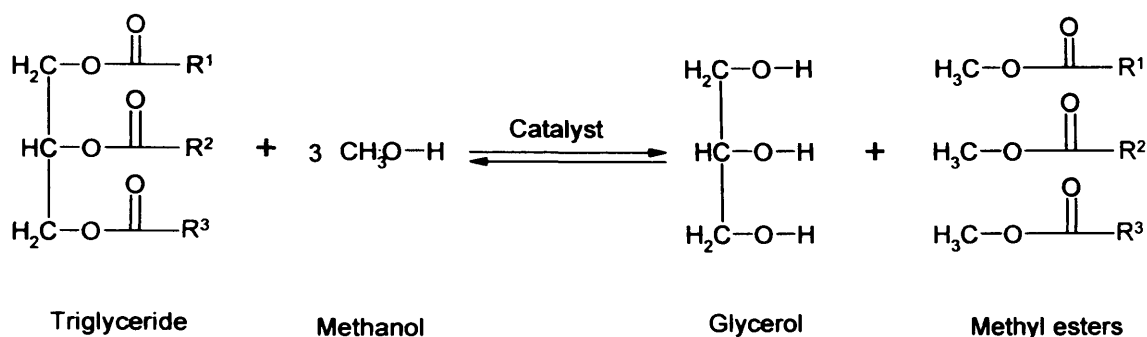


Figure 6.1.1: The general equation of transesterification for a triglyceride using methanol

During transesterification, due to the reversible nature of the reaction, an excess of alcohol is required to shift the reaction equilibrium to favour the formation of the alkyl esters. The reaction between an alcohol and a triglyceride occurs as three stepwise reactions with each fatty alkyl chain forming an ester with the reacting alcohol, eventually leaving a glycerol molecule as a by-product.

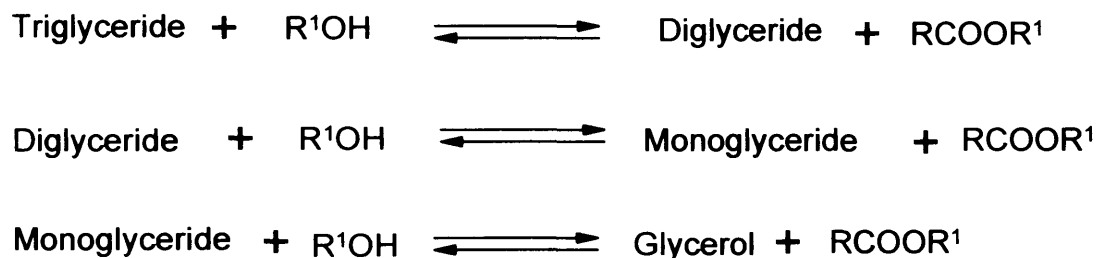


Figure 6.1.2: General stepwise reactions of an alcohol and a triglyceride

The production of bio-diesel is usually carried out with methanol, due to the low cost of methanol and ease of separation of the resulting fatty acid methyl esters (FAME), remaining methanol present and glycerol. Other methods of bio-diesel production involve the use of super-critical methanol<sup>(2)</sup>, ion-exchange resins<sup>(3)</sup>, zeolites<sup>(3)</sup>, sulphated zirconia<sup>(3)</sup> lipases<sup>(4)</sup> calcium oxides<sup>(5)</sup>, MgAl hydrotalcites<sup>(6)</sup> and ultrasonic and hydrodynamic cavitation<sup>(7)</sup>.



The sodium hydroxide method is the most widely used and relatively inexpensive, proceeds at relatively low temperatures and achieve high conversions relatively quickly, but the catalyst is not reusable and the process requires that the reactants be completely free of water, as soap formation can result, a process known as saponification. Most vegetable oils have high levels of free fatty acids (FFA), which have to be transesterified using an acid catalyst before using an alkali catalyst to prevent saponification<sup>(1)</sup>.

Acid catalysed transesterification can be done, but this route requires a higher alcohol to vegetable oil ratio, higher temperatures and longer reaction times to reach the same conversions as the base catalysed route.

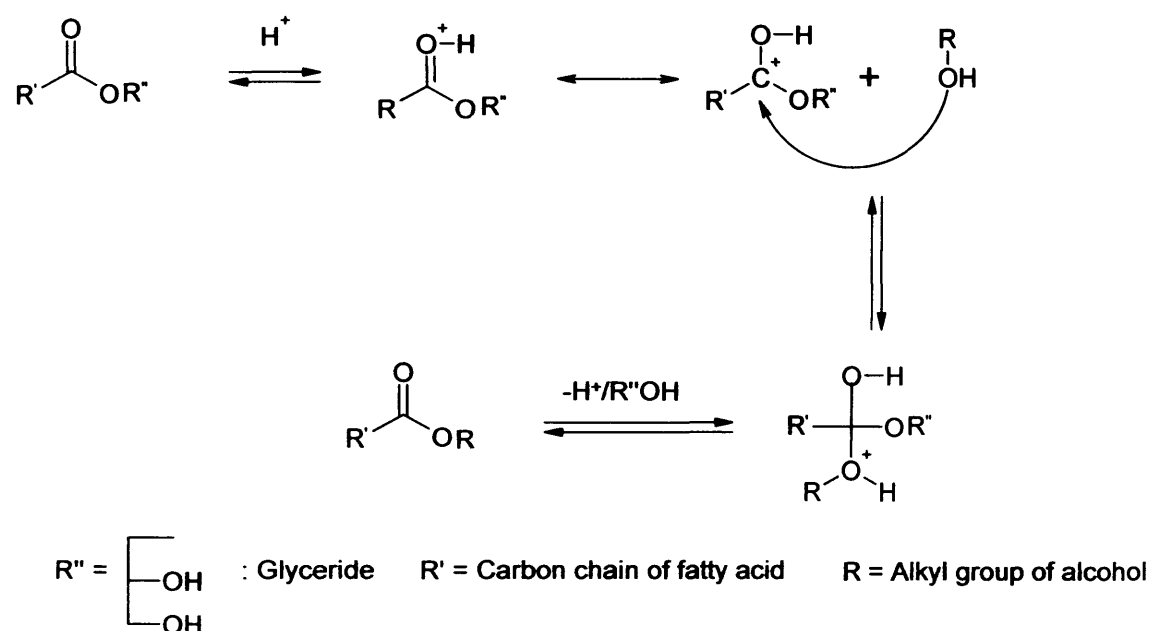


Figure 6.1.3: Mechanism of the acid catalysed transesterification of a triglyceride

One advantage of acid catalysed transesterification over base catalysed transesterification is that the tolerance to water is much greater, as there are no metal cations available to create the soap<sup>(1)</sup>. In the case of heteropoly acids, the super acidic

properties may enable small quantities of HPAs to be used in amounts comparable to, or better than, the current process using sodium methoxide.

Due to the large quantities of waste cooking oils available and the low quality of such oils, base catalysed transesterification of these oils require additional processing to remove the FFAs to stop saponification and the removal of water. The use of supported HPAs could eliminate the need for additional steps in the transesterification of a wide range of triglycerides into bio-diesel.

## 6.2 Reactions

### 6.2.1 Initial Reactions

Initial reactions were carried out in a round-bottomed flask using a methanol: rapeseed oil (RSO) molar ratio of 8.8 gave no conversion with 0.05g of unsupported STA at 40°C. Conversion of RSO to FAME was calculated by using an <sup>1</sup>H NMR method <sup>(1)</sup> to monitor the reaction. The signal due to the methylene protons next to the ester group in the triglycerides appears at 2.3ppm and after the reaction the methoxy protons of the FAME appear at 3.7ppm. The following equation:

$$C = 100 \times \left( \frac{2A_{ME}}{3A_{CH_2}} \right)$$

Where C is the percentage conversion of RSO to FAME, A<sub>ME</sub> is the integration value of the protons of the FAME and A<sub>CH<sub>2</sub></sub> is the integration value of the methylene protons.

Upon doubling the amount of catalyst to 0.1g, the conversion was 14% after 30 minutes reaction time and remained at 14% conversion after 120 minutes reaction time. Performing the reaction in an autoclave with the same amounts of reactants with 0.05g of STA catalyst resulted in 22% conversion of RSO to bio-diesel after 15

minutes reaction at 80°C. It was noticed that the temperature during the reaction increased from 80°C to 170°C

### 6.2.2 Transesterification of rapeseed oil to bio-diesel using an autoclave

To test if the reaction would proceed by heat and pressure alone, RSO (20ml) and methanol (7.6ml) were loaded into the autoclave and the reaction started at 80°C. After 15 minutes the reaction was stopped and a portion of the RSO/FAME layer taken for analysis. The reaction was restarted again but with 0.05g unsupported CsSTA added to determine if the addition of catalyst would increase conversion. After 15 minutes the reaction was stopped and the RSO/FAME layer taken for analysis. The results are shown in the table below:

	15 minutes, no catalyst	15 minutes, 0.05g catalyst (30minutes reaction time)
% RSO conversion to FAME	0	25

**Table 6.2.2.1 Conversion of RSO to FAME using catalyst**

It can be shown that the effect of temperature and pressure alone do not contribute to the formation of FAME in the absence of catalyst.

Catalyst	30 minutes reaction time	60 minutes reaction time	120 Minutes reaction time	240 minutes reaction time
0.05g STA	2	2	9	15
0.1g STA	2	5	6	24
0.05g CsSTA	3	2	3	3
0.1g CsSTA	1	1	16	34

**Table 6.2.2.2: Conversions of RSO to FAME at 160°C determined using NMR method**

Conversion of RSO to FAME increases with the amount of catalyst used. (See table 6.2.2.2) after 240 minutes reaction time the conversion of RSO using 0.1g of CsSTA is over ten times that of the 0.05g CsSTA. Kinetic analysis of the rate of reaction was calculated and the results are given in table 6.2.2.4 and figure 6.2.2.3.

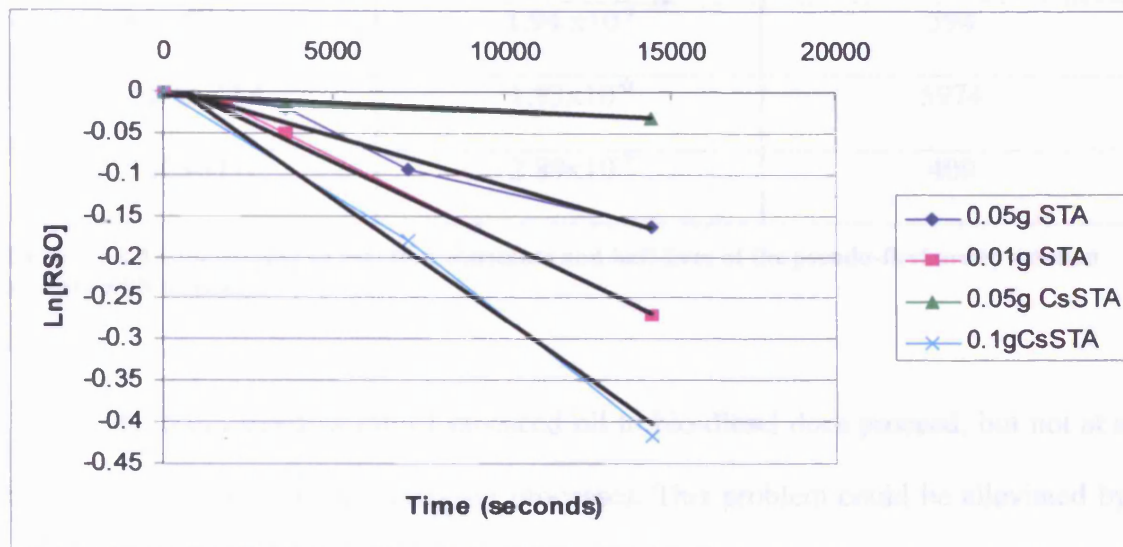


Figure 6.2.2.3: First order plot of the transesterification of RSO to FAME at 160°C

The first order plots agree with the literature, as the kinetics of RSO to FAME is pseudo-first order. The fastest rate is with the 0.1g CsSTA while the slowest rate is with the 0.05g CsSTA. The 0.05g CsSTA was expected to have the slowest rate of the catalysts investigated, due to the neutralisation of the most acidic proton of the HPA, the fastest rate as seen in the graphs is with the 0.1g CsSTA could be explained by the insolubility of the HPA in methanol, forming a phase transfer region between the methanol and the RSO which would enhance the initial reaction between the reactants. It is known that in the transesterification of RSO to FAME that the mixing of the two phases is important to start the reaction, as the two reactants are immiscible and the catalyst usually resides in the methanol phase.<sup>(1)</sup> Once the reaction between the reactants has started, the mixing is less important as the products are a mixture of di and mono-glycerides, which have polar and non-polar groups and act as surfactants

in the reaction mixture, which help emulsify the RSO and methanol to enhance mixing.<sup>(1)</sup>

Catalyst	Rate constant $k$ ( $s^{-1}$ )	Half-life (minutes)
0.05g STA	$1.19 \times 10^{-5}$	972
0.1g STA	$1.94 \times 10^{-5}$	594
0.05g CsSTA	$1.93 \times 10^{-6}$	5974
0.1gCsSTA	$2.89 \times 10^{-5}$	400

Table 6.2.2.4 Comparison of reaction constants and half-lives of the pseudo-first order reaction of RSO with methanol

The transesterification of rapeseed oil to bio-diesel does proceed, but not at a rate to compete with alkali catalysed processes. This problem could be alleviated by grafting the HPA onto the support so as to minimise the leaching. The catalyst could then be reusable and offers a distinct advantage over sodium hydroxide.

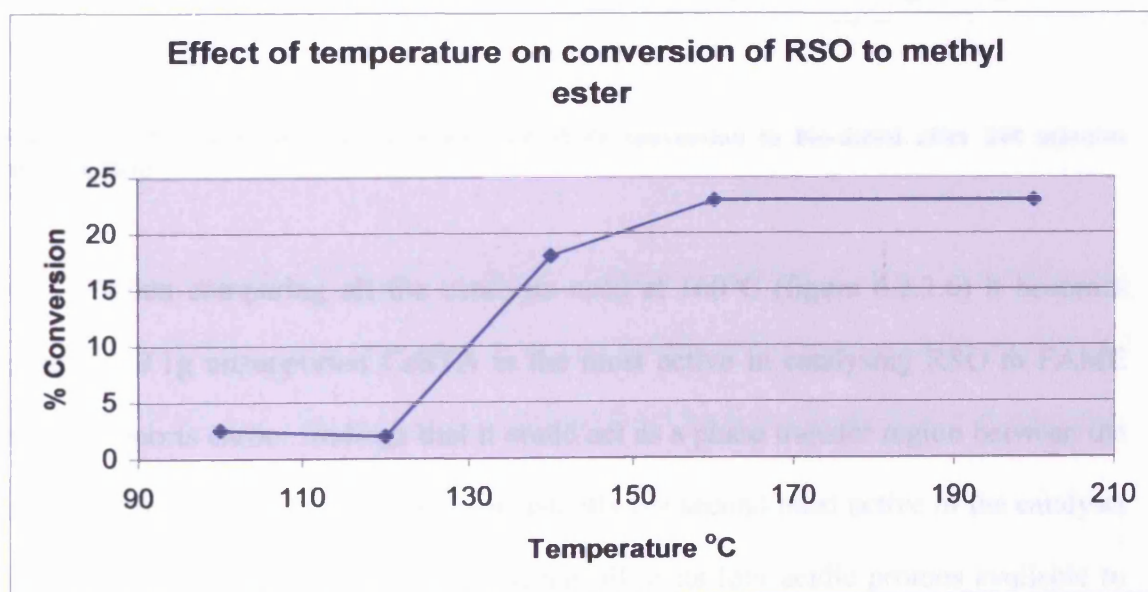


Figure 6.2.2.5 Effect of temperature on RSO conversion using 0.1g silica supported STA. Time 240 minutes

Reactions of transesterification of RSO to FAME were carried out at various temperatures to see if an increase of temperature would effect the conversion. It was found that when using 0.1g of silica supported STA there was no increase of conversion from 160°C to 200°C. Temperature does influence the reaction and under the conditions investigated found that a reaction temperature of 160°C gave the highest conversion.

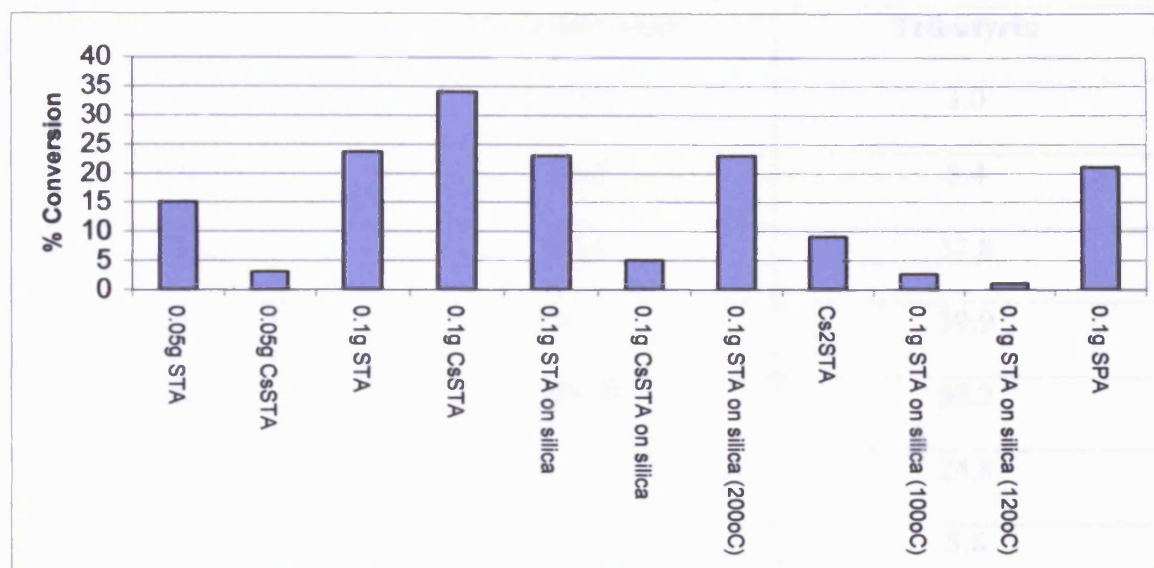


Figure 6.2.2.6 Comparison of catalysts with RSO conversion to bio-diesel after 240 minutes reaction time

When comparing all the catalysts used at 160°C (figure 6.2.2.6) it becomes clear that 0.1g unsupported CsSTA is the most active in catalysing RSO to FAME which supports earlier findings that it could act as a phase transfer region between the methanol and RSO. 0.1g STA was consistently the second most active of the catalysts investigated as would be expected as it has all of its four acidic protons available to catalyse the reaction. Silica supported phosphoric acid has been reported for the transesterification of triacetin with methanol<sup>(11)</sup> The activity of the catalyst was very low at 10%, this was attributed to the low surface area of the catalyst (2.6m<sup>2</sup>/g) and

weak acid site concentration (approximately 986 $\mu$ mol/g.) Cs salts of PTA have been investigated in the esterification of palmitic acid and the transesterification of tributyrin with methanol<sup>(12)</sup>. The reactions were carried out at 60°C with PTA and conversion was found to increase with increasing Cs substitution of PTA and reached a maximum at Cs<sub>2,3</sub>PTA and decreases with further Cs substitution.

Catalyst	Conversion (%)	
	Palmitic Acid	Tributyrin
Cs <sub>0,9</sub>	70.7	3.0
Cs <sub>1,9</sub>	80.2	5.4
Cs <sub>2,0</sub>	85.6	37.8
Cs <sub>2,1</sub>	86.3	39.9
Cs <sub>2,3</sub>	100.0	50.2
Cs <sub>2,4</sub>	80.4	24.8
Cs <sub>2,7</sub>	20.6	5.8
Cs <sub>3,0</sub>	8.5	10.1

**Table 6.2.3.8 Conversion of palmitic acid and tributyrin with methanol at 60°C<sup>(12)</sup>**

The conversion of RSO with silica supported CsSTA at 160°C was 34% after four hours reaction time, this is greater than the result for the Cs<sub>0,9</sub>PTA used in the tributyrin. However, the greater conversion would be down to the higher temperature in the RSO and the difference of the reactants. It is interesting to note that the highest conversion is with the Cs<sub>2,3</sub>PTA whereas most literature sources identify Cs<sub>2,5</sub>HPA salts as more active in many different reactions. Cs substituted HPAs can form an emulsion like slurry when used in reactions of the transesterification of ethanol and triolein<sup>(13)</sup> which makes the separation of the catalysts difficult, however these

catalysts are more active in the transesterification of triolein with ethanol. Sunflower transesterification with methanol catalysed by zirconia supported STA and PTA<sup>(14)</sup> gave conversions of 71 and 80% respectively in five hours at 180°C. The higher conversions can be attributed to higher catalyst loading and higher temperature used.

### 6.2.3 Comparisons with other acid catalysts

Different mineral acids were used to compare the HPA to cheaper alternatives.

Catalyst	Conversion of RSO
0.1g STA on silica	18 (temp 140°C)
0.2ml of 0.05M sulphuric acid	90
0.1ml of 0.1M hydrochloric acid	77
0.1g STA on silica	21
Reuse of STA on silica	14
Unsupported Cs <sub>2.5</sub> STA	3
Silica supported Cs <sub>2.5</sub> STA (20% loading)	5

**Table 6.2.3.8 Comparison of mineral acids versus HPA in RSO transesterification after 240 minutes at 160°C**

It appears that the conventional mineral acids used (sulphuric and hydrochloric acid) are more effective at catalysing the conversion of RSO to the methyl ester. The Cs<sub>2.5</sub>STA and the supported Cs<sub>2.5</sub>STA, while having larger surface areas than the non-cation exchanged STA, are the least active of the catalysts when tested under the same conditions. Calculations to determine the moles of H<sup>+</sup> in solution show that the concentration of the mineral acids, hydrochloric acid and sulphuric acid are  $1 \times 10^{-5}$  and  $2 \times 10^{-5}$  respectively whereas the moles of H<sup>+</sup> in solution available from STA and silica supported Cs<sub>2.5</sub>STA is  $2.4 \times 10^{-5}$  and  $9.4 \times 10^{-6}$  moles respectively.



Caesium is known as a strong base and could react with the methanol present and produce caesium methoxide, this may result in saponification of the RSO due to the water present in the methanol. This, in combination with the effect of fewer acidic protons present per caesium cation would reduce the production of FAME in the reaction.

### 6.3 Conclusions

It is possible to conclude that the transesterification of RSO to bio-diesel has been partially successful. The HPA catalysts were possible of converting RSO to bio-diesel with moderate results however, the unsupported catalysts are not recoverable as they dissolve into the methanol phase, while the caesium salts produce an emulsion with the RSO layer. This is in agreement with the literature<sup>(13)</sup>

The best results were obtained using a higher temperature and a higher loading of catalyst. It appears that during the use of the lower weight of catalyst, the unsubstituted STA is more active than the CsSTA, while at the higher weight of catalyst, the CsSTA is more active than the unsubstituted STA.

### References

1. L.C. Meher D. Vidya Sagar, S.N. Naik Renewable and Sustainable Energy Reviews 10 (2006) 248-268
2. E. Minami, S. Saka Fuel 85 (2006) 2479–2483
3. L. Guerreiro, J.E. Castanheiro, I.M. Fonseca, R.M. Martin-Aranda, A.M. Ramos, J. Vital Catalysis Today 118 (2006) 166–171
4. H. Chang, H. Liao, C. Lee, C. Shieh Journal of Chemical Technology and Biotechnology 80 (2005) 307–312
5. C. Reddy, V. Reddy, R. Oshel, J.G Verkaade Energy & Fuels 20 (2006) 1310-1314

6. D.G. Cantrell, L.J. Gillie, A.F. Lee, K. Wilson *Applied Catalysis A: General* 287 (2005) 183–190
7. J. Ji, J. Wang, Y. Li, Y. Yu, Z. Xu *Ultrasonics* 44 (2006) e411–e414
8. Y.C. Lin, W.J. Lee, T.S. Wu, C.T. Wang *Fuel* 85 (2006) 2516–2523
9. S. Machado Correâ, G. Arbilla *Atmospheric Environment* 40 (2006) 6821–6826
10. C.D. Rakopoulos, K.A. Antonopoulos, D.C. Rakopoulos, D.T. Hountalas, E.G. Giakoumis *Energy Conversion and Management* 47 (2006) 3272–3287
11. M. Zabeti, W. M. A. W. Daud, M. K. Aroua *Fuel Processing Technology* 90 (2009) 770-777
12. K. Narasimharao, D.R. Brown, A.F. Lee, A.D. Newman, P.F. Siril, S.J. Tavener, K. Wilson *Journal of Catalysis* 248 (2007) 226-234
13. N. Katada, T. Hatanaka, M. Ota, K. Yamada, K. Okumura, M. Niwa *Applied Catalysis A: General* 363 (2009) 164-168
14. G. Sunita, B.M. Devassy, A. Vinu, D. P. Sawant, V.V. Balasubramanian, S.B. Halligudi *Catalysis Communications* Volume 9 Issue 5 (2008) 696-702

# Chapter Seven: Conclusions and Future Work

## 7.1 Conclusions

The silicotungstic Keggin-type heteropoly acid as the free acid or supported and its caesium salts have been synthesised, characterised and their catalytic activity tested in various reactions, both in the gas phase and liquid phase and as homogeneous and heterogeneous catalysts against other mineral acids.

The characterisation of the catalysts prepared agrees with the literature. The surface areas of the substituted HPAs increase to a maximum when three or four protons are substituted and decreasing once all the protons are substituted. The pores of the supports investigated are filled with solid HPA. Raman spectroscopy and powder X-ray diffraction support the evidence that the primary structure of the Keggin anion. Thermal gravimetric analysis on the supported STA show that there is a loss of weight corresponding to the decomposition of the Keggin unit on the support. The temperature programmed desorption of ammonia shows that the support has an effect on the Keggin unit. When supported on silica, STA showed evidence of strong acidity and less reducibility with strong, defined peaks at 225°C. The STA on carbon coated supports lack the sharp peaks above 225°C showing that the HPA does interact with the carbon coated supports.

The cyclodehydration of BTD in both the liquid and gas phases was inconclusive, as the reaction could not be monitored appropriately. It was impossible to make any kinetic comparisons between the liquid and gas phase reactions due to the problems encountered. It was found that the mass balance for both the gas phase reaction and the liquid phase reaction were very low. It would appear that under the

conditions tested the reaction in the gas phase either initiated the polymerisation of any THF <sup>(1)</sup> produced and deposited on the walls of the tubes of the gas phase apparatus or that the BTD/THF encountered a hot-spot in the reactor and carbonised on the walls of the tubes.

The reactions of geraniol with supported and unsupported HPAs showed that the reaction is sensitive to competitive adsorption during the reaction, but is able to be catalysed by HPAs whereas the same concentration of mineral acids cannot. It was also found that a neutralised caesium salt of STA was unable to catalyse the reaction, giving evidence that the super-acidic nature of HPAs play a part in the reaction. The selectivity to linalool could be explained as the rearrangement of geraniol after losing a water molecule and forming linalool after the re-uptake of the water molecule. Immobilisation of the catalyst in a support would enable the separation of the products from the catalyst with a decreased risk of catalyst in the final product, which may be added to cosmetics as an aroma compound.

The synthesis of bio-diesel shows that HPAs can be used to catalyse the transesterification of methanol and vegetable oil to glycerol and bio-diesel. The catalysts suffer from leaching as evidenced by the emulsion seen when using the CsSTA catalysts. While not as efficient as sodium hydroxide, the reaction does show that HPA is capable of catalysing the reaction. The benefit of using an acid catalyst is that lower quality feedstocks can be used without the risk of contaminating the product with saponification products. Simply depositing the HPA or its salts on a support is not enough to prevent it from significantly leaching off the support. The risk of contaminating the bio-diesel with dissolved catalyst would be decreased if the catalyst were immobilised on a support. This would be likely to increase the reusability of the HPA catalysts.

While HPAs are easier to safer to handle, store and offer super-acidic properties, they are more expensive than typical mineral acids used in acid catalysed reactions. This would hinder the introduction of HPAs into widespread use in industry.

### 7.2 Further Work

Although some promising results have been obtained, in particular, in the transesterification of vegetable oil, there is a case for grafting the HPA onto the support to help minimise the leaching. This would enable the catalyst to be easily recovered and reused. It may be possible that the reactions performed in the bio-diesel experiments may proceed without the high temperatures and pressures developed in an autoclave and could be performed in a glass vessel at normal atmospheric pressure. These milder conditions would be beneficial for bio-diesel producers as the energy requirement and therefore cost of goods (COG) would be lower. This would help bio-diesel compete with fossil diesel in a financial sense and attract investment.

The cyclodehydration of BTD failed to yield positive results. A more robust and validated method of analysing BTD would certainly yield more meaningful results in both the gas phase and liquid phase. The product distribution of the geraniol experiments is an area that requires more investigation. If a method of driving off the water during the reaction was employed, for instance a fractionating column or Dean-Stark apparatus, it may change the selectivity of the products towards limonene.

### References

1. I. V. Kozhevnikov *Chemical Reviews* 98 (1998) 171-198

# Appendix

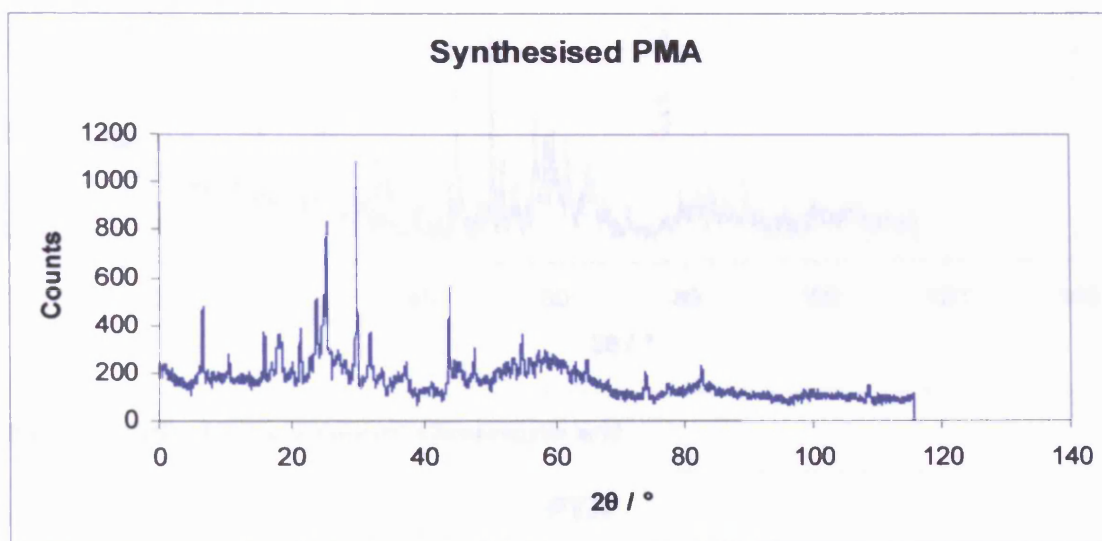


Figure 1 XRD of synthesised phosphomolybdic acid

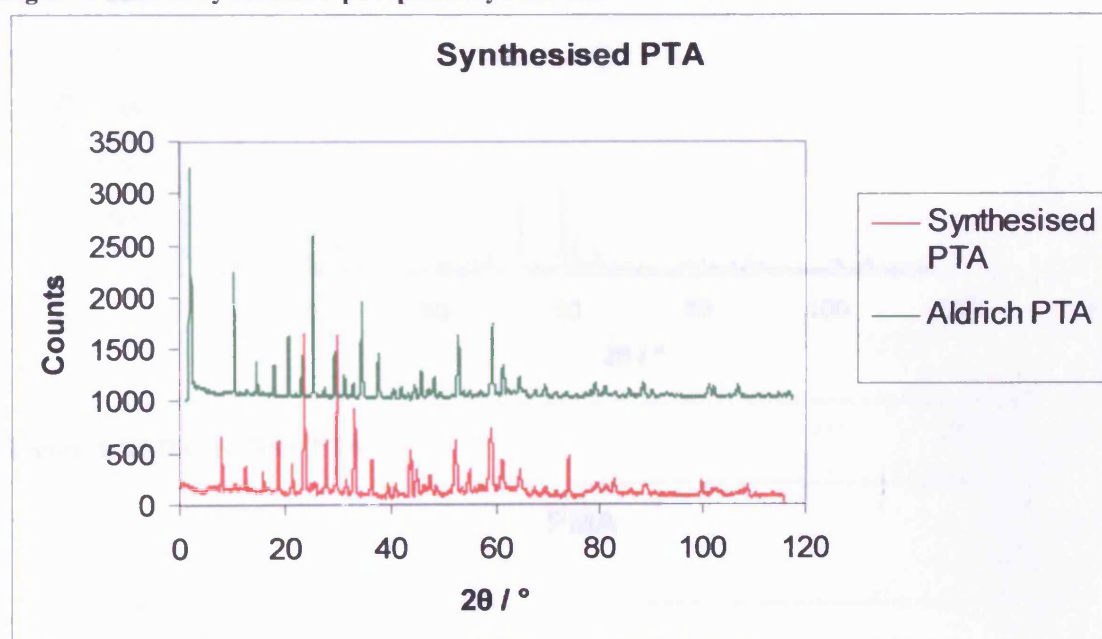


Figure 2: XRD of synthesised phosphotungstic acid and Aldrich bought PTA

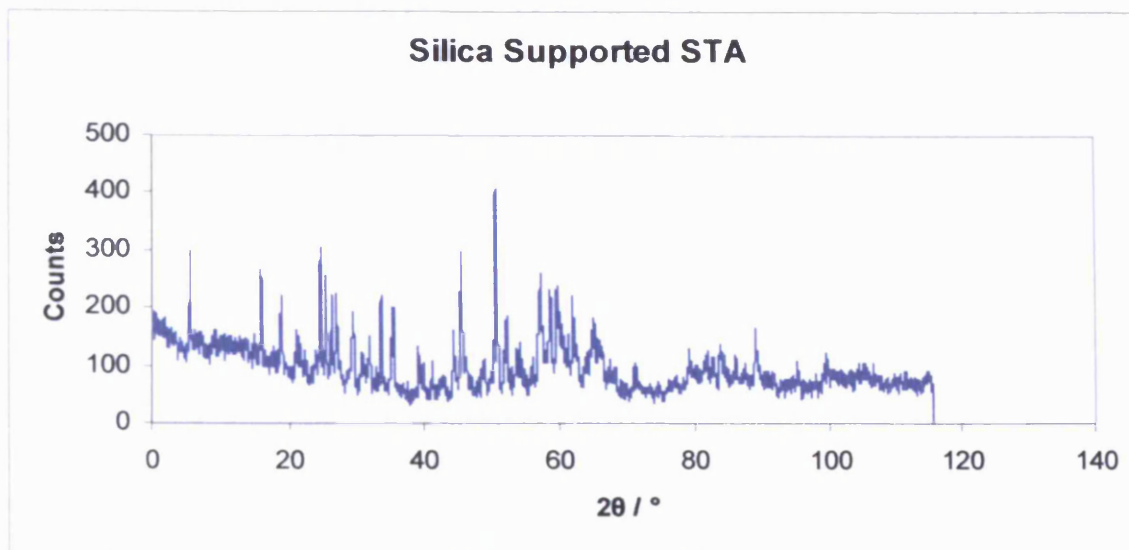


Figure 3: XRD of Silica supported silicotungstic acid

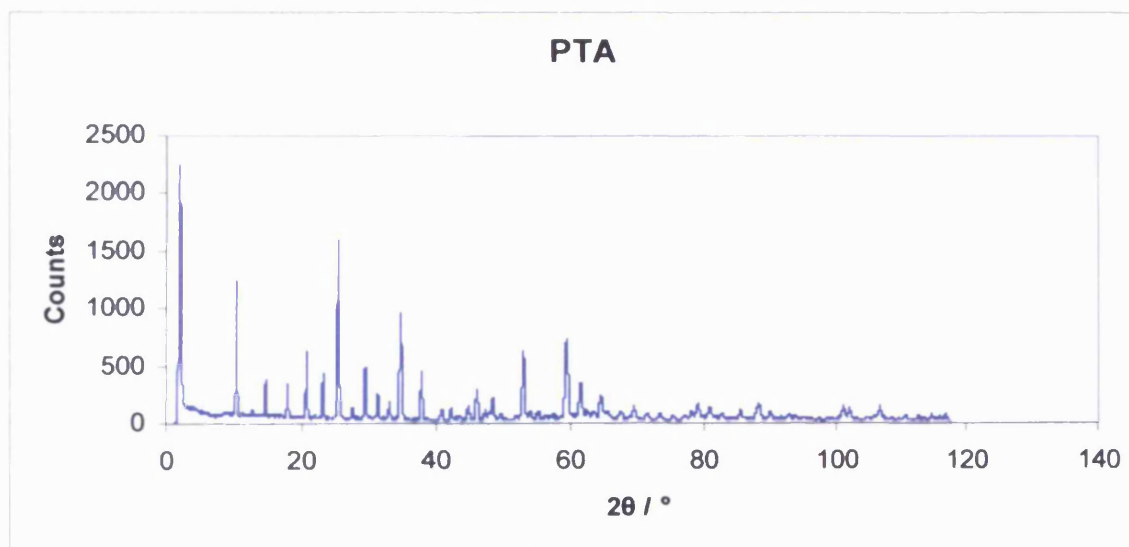


Figure 4: XRD of Aldrich PTA

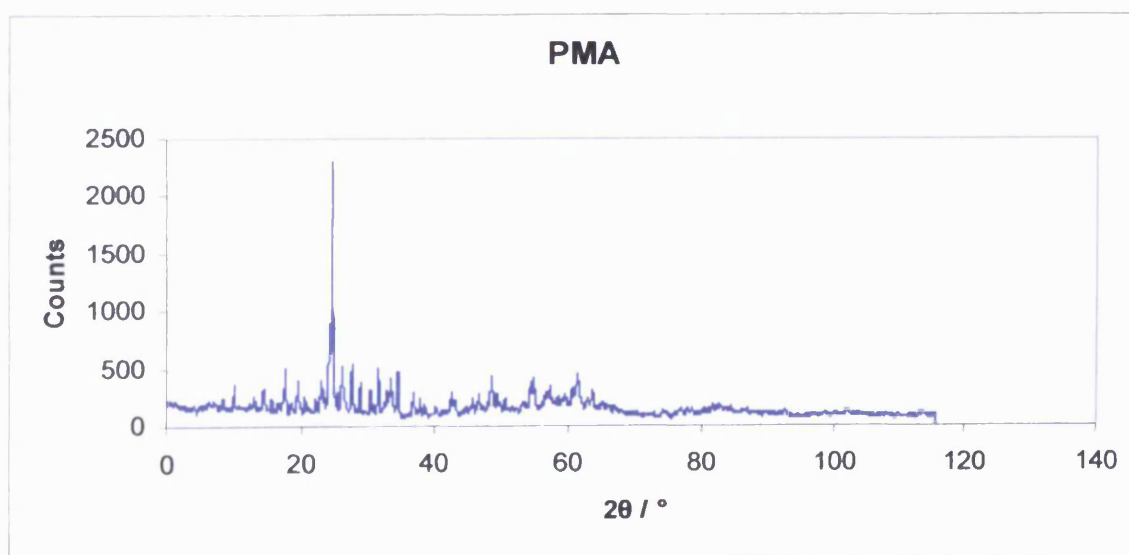


Figure 5: XRD Aldrich phosphomolybdic acid

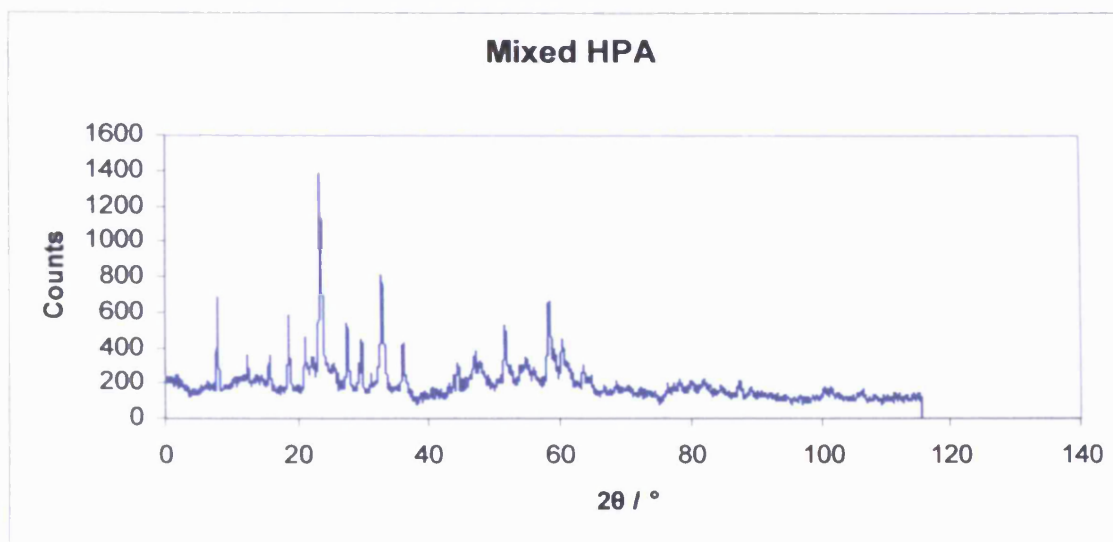


Figure 6: XRD of PMA/PTA mix

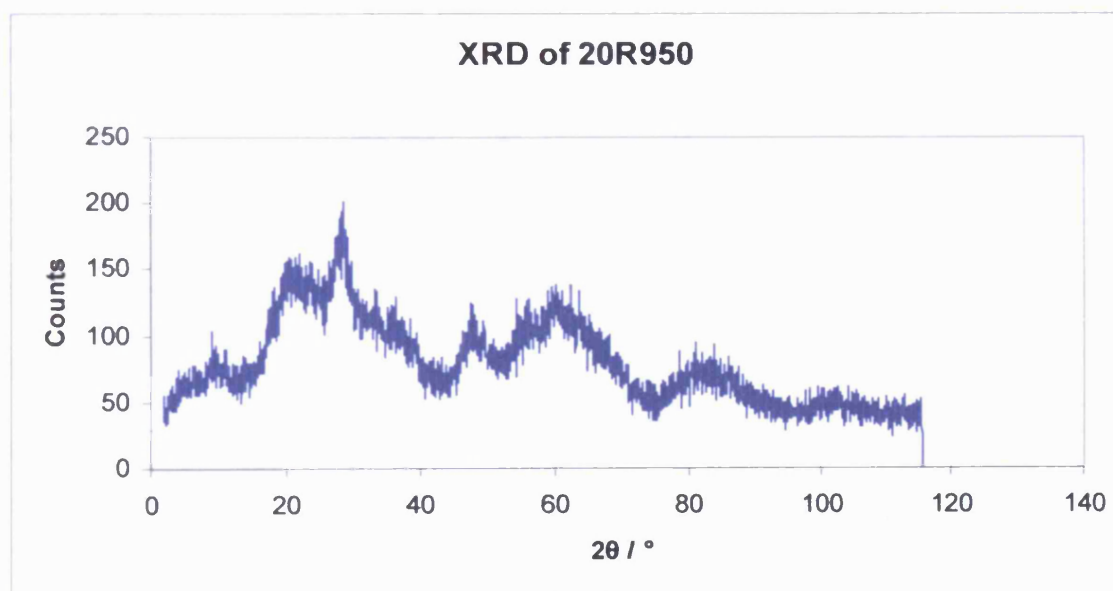


Figure 7: XRD of Course grain silica supported STA



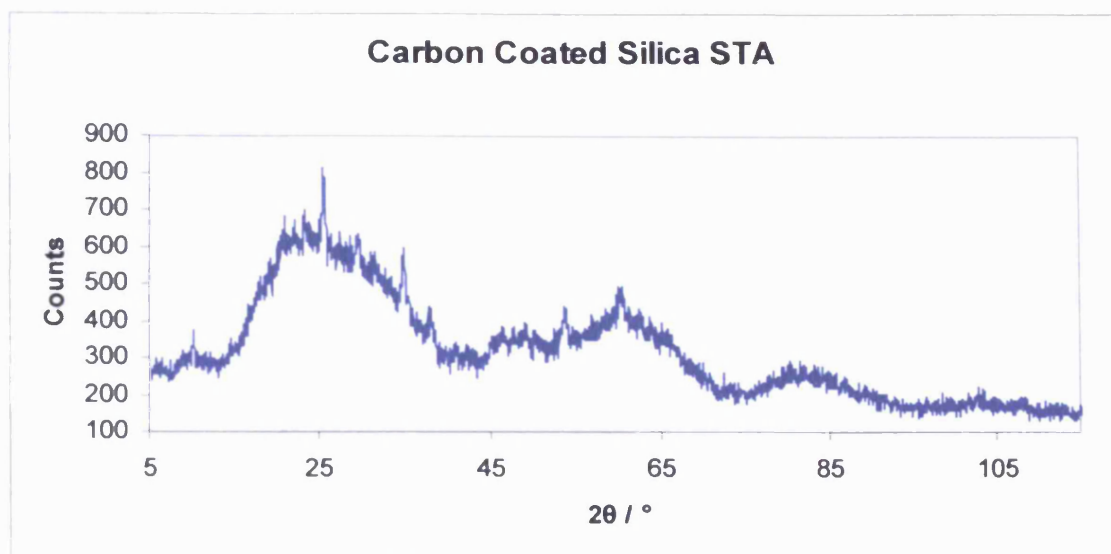


Figure 8: XRD of carbon coated silica supported STA

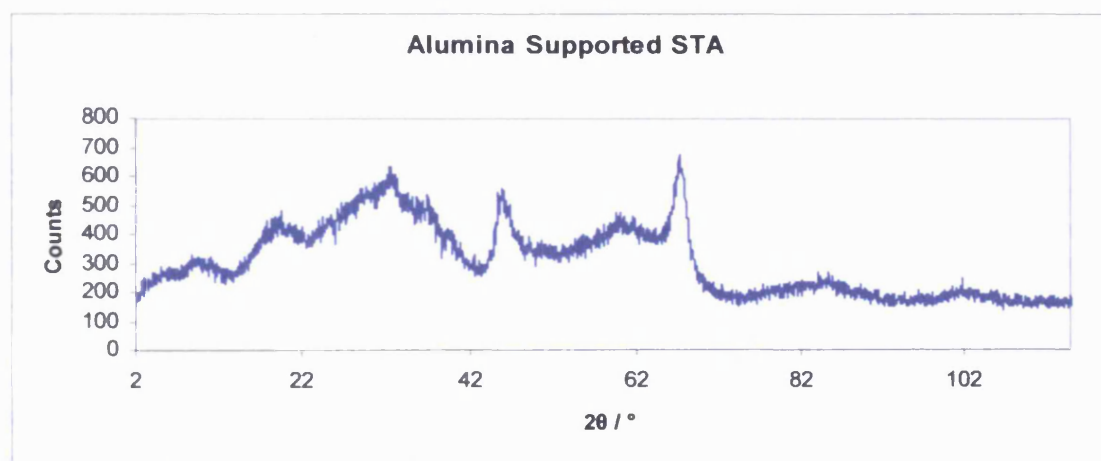


Figure 9: XRD of alumina supported STA

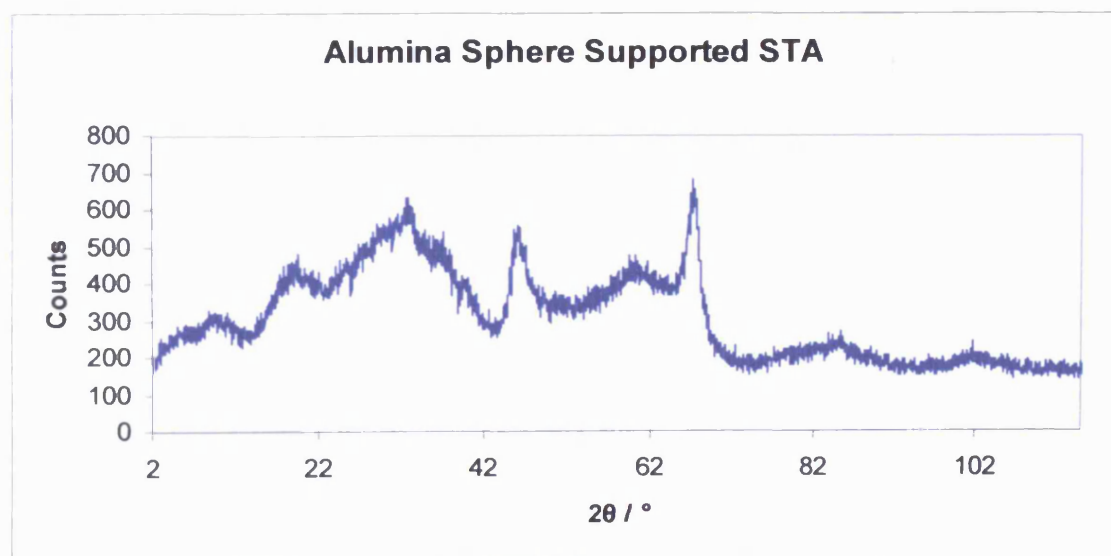


Figure 10: XRD of alumina sphere supported STA

He flow rate: 80ml/min

Weight of STA/silica 0.05g

Vaporiser set at 60°C

Furnace set at 55-70°C

Septum split ratio: 200

<b>Injection</b>	<b>Ratio butanediol/dioxane</b>
1	2.120
2	1.423
3	1.300
4	2.056
5	1.282
6	1.439
7	2.253
8	1.649
9	2.016
10	2.891

**Table 1**

Septum split ratio: 500

<b>Injection</b>	<b>Ratio butanediol/dioxane</b>
1	2.017
2	2.193
3	1.789
4	2.518
5	1.965
6	2.097
7	1.970
8	1.953
9	1.384
10	1.808

**Table 2**

Septum split ratio: 1000

<b>Injection</b>	<b>Ratio butanediol/dioxane</b>
1	6.079
2	2.782
3	0.642
4	1.220
5	1.201
6	0.429
7	1.985
8	1.246
9	0.975
10	1.671

**Table 3**

Septum split ratio:1000

<b>Injection</b>	<b>Ratio butanediol/dioxane</b>
1	0.436
2	1.250
3	1.927
4	1.103
5	2.200
6	0.951
7	0.918
8	0.979
9	2.156
10	1.019

Table 4

Septum split ratio:1000

<b>Injection</b>	<b>Ratio butanediol/dioxane</b>
1	0.370
2	1.334
3	3.944
4	1.349
5	1.192
6	1.575
7	1.034
8	3.307
9	1.319
10	3.280

Table 5

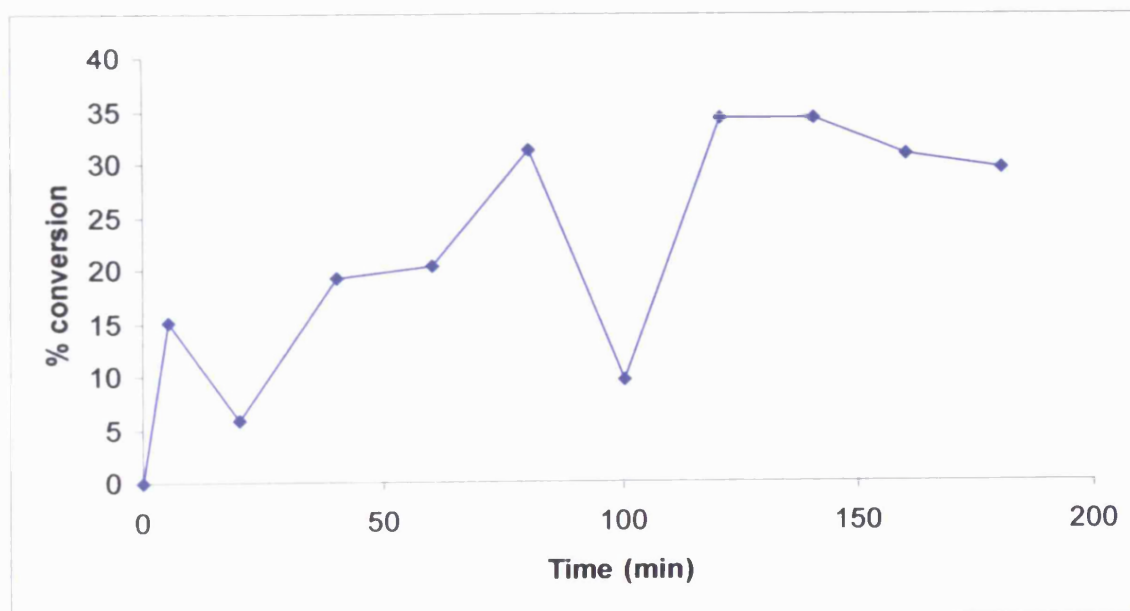


Figure 20: Conversion of BTD at 100°C using 0.05g PTA free acid

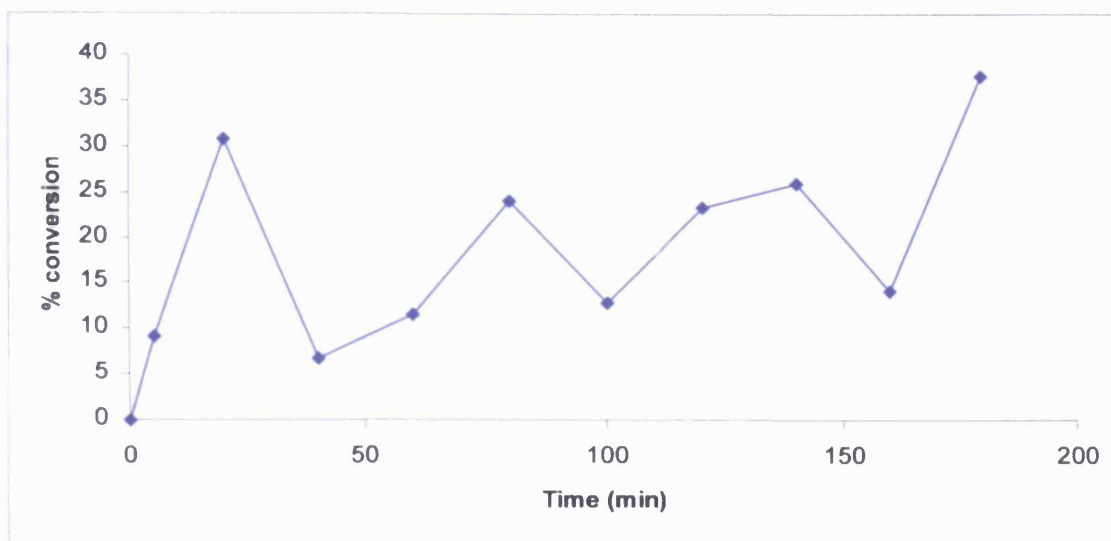


Figure 21: Conversion of BTB at 100°C using 0.05g SMA free acid

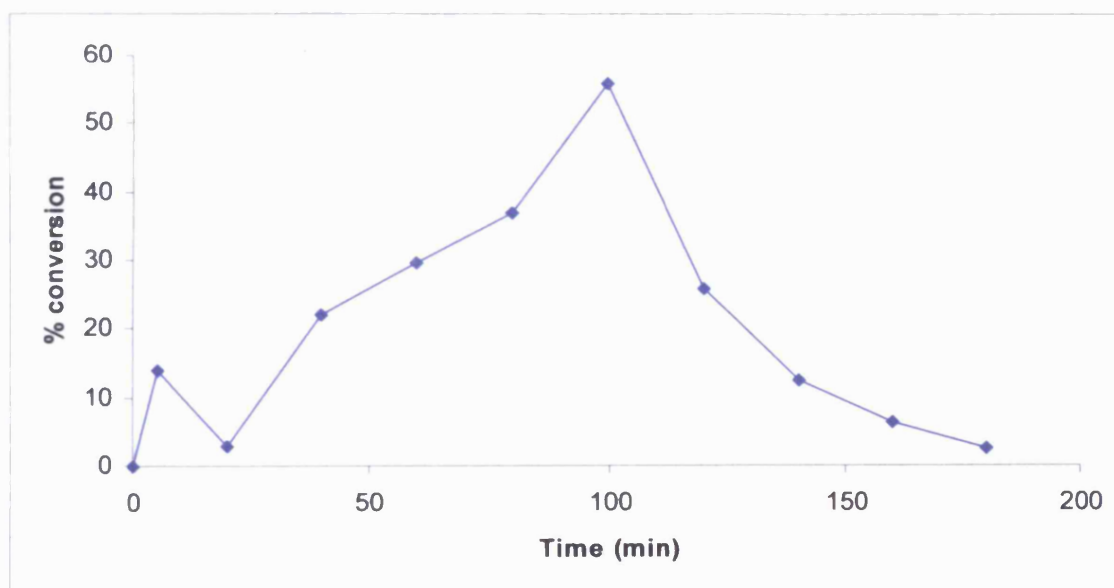


Figure 22: Conversion of BTB at 100°C using 0.05g CsSMA

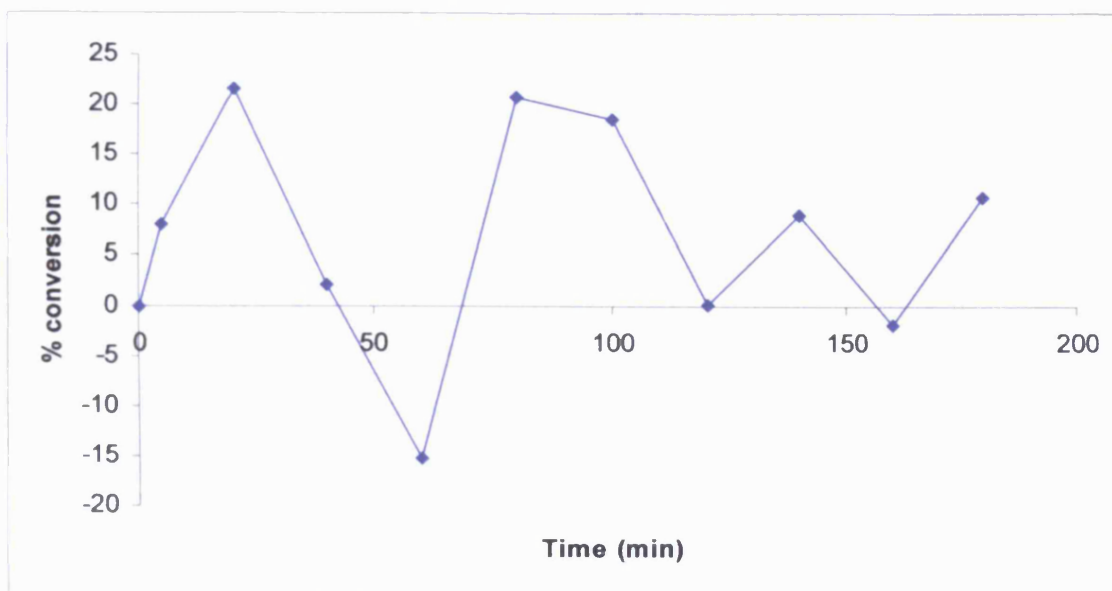


Figure 23: Conversion of BTD at 100°C using 0.05g CsPMA

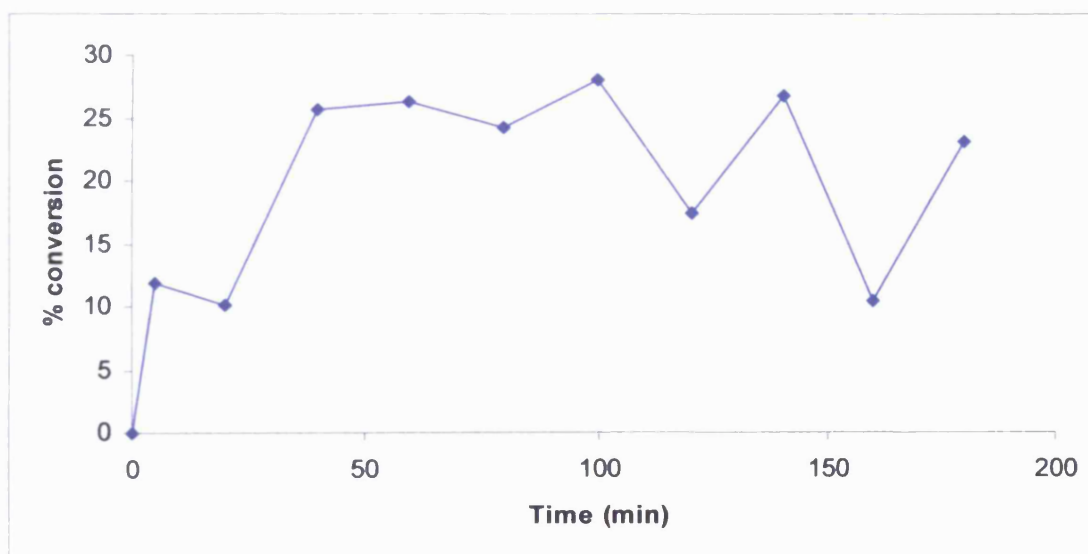


Figure 24: Conversion of BTD at 100°C using 0.05g Cs<sub>3</sub>SMA

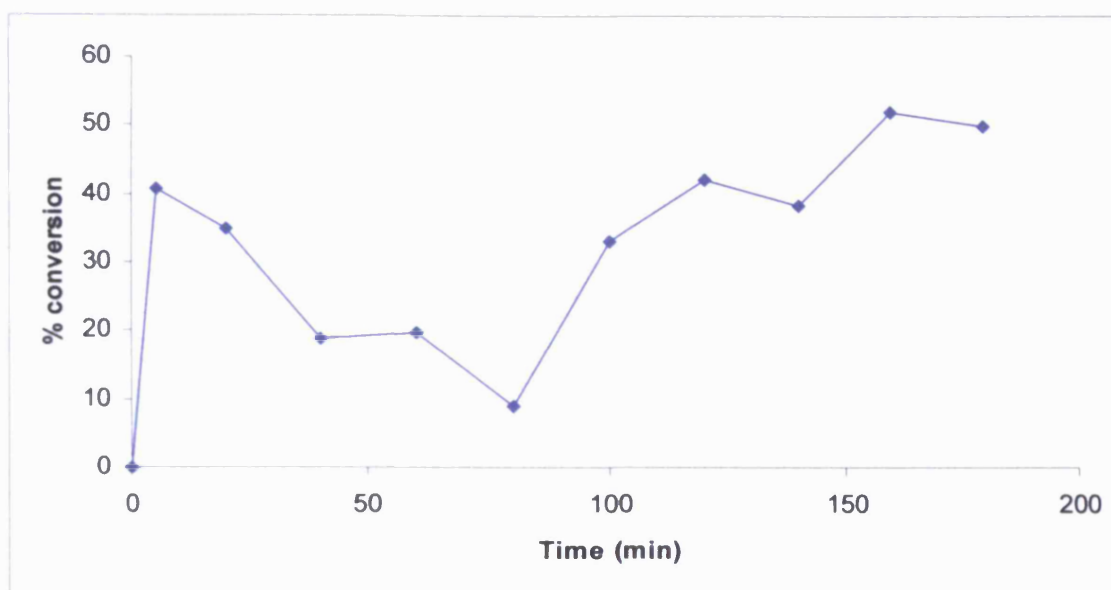


Figure 25: Conversion of BTB at 100°C using 0.05g CsSTA

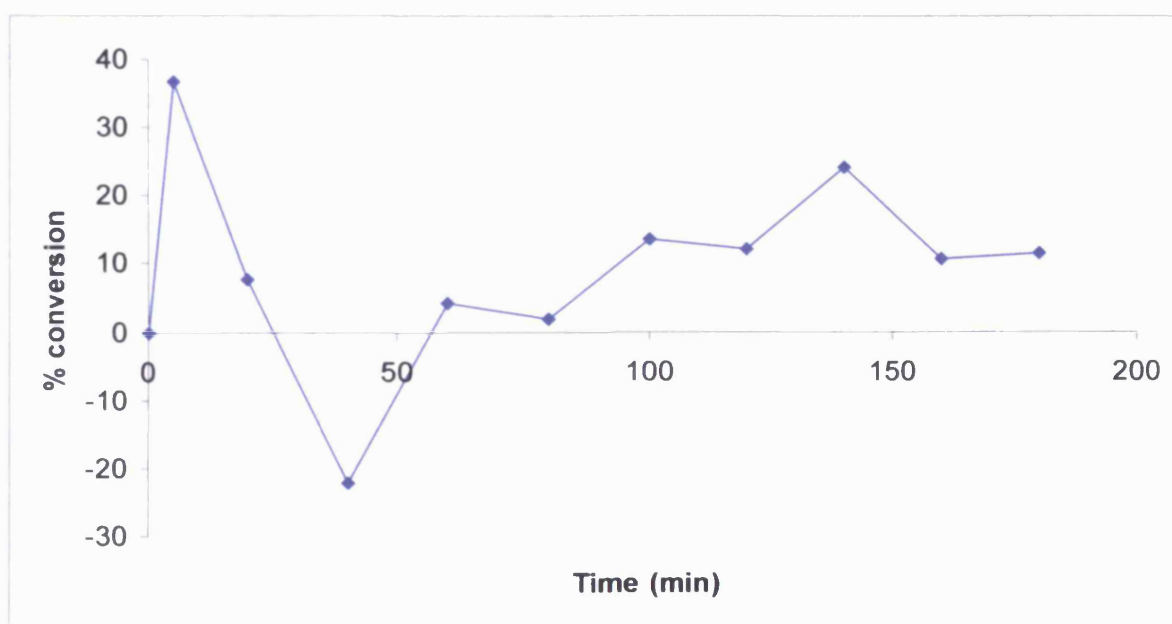


Figure 26: Conversion of BTB at 100°C using 0.05g Cs<sub>2</sub>STA

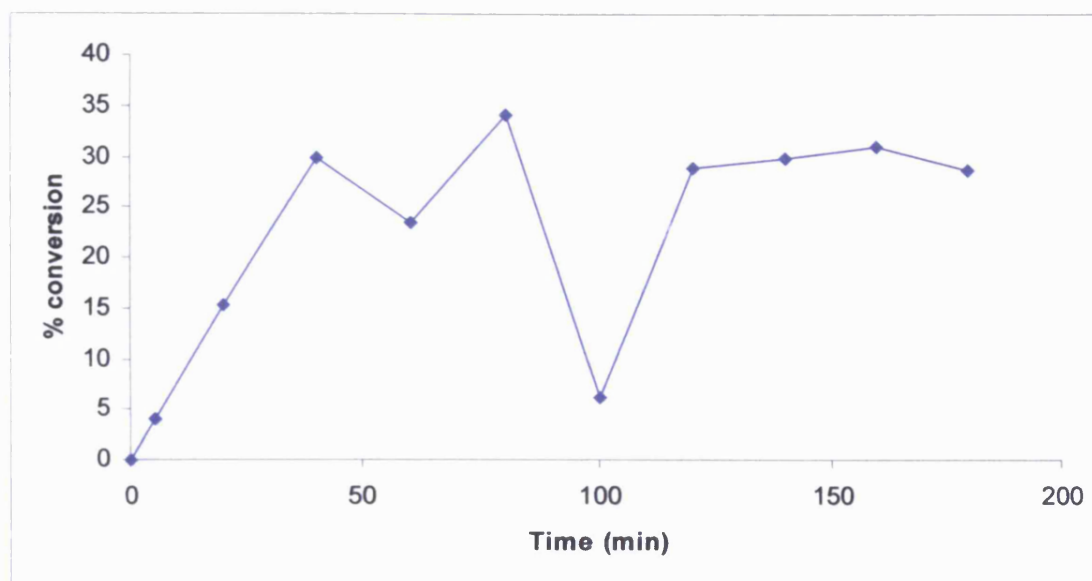


Figure 27: Conversion of BTD at 100°C using 0.05g Cs<sub>2</sub>PMA

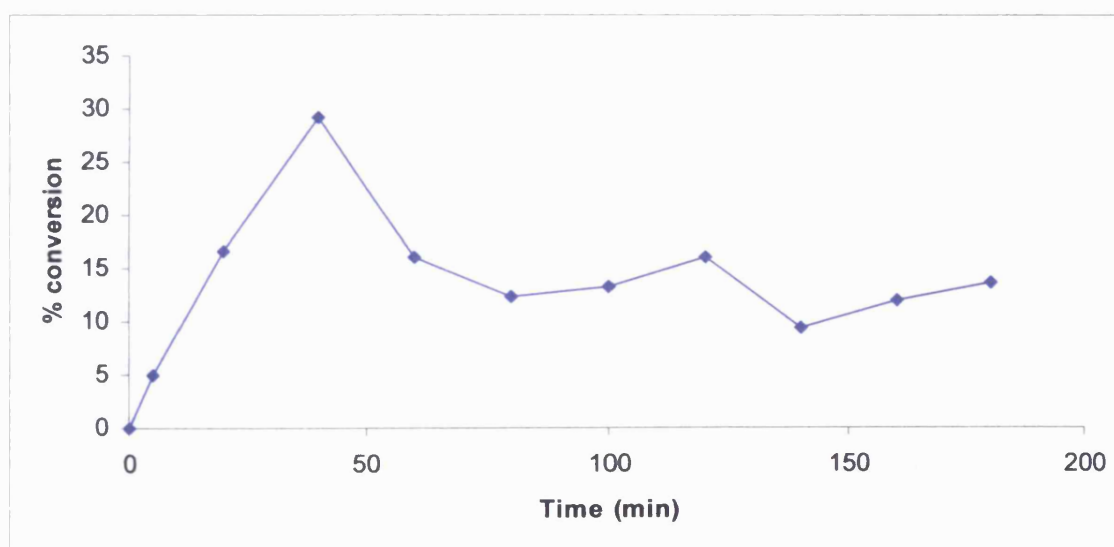


Figure 28: Conversion of BTD at 100°C using 0.05g Cs<sub>3</sub>PTA

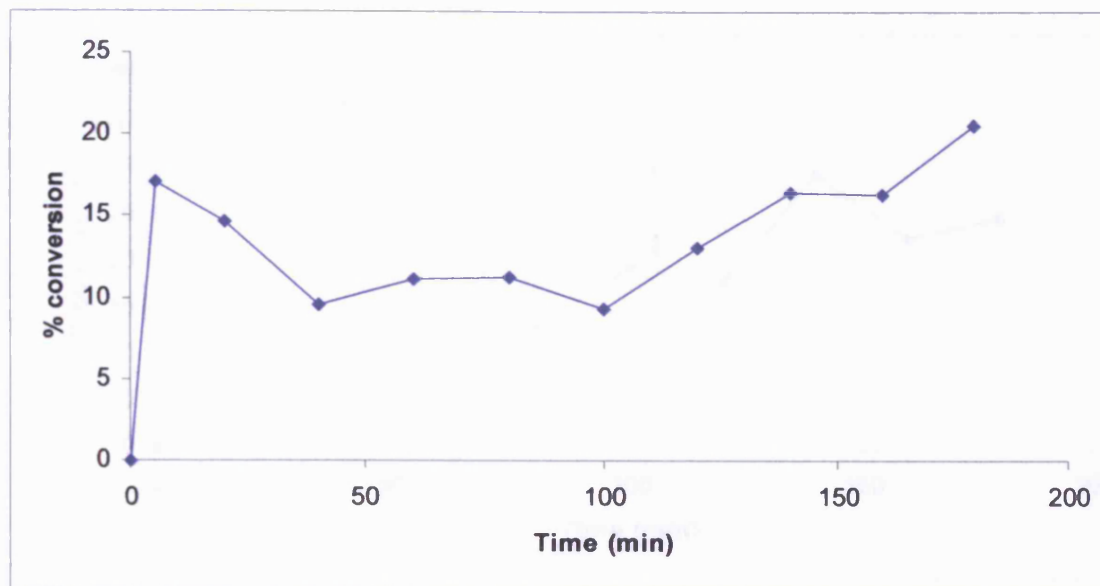


Figure 29: Conversion of BTB at 100°C using 0.05g Cs<sub>3</sub>STA

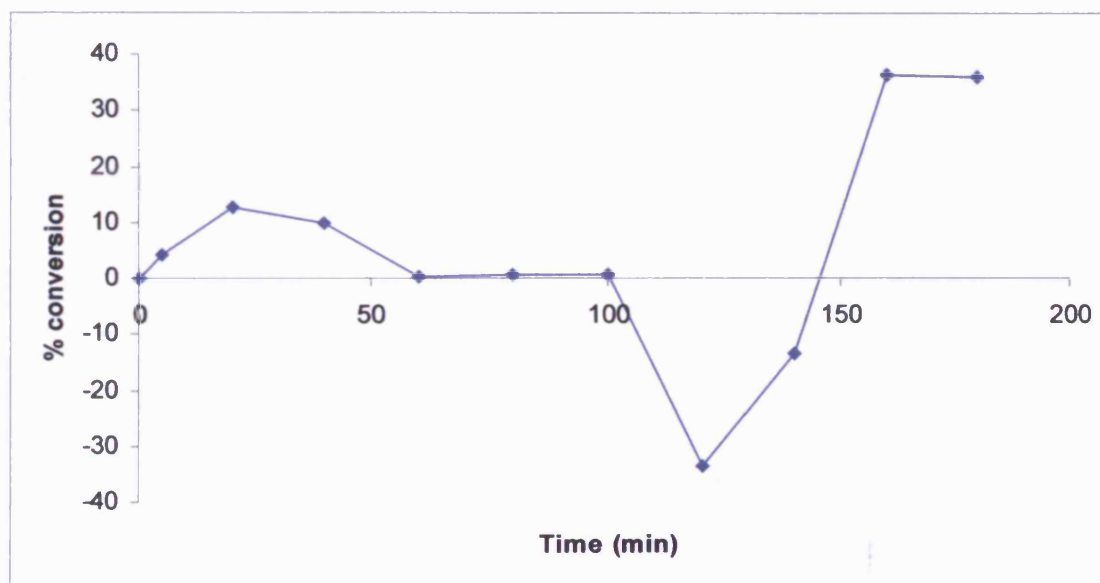


Figure 30: Conversion of BTB at 100°C using 0.05g Cs<sub>4</sub>STA



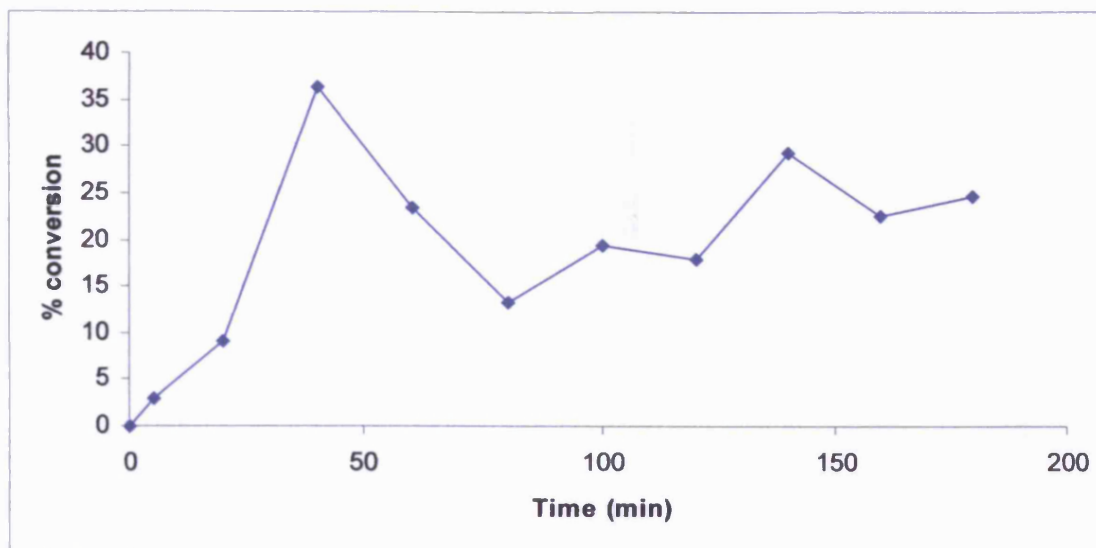


Figure 31: Conversion of BTB at 100°C using 0.05g Cs<sub>3</sub>PMA

